TECHNOECONOMIC EVALUATION OF SOLID OXIDE FUEL CELL HYDROGEN-ELECTRICITY CO-GENERATION CONCEPTS

JOHN ESLICK, ALEXANDER NORING, NARESH SUSARLA, CHINEDU OKOLI, DOUGLAS ALLAN, MAOJIAN WANG, JINLIANG MA, MIGUEL ZAMARRIPA, ARUN IYENGAR, ANTHONY BURGARD

March 31, 2023

DOE/NETL - 2023/4322

Disclaimer

This project was funded by the United States Department of Energy, National Energy Technology Laboratory, in part, through a site support contract.

All images in this report were created by NETL, unless otherwise noted.

John Eslick[1,2]*: Conceptualization, Methodology, Writing – Original Draft, Formal Analysis, Supervision;* ***Alexander Noring***[1,2]*: Conceptualization, Methodology, Formal Analysis, Writing – Original Draft;* ***Naresh Susarla***[1,2]*: Conceptualization, Methodology, Formal Analysis, Writing – Original Draft;* ***Chinedu Okoli***[1,2]*: Conceptualization, Methodology, Formal Analysis, Writing – Original Draft;* ***Douglas Allan***[1,2]*: Conceptualization, Methodology, Formal Analysis, Writing – Original Draft;* ***Maojian Wang***[1,2]*: Conceptualization, Methodology, Formal Analysis, Writing – Original Draft;* ***Jinliang Ma***[1,2]*: Conceptualization, Methodology, Writing – Original Draft, Formal Analysis, Supervision;* ***Miguel Zamarripa***[1,2]*: Conceptualization, Methodology, Writing – Original Draft, Formal Analysis, Supervision;* ***Arun Iyengar***[1,2]*: Conceptualization, Supervision;* ***Anthony Burgard***[2]**: Conceptualization, Supervision*

[1]National Energy Technology Laboratory (NETL) support contractor
[2]NETL
*Corresponding contact: Anthony.Burgard@netl.doe.gov, 412.386.5056

The authors wish to acknowledge the cooperation, suggestions, and contributions from the following team members:

Jaffer Ghouse, *NETL support contractor*
Alexander Dowling, *University of Notre Dame (UND)*
David Miller, *NETL*
Debangsu Bhattacharyya, *West Virginia University (WVU)*
Samuel Bayham, *NETL*

Suggested Citation:

J. Eslick, A. Noring, N. Susarla, C. Okoli, D. Allan, M. Wang, J. Ma, M. Zamarripa, A. Iyengar, A. Burgard, "Technoeconomic Evaluation of Solid Oxide Fuel Cell Hydrogen-Electricity Co-generation Concepts," National Energy Technology Laboratory, Pittsburgh, March 31, 2023.

This page intentionally left blank.

TABLE OF CONTENTS

LIST OF EXHIBITS

ACRONYMS AND ABBREVIATIONS

°C	Degrees Celsius
K	Degrees Kelvin
µm	Micrometer
Ωm	Ohm meter
A	Ampere
AC	Alternating current
ALAMO	Automatic Learning of Algebraic Models
Ar	Argon
AR5	Intergovernmental Panel on Climate Change Fifth Assessment Report
Aspen	Aspen Plus®
ASU	Air separation unit
BEC	Bare erected cost
BOP	Balance of plant
Btu, BTU	British thermal unit
CAES	Compressed air energy storage
C_2H_6	Ethane
C_3H_8	Propane
C_4H_{10}	Butane
CCS	Carbon capture and storage
CH_4	Methane
cm^2	Square centimeter
CO_2	Carbon dioxide
CO_2e	CO_2 equivalents
CPU	Carbon purification unit
DNN	Deep neural network
DOE	Department of Energy
EoS	Equation of state
EPA	Environmental Protection Agency
EPC	Engineering, Procurement, and Construction
EPCC	Engineering, Procurement, and Construction Cost
EPRI	Electric Power Research Institute
FEB	Fossil Energy Baseline report
FCR	Fixed charge rate
GHG	Greenhouse gas
GWP	Global warming potential
h, hr	Hour
H_2	Hydrogen
H_2O	Water
HHV	Higher heating value
HP	High pressure
hr	Hour
HRSG	Heat recovery steam generator
HX, HTX	Heat exchanger
IDAES	Institute for the Design of Advanced Energy Systems
IES	Integrated energy systems
IP	Intermediate pressure
J	Joule
kg	Kilogram
kJ	Kilojoule
kmol	Kilomole
kPa	Kilopascal
LCA	Life cycle analysis
LHV	Lower heating value
LP	Low pressure
LSM	Lanthanum Strontium Manganite
m	Meter
m^2	Square meter
mA	Milliampere
MJ	Megajoule
MM	Million
mol	Mole
mol%	Mole percent
MPa	Megapascal
MW, MW_e	Megawatt electric
MWh	Megawatt hour
MW_{th}	Megawatt electric thermal
N_2	Nitrogen
N_2O	Nitrous oxide
NETL	National Energy Technology Laboratory
NG	Natural gas
NGCC	Natural gas combined cycle
NGFC	Natural gas fuel cell
Ni	Nickel
NREL	National Renewable Energy Laboratory

O_2	Oxygen
O&M	Operating and maintenance
Pa	Pascal
ppm	Parts per million
PV	Photovoltaic
PZ	Piperazine
PZAS™	Piperazine Advanced Stripper
QGESS	Quality Guidelines for Energy System Studies
ROM	Reduced-order model
rSOC	Reversible solid oxide cell
s	Second
SMR	Steam methane reforming
SOC	Solid oxide cell
SOEC	Solid oxide electrolysis cell
SOFC	Solid oxide fuel cell
SOFC-MP	SOFC-multi-physics
SMR	Steam methane reforming
SRD	Specific reboiler duty
TASC	Total as spent cost
TOC	Total overnight cost
tonne	Metric ton (1,000 kg)
TPC	Total plant cost
TRL	Technology readiness level
U.S.	United States
V	Volt
V-I	Voltage-current
vol%	Volume percent
W	Watt
WVU	West Virginia University
yr	Year
YSZ	Yttria-stabilized zirconia

EXECUTIVE SUMMARY

Fossil energy systems with carbon capture, such as natural gas combined cycle (NGCC) plants equipped with carbon capture and storage (CCS) and energy storage technologies are expected to play an important role in maintaining electric grid reliability in the transition to a decarbonized energy sector. In the long-term, as the world moves toward environmentally sustainable resources, hydrogen (H_2) is expected to play a key role in economy-wide decarbonization. Accordingly, the United States (U.S.) Department of Energy (DOE) aims to reduce levelized costs of low-carbon power and H_2 to aid in the decarbonization of the energy sector by 2030 and the broader economy by 2050.

Integrated energy systems (IES) capable of co-producing power and H_2 provide a promising means for lowering overall production costs of both while enhancing flexibility to work effectively in tandem with intermittent renewable technologies. For example, in comparison to standalone systems for power and H_2 generation, IES can enable significant savings in capital and maintenance costs due to the sharing of much of the same equipment, such as the carbon capture and compression system, as well as lower variable costs through process and heat integration. Additionally, IES with the flexibility to produce H_2 from electricity when electricity prices are low would be expected to operate at a higher capacity factor than a more standard power plant that would be forced to turn down under these conditions. In general, the power generating system also benefits from spending longer periods operating near design conditions, limiting adverse cycling-related effects on plant life.

This report evaluates the cost and performance of several types of IES based on solid oxide fuel cells (SOFCs) to generate power and solid oxide electrolysis cells (SOECs) to produce H_2. As a baseline for comparison, NGCC systems are included as they are currently widely deployed. All cases feature carbon capture at rates exceeding 97 percent. The NGCC-based systems use a solvent-based post combustion capture system, while the SOFC-based systems employ a cryogenic distillation process to provide pure oxygen (O_2) for combustion resulting in a concentrated carbon dioxide (CO_2) stream. A total of seven cases were investigated, as summarized in Exhibit ES-1.

Exhibit ES-1. Case summary

Case	Description	Power Capacity ($MW_{e,net}$)	H_2 Capacity (kg/s)
0	NGCC	650	-
1	SOFC	650	-
2	SOFC+CAES (CAES off)	650	-
	SOFC+CAES Charging	397	-
	SOFC+CAES Discharging	798	-
3	NGCC+SOEC	650	5
4	rSOC	650	5
5	SOFC+SOEC	712	5
6	SOEC	-	5

The power capacities were chosen to be near 650 $MW_{e,net}$ to be consistent with previous National Energy Technology Laboratory (NETL) baseline reports. The SOFC+SOEC system was adjusted such that the SOFC portion of the process can generate 712 MW to provide all the electricity required by the SOEC, while the NGCC+SOEC system must import some power at full H_2 production. The 5 kg/s H_2 capacity was chosen because it requires roughly 650 MW_e. Since current density is generally higher in SOEC systems than SOFC systems, the SOEC stack required to generate 5 kg/s H_2 is roughly one-third the size of an SOFC stack required to generate 650 MW_e. The reversible solid oxide cell (rSOC) balance of plant sizing is done to be consistent with other cases generating 5 kg/s H_2. There is a tradeoff in the rSOC capacities, where a smaller H_2 generation capacity reduces the cost of electricity but increases the cost of H_2. The optimal rSOC capacities can only be decided in the context of market analysis where the time spent operating in electricity production mode and in H_2 mode can be estimated.

PROBLEM DESCRIPTION

The goal of this work is to identify which systems enable lowest cost production of power and H_2 given various sets of assumptions. This report describes the development of optimized steady state process models for each system described in Exhibit ES-1. The models are used to calculate overall production costs using a consistent methodology that facilitates comparisons of these cases to one another and to prior NETL cost and performance estimates. The models will also be leveraged by supplementary work outside the scope of this report that will analyze the potential profitability of each system in different regional markets using time varying electricity price signals.

In contrast to the mature NGCC technology, SOFC systems are currently in a demonstration phase, where kW-MW class systems are being commercialized, corresponding to a technology readiness level (TRL) of 6. The SOEC systems are at a TRL of 4–6, with incipient but growing demonstrations at a small scale. The SOFC and SOEC costs and performance in the present analysis are based on nth-of-a-kind systems and include research and development and learning associated with mass-scale commercial deployment of the technology over the next decade

required for commercial utility-scale systems, consistent with the technology developmental timeline projected by DOE.

RESULTS OVERVIEW

This report considers instantaneous operating points given fixed electricity, H_2, and natural gas (NG) prices. First, the trends in systems producing only power are examined. The NGCC systems with 97 percent CO_2 capture can achieve 47.6 percent higher heating value (HHV) efficiency for power generation at full load, while SOFC-based systems can achieve 65.3 percent HHV efficiency at full load with 98 percent CO_2 capture. Exhibit ES-2 shows the cost breakdown for the different cases at 100 percent electrical power capacity and no H_2 production. Due to their relatively higher efficiency (which lowers the variable operating and maintenance [O&M] costs) as well as lower capital and fixed O&M costs, SOFC-based systems perform significantly better than NGCC-based systems. The SOFC case is the cheapest option among the solid oxide cell-based systems. However, if H_2 production is desired, the rSOC and SOFC+SOEC cases provide the flexibility to do so with a relatively small increase in the cost of electricity produced compared to the SOFC, with the rSOFC being only slightly less costly than the SOFC+SOEC.

Exhibit ES-2. Cost breakdown for electricity production (2018 dollars)

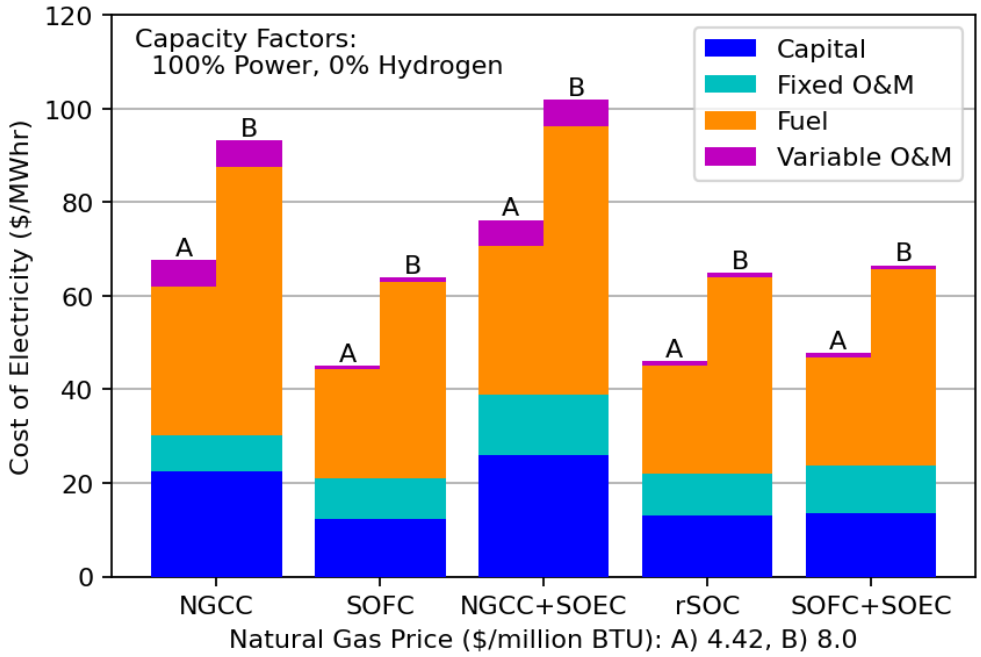

Exhibit ES-3 shows the break-even electricity price as a function of the NG price. This plot also shows approximately how the price of electricity could be expected to vary as a function of gas price.

Exhibit ES-3. Break-even electricity price (2018 dollars)

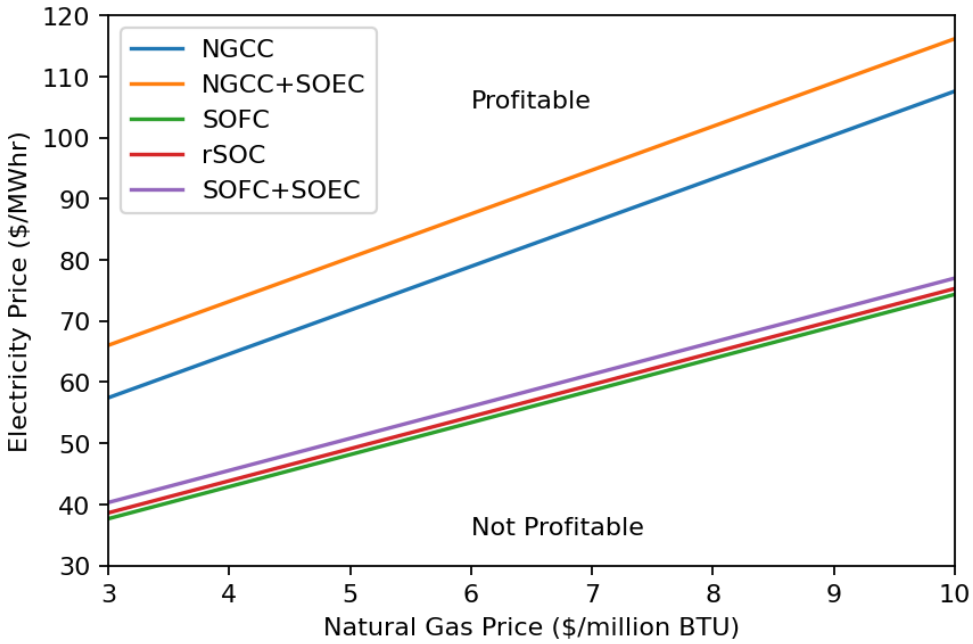

Exhibit ES-4 shows the cost breakdown for systems producing 5 kg/s of H_2 (100 percent capacity). Notably, the system capable of producing H_2 at the lowest cost depends on the assumed electricity and NG prices. At the lowest electricity price ($30/MWh), the SOEC enables lowest cost H_2 production followed closely by the SOFC+SOEC and rSOC systems. The SOEC case is like the rSOC case, but the stack size is significantly smaller, and it does not require CO_2 capture and other equipment associated with power generation allowing for substantial capital cost savings. At the highest electricity price ($100/MWh), the systems with the flexibility to produce their own electricity for H_2 generation, the SOFC+SOEC and NGCC+SOEC, are the lowest cost. The cost of H_2 produced from the NGCC+SOEC system is more dependent on NG price than the SOFC+SOEC due to the lower efficiency of NGCC compared to SOFC-based power generation.

Exhibit ES-4. H_2 production cost breakdown (2018 dollars)

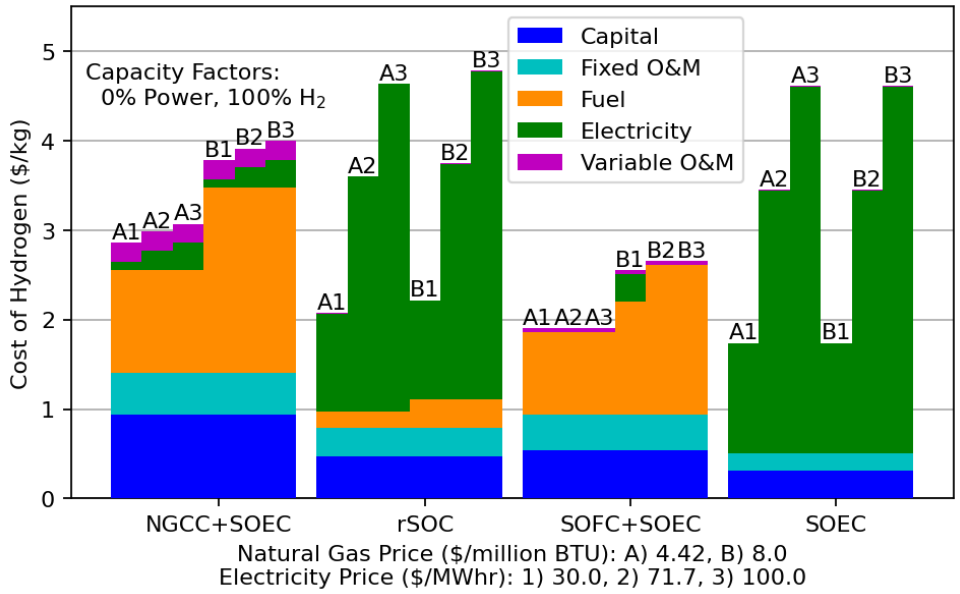

Exhibit ES-5 shows the electricity and H_2 break-even prices at $4.42/MMBtu NG for the various systems. These were obtained by solving an optimization problem to minimize the H_2 selling price required to achieve zero overall profit at different electricity prices. The individual lines for the various systems imply that just enough revenue is generated to provide the modest return on investment assumed by the cost estimation methodology. Key observations include the following:

- At low electricity prices, the standalone SOEC is the lowest cost system for H_2 production, followed by the rSOC, SOFC+SOEC, and NGCC+SOEC, respectively.
- At electricity prices higher than $38/MWh, the SOFC+SOEC system becomes more favorable than the standalone SOEC due to its ability to generate its own electricity for H_2 production.
- At electricity prices higher than $60/MWh, the NGCC+SOEC system becomes more advantageous than the standalone SOEC.

Exhibit ES-5. Break-even curves for electricity and H_2 production, NG price $4.42 (2018 dollars)

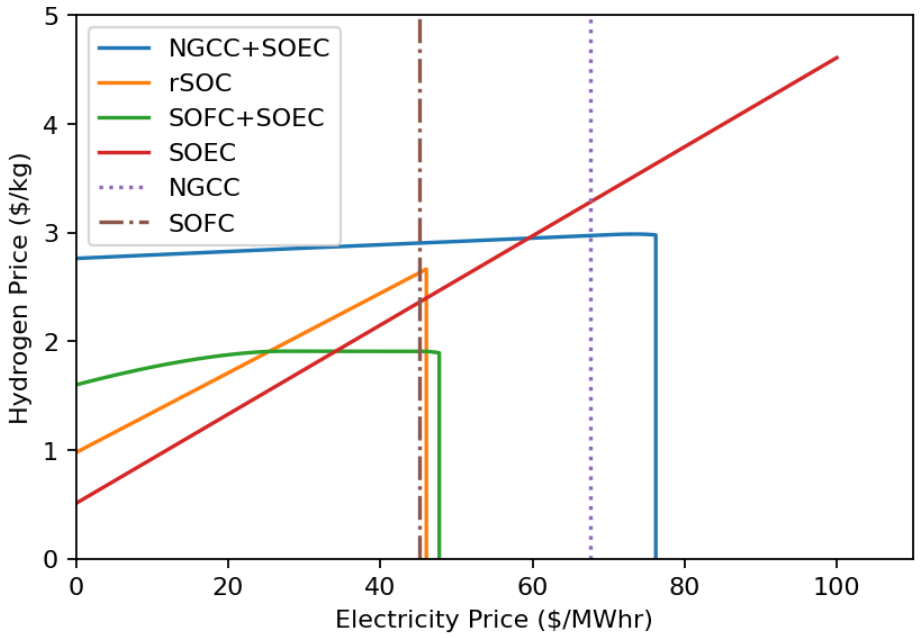

Regarding the integrated systems, there are different price points where the rSOC or SOFC+SOEC are the most favorable, due to the rSOC using mostly purchased electricity from the grid and the SOFC+SOEC mostly generating its own electricity. For example, the rSOC system is preferred over the SOFC+SOEC system below $25/MWh and above $45/MWh. Between those ranges, the SOFC+SOEC process is the preferred system due to its ability to generate its own electricity for H_2 production. The NGCC+SOEC is the least favorable of the IES processes.

This analysis suggests that the value proposition for the SOFC/SOEC IES concepts centers on future electricity prices being bimodal (e.g., distinct periods of low and high electricity prices), a reasonable possibility in future high variable renewable energy grids. If electricity prices are anticipated to be consistently low, the standalone SOEC process (or even reforming-based processes) will outperform the integrated systems. If electricity prices are anticipated to be very high, the standalone SOFC process will outperform the integrated systems as it is the cheapest means to generate electricity. However, if electricity prices are expected to fluctuate frequently between low and high values, then the rSOC process may confer a distinct advantage over the standalone systems by enabling a higher overall capacity factor. Furthermore, although the SOFC+SOEC process is higher cost than the rSOC process under most electricity-H_2 price pairings, it has a major advantage over the rSOC in that it can insulate itself from high electricity prices by producing its own electricity. This can be quite useful if minimum H_2 demands are placed on the system and turning down at high electricity prices is not possible.

A life cycle analysis was carried out for the technology options in both power and H_2 generation modes. Emissions considered across all modes include emissions associated with the import of NG and electricity, and the direct emissions from the plant. In the case of the power production technologies, the emissions of each technology are evaluated at the base case net power production (650 MW_e), while for the H_2 production technologies the emissions are evaluated at

the base case H_2 production (5 kg/s H_2). The following observations can be made for the power production technology results shown in Exhibit ES-6.

- The technology with the highest global warming potential (GWP) (as anticipated) is the NGCC without capture, which has emissions of ~436 kg carbon dioxide equivalents (CO_2e)/MWh-net, while the technology with the lowest GWP is the SOFC with capture, which has emissions of ~86 kgCO_2e/MWh-net. The rSOC operating in the power production mode degenerates to the SOFC case with identical emissions.
- The SOFC+SOEC technology has the second lowest emissions (kgCO_2e/MWh-net) after the SOFC with capture. This is because even when the SOFC+SOEC produces the maximum power possible, the SOEC is not completely shutdown. A minimum amount of H_2 (0.5 kg/s) is still produced, so extra power and thus extra NG (and its associated emissions) is needed in comparison to the SOFC.

Exhibit ES-6. CO_2e life cycle emissions for technologies in power production mode

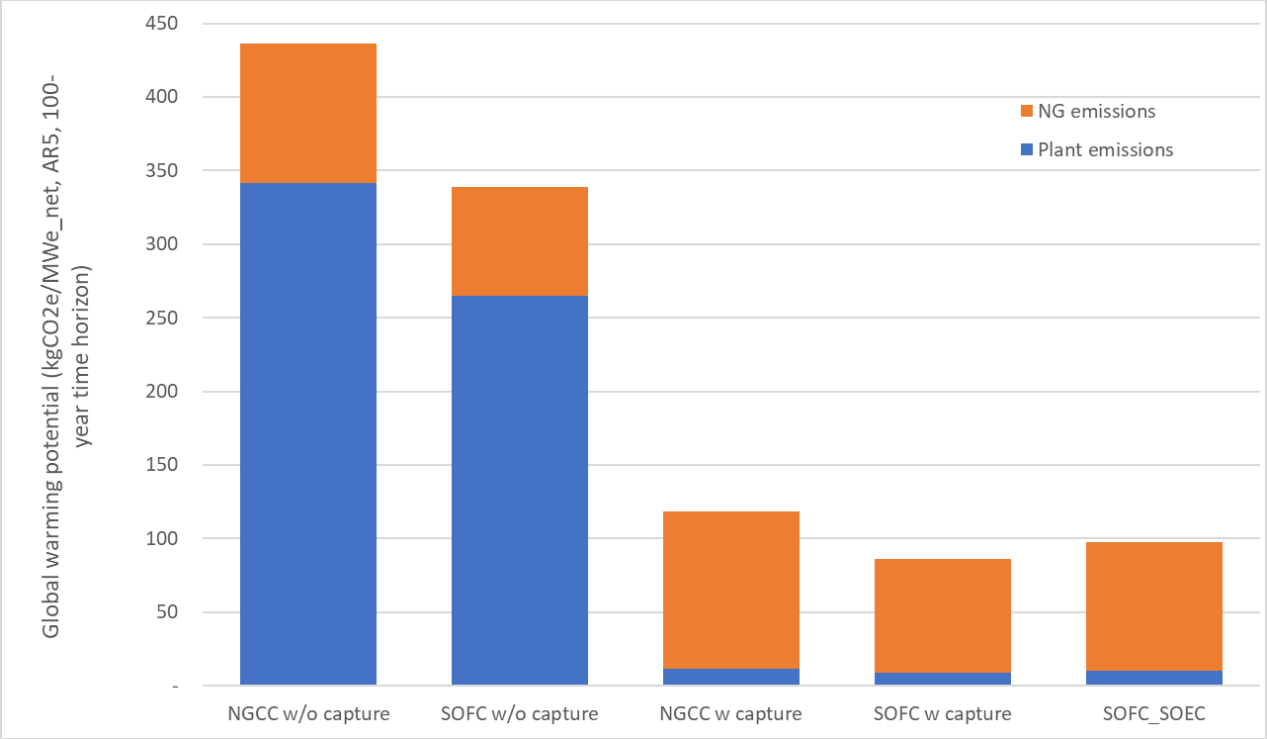

Two scenarios are evaluated for the H_2 production technologies. In the first scenario, electricity import is assumed to have emissions equivalent to a grid with 2019 U.S. average generation mix, while for the second scenario electricity import is assumed to have emissions equivalent to a solar photovoltaic (PV)-based grid. These scenarios allow the impact of different electricity grids on the GWP of each technology to be evaluated.

Two separate scenarios are evaluated for the SOFC+SOEC technology. In the first scenario, the SOFC is run at minimum load and the electricity is imported from the grid to run the SOEC. In the second scenario, there is no electricity import nor export and the SOFC is run to provide only the amount of electricity needed to run the SOEC and balance of plant equipment.

- The following observations can be made for the H_2 production technology results shown in Exhibit ES-7. The type of grid has a major impact on which technology has the highest and lowest emissions. For example, when a U.S. average grid is considered, the standalone SOEC has the highest emissions of ~17 $kgCO_2e/kgH_2$, while for the solar PV grid it has the lowest emissions of ~2 $kgCO_2e/kgH_2$.
- The rSOC has a similar emissions profile to the standalone SOEC but with slightly less extremes. When the U.S. average grid is considered, the rSOC has the second highest emissions of ~16.2 $kgCO_2e/kgH_2$, while for the solar PV grid it has the second lowest emissions of ~2.7 $kgCO_2e/kgH_2$. For the U.S. average grid scenario, the grid electricity emissions constitute 94 percent of the rSOC emissions, while it accounts for 64 percent of the emissions of the corresponding case for the solar PV scenario albeit at a significantly lower value.
- The SOFC+SOEC with zero power import has the third lowest emission profile among the technologies considered for both the U.S. average grid and the solar PV grid (both have emissions of ~3.6 $kgCO_2e/H_2$), as no electricity import emissions are associated with it. However, the SOFC+SOEC with maximum electricity import has the second highest emissions (~14.4 $kgCO_2e/kgH_2$) for the U.S. average grid scenario because of the large amount of electricity import (~506 MW_e) needed.
- When the current U.S. average grid is considered, steam methane reforming (SMR) without carbon capture has lower emissions than several of the assessed technologies such as the standalone SOEC, the rSOC and the SOFC+SOEC with maximum electricity import, which all consume a large amount of electricity for water electrolysis. This highlights the need for these technologies to use low carbon electricity to play an attractive role in decarbonization.

Exhibit ES-7. CO_2e life cycle emissions for technologies in H_2 production mode

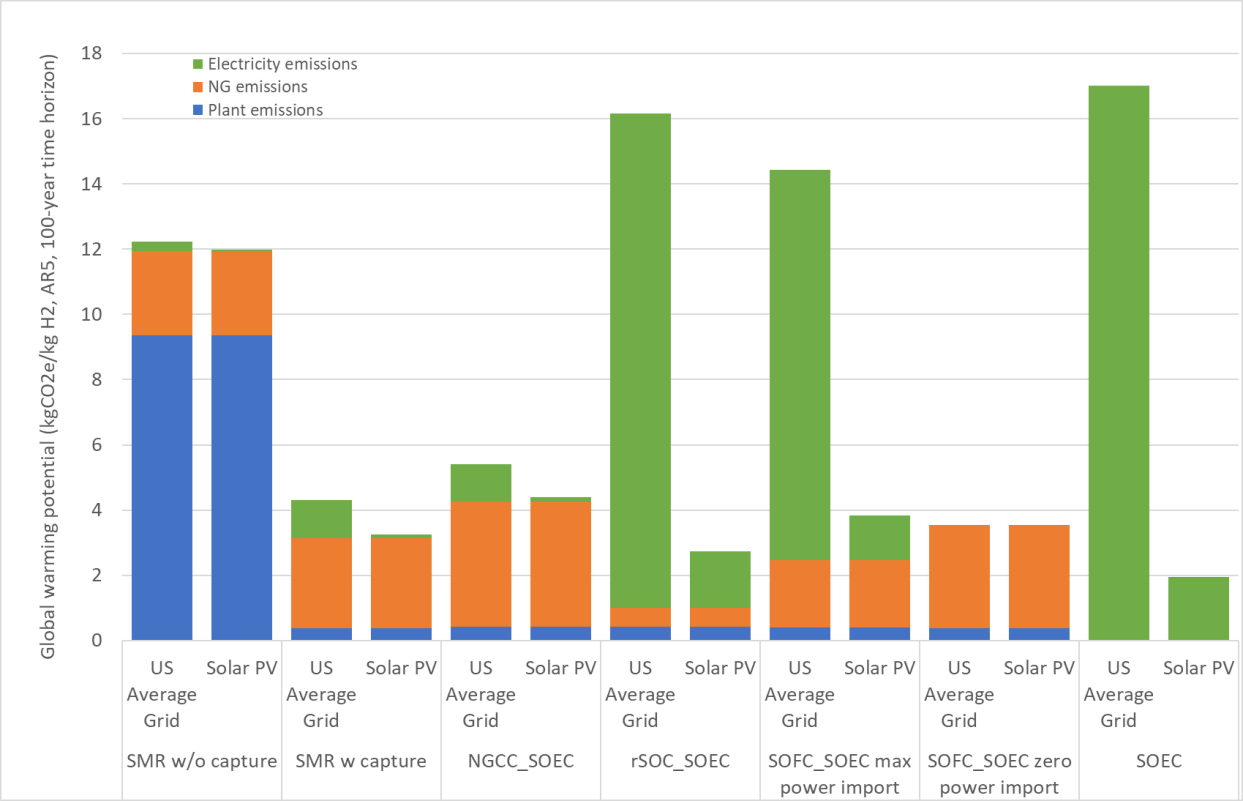

When considering IES technology options and looking at the CO_2 emissions results from both the power production and H_2 production modes, it can be observed that the rSOC technology is promising across both modes only when electricity imports from a renewable-based grid (such as a solar PV) is an option. However, the SOFC+SOEC technology is promising across both power and H_2 production modes when H_2 production is carried out without electricity import from the grid (SOFC+SOEC zero-power import case).

CONCLUSIONS

The results clearly show that in almost all scenarios SOFC-based systems are expected to be less costly to build and operate than NGCC-based systems having both lower expected capital costs and higher efficiency.

Depending on the grid power generation makeup, the expected price of electricity and gas can vary widely, so when considering the choice between rSOC and SOFC+SOEC for H_2 producing IES, market conditions will be an important consideration. Market analysis of these systems will be provided in a follow-up publication to this work.

1 INTRODUCTION

Fossil energy systems with carbon capture, such as such as natural gas combined cycle (NGCC) plants equipped with carbon capture and storage (CCS) and energy storage technologies are expected to play an important role in maintaining electric grid reliability in the transition to a decarbonized energy sector. As the world moves toward an environmentally sustainable economy, hydrogen (H_2) is expected to play a key role in decarbonization. Accordingly, the United States (U.S.) Department of Energy (DOE) aims to reduce levelized costs of low-carbon power and H_2 to aid in the decarbonization of the energy sector by 2030 and the broader economy by 2050.

Integrated energy systems (IES) capable of co-producing power and H_2 provide a promising means for lowering overall production costs of both electricity and H_2 while enhancing flexibility to work effectively in tandem with intermittent renewable technologies. In comparison to standalone systems for power and H_2 generation, IES can enable significant savings in capital and maintenance costs due to the sharing the same equipment, such as the carbon capture and compression system, as well as savings through lower variable costs through process and heat integration. Additionally, IES with the flexibility to produce H_2 from electricity when electricity prices are low would be expected to operate at a higher capacity factor than a conventional power plant that would be forced to turn down under these conditions. In general, the power generating system also benefits from operating near design conditions most of the time, limiting adverse cycling-related effects on plant life.

This report evaluates the cost and performance of several types of IES based on solid oxide fuel cells (SOFCs) to generate power and solid oxide electrolysis cell (SOECs) to produce H_2. NGCC systems are currently widely deployed, so they are included as a baseline for comparison. All cases feature carbon capture at rates exceeding 97 percent. The NGCC-based systems use a solvent-based post combustion capture system, while the SOFC-based systems employ a cryogenic distillation process. A total of seven cases were investigated as summarized in Exhibit 1-1.

While NGCC is a mature technology, SOFC systems are currently in a demonstration phase, where kW-MW class systems are being commercialized, corresponding to a technology readiness level (TRL) of 6. The SOEC systems are at a TRL of 4–6, with incipient but growing demonstrations at a small scale. The SOFC and SOEC costs and performance in the present analysis are based on nth-of-a-kind systems and include research and development and learning associated with mass-scale commercial deployment of the technology over the next decade required for commercial utility-scale systems, consistent with the technology developmental timeline projected by DOE.

Exhibit 1-1. Case summary

Case	Description	Power Capacity ($MW_{e,net}$)	H_2 Capacity (kg/s)
0	NGCC	650	-
1	SOFC	650	-
2	SOFC+CAES (CAES off)	650	-
	SOFC+CAES Charging	397	-
	SOFC+CAES Discharging	798	-
3	NGCC+SOEC	650	5
4	rSOC	650	5
5	SOFC+SOEC	712	5
6	SOEC	-	5

The power capacities were chosen to be 650 $MW_{e,net}$ to be consistent with previous National Energy Technology Laboratory (NETL) baseline reports, except the SOFC+SOEC system where the 712 MW capacity was chosen to cover the heat and power requirement when producing H_2 at full capacity. The 5 kg/s H_2 capacity was chosen because it uses roughly 650 MW_e. Since current density is generally higher in SOEC systems than SOFC systems, the SOEC stack required to generate 5 kg/s H_2 is roughly one-third the size of an SOFC stack required to generate 650 MW_e. The reversible solid oxide cell (rSOC) balance of plant (BOP) sizing is done to be consistent with other cases generating 5 kg/s H_2. There is a tradeoff in the rSOC capacities, where a smaller H_2 generation capacity reduces the cost of electricity but increases the cost of H_2. The most optimal rSOC capacities can only be decided in the context of market analysis where the time spent operating in electricity production mode and in H_2 mode is known.

1.1 Case 0: NGCC with Carbon Capture

Case 0, an NGCC plant with 97 percent carbon capture, is provided as a baseline for comparison. The NGCC is based heavily on the NETL fossil energy baseline report (FEB), Case B31B [1], albeit with a higher capture rate.

1.2 Case 1: SOFC

Case 1 consists of a natural gas (NG)-fed SOFC plant with a steam turbine bottoming cycle. This standalone SOFC case serves as a reference case for integrated systems featuring H_2 production. SOFC technology is assumed to be sufficiently advanced to where NG can be fully reformed within the stack without the need for external reforming equipment. The model is based on the NETL natural gas fuel cell (NGFC) report, Case ANGFC3B [2].

1.3 Case 2: SOFC with CAES

In Case 2, a compressed air energy storage (CAES) system is integrated with the SOFC system in Case 1. Heat and power from the SOFC plant are used for the operation of the CAES system. During periods of low electricity prices, power produced by the SOFC is used to compress and

store air in an underground cavern. This compressed air is heated and expanded in an air turbine to produce additional electricity when the electricity prices are higher.

1.4 CASE 3: NGCC WITH CARBON CAPTURE AND SOEC

Case 3 integrates an SOEC system with the NGCC from Case 0. The SOEC uses both electricity and steam from the NGCC to produce H_2. Depending on the electricity and H_2 prices, the system can operate at an optimal combination of power generation and H_2 production to maximize revenue. Producing H_2 allows the NGCC to operate at outputs closer to maximum efficiency at or near full load most of the time. At some combination of NG and electricity prices, selling electricity may not be profitable, but H_2 can be produced at low cost if gas prices are low.

1.5 CASE 4: REVERSIBLE SOC

Case 4 is a rSOC, which can be operated in either fuel cell (SOFC) or in an electrolysis (SOEC) mode. The primary advantage of the rSOC is that for a modest increase in capital cost over the SOFC system, the process can be operated in either power-generation or H_2-generation mode depending on market prices for electricity and H_2. However, frequent switching between power and H_2 production modes may reduce the lifetime of the equipment, and the additional capital cost relative to Case 1 may not be justified if H_2 production is expected to be relatively low (e.g., if high electricity prices are expected).

1.6 CASE 5: SOFC WITH SOEC

Case 5 comprises SOFC modules paired with SOEC modules, which allows for simultaneous electricity and H_2 production. The IES may be beneficial depending on electricity and H_2 prices and demands. The capital costs of this system will be greater than the rSOC case. The overall economics of the system may be attractive if the SOFC can produce electricity more cheaply than it can be purchased from the grid. Unlike Case 4, this system does not suffer from the adverse effects of cycling between SOFC and SOEC modes.

2 METHODOLOGY

Detailed first-principles flowsheet models capable of off-design performance and cost prediction were constructed for each process concept using the open-source, Institute for the Design of Advanced Energy Systems (IDAES) Integrated Platform [3]. This section discusses the design basis, flowsheet components, and cost assumptions shared between case studies.

2.1 DESIGN BASIS AND COMPONENTS

This section describes the design parameters and process models that form a common basis for comparison between cases. Where possible, models are shared between cases to enhance maintainability and consistency.

2.1.1 Design Basis

The FEB is the primary literature source for fuel, air, and location parameters [1]. The NGCC with carbon capture, Case B31B, was used as a baseline for economic comparison. As such, the NGCC design parameters were used to the extent possible in each case.

2.1.1.1 Power Generation

Each concept was designed to generate 650 to 712 $MW_{e,net}$ including carbon capture, but without H_2 production. Capital cost for smaller systems can be obtained by scaling appropriately. The costing methodology is outlined in Section 2.2.

2.1.1.2 Hydrogen Production

The baseline H_2 capacity is 5 kg/s, which is approximately the flow that can be produced by SOEC technology using 650 MW_e. The specification for delivering H_2 is 6.479 MPa with less than 10 ppm water (H_2O) [4].

2.1.1.3 Ambient Air/Location

Plant location and air specifications are taken from the FEB [1]. The plant is assumed to be built in the Midwestern United States. Air is assumed to be 101 kPa, 15 °C (288.15 K), with a relative humidity of 60 percent. The air composition is shown in Exhibit 2-1.

Exhibit 2-1. Air composition

Component	Mass Fraction (%)	Mole Fraction (%)
N_2	75.055	77.320
O_2	22.998	20.74
Ar	1.280	0.92
H_2O	0.616	0.99
CO_2	0.050	0.03

Based on the ambient conditions above, the cooling water temperature is assumed to be 15.6 °C (288.75 K).

2.1.1.4 Fuel

Exhibit 2-2 shows the NG composition. The higher heating value (HHV) is 52,295 kJ/kg, and the lower heating value (LHV) is 47,201 kJ/kg. Based on the HHV, the baseline NG cost is $4.42 per million (MM)Btu [1].

Exhibit 2-2. NG composition

Component	Volume Fraction (%)
CH_4	93.1
C_2H_6	3.2
C_3H_8	0.7
C_4H_{10}	0.4
CO_2	1.0
N_2	1.6

2.1.1.5 Water

H_2O cost is assumed to be $1.90 per 1,000 gallons, and H_2O treatment chemicals are assumed to cost $1.64 per 1,000 gallons treated.

2.1.1.6 Emissions Targets

All IES studied in this report are designed to capture at least 97 percent of the carbon dioxide (CO_2) produced.

2.1.2 Air Separation Unit

A conventional cryogenic air separation unit (ASU) generates oxidant for oxy-combustion in the SOFC, rSOC, and SOFC+SOEC cases. Specifications and performance of the ASU were taken from the NGFC Pathways study [5]. The ASU generates 99.5 percent pure oxygen (O_2) at an outlet pressure and temperature of 0.16 MPa and 26.7°C, respectively. The nitrogen (N_2) product is unused and vented.

The ASU model is a hybrid model that uses a simplified representation of the ASU where models calculate mass and energy balances, and constant energy requirements per O_2 generated for parasitic electricity and heat requirements. The electricity requirement of the ASU was assumed to be 202 kW_eh/tonne O_2. The regenerative steam required is 93.43 $kW_{th}h$/tonne O_2. Regenerative steam is supplied by the heat recovery steam generator (HRSG).

The models used for the mass and energy balances consist of a two-stage main air compressor with intercooling and aftercooling, a separator, and a heater. The main air compressor discharge pressure was set to 0.5 MPa, with intercooling and aftercooling temperature set to 37.8°C. The cooling duty of the intercoolers was directly used in the sizing and costing of the cooling water system. The separator splits the incoming stream by component to achieve the 99.5 percent pure O_2 product.

2.1.3 Carbon Purification Unit

A carbon purification unit (CPU) generates a pipeline-ready, high-purity CO_2 stream from flue gas in the SOFC, rSOC, and SOFC+SOEC cases. The flue gas in these cases is primarily composed of CO_2 and H_2O allowing for an auto-refrigerated distillation process that is less costly than the solvent-based capture system used by the NGCC and NGCC+SOEC. The CPU results in a carbon capture rate of 98 percent while achieving a CO_2 purity of 99.99 percent to meet O_2 concentration requirement of 10 ppm or less [6] for CO_2 transportation and for use in enhanced oil recovery.

Exhibit 2-3 depicts the block flow diagram of the CPU process based on NETL's advanced oxy-combustion study [7]. Moisture is removed from the wet CO_2-rich flue gas in the intercoolers of a multi-stage CO_2 compressor followed by a drier. The dried CO_2-rich gas is cooled and liquified before undergoing a flash phase separation and distillation to achieve the desired purity. The refrigeration needs of the process are achieved entirely through the expansion of a portion of the pure CO_2 product.

Exhibit 2-3. Auto-refrigerated CPU process serving as the basis for the CPU surrogate model

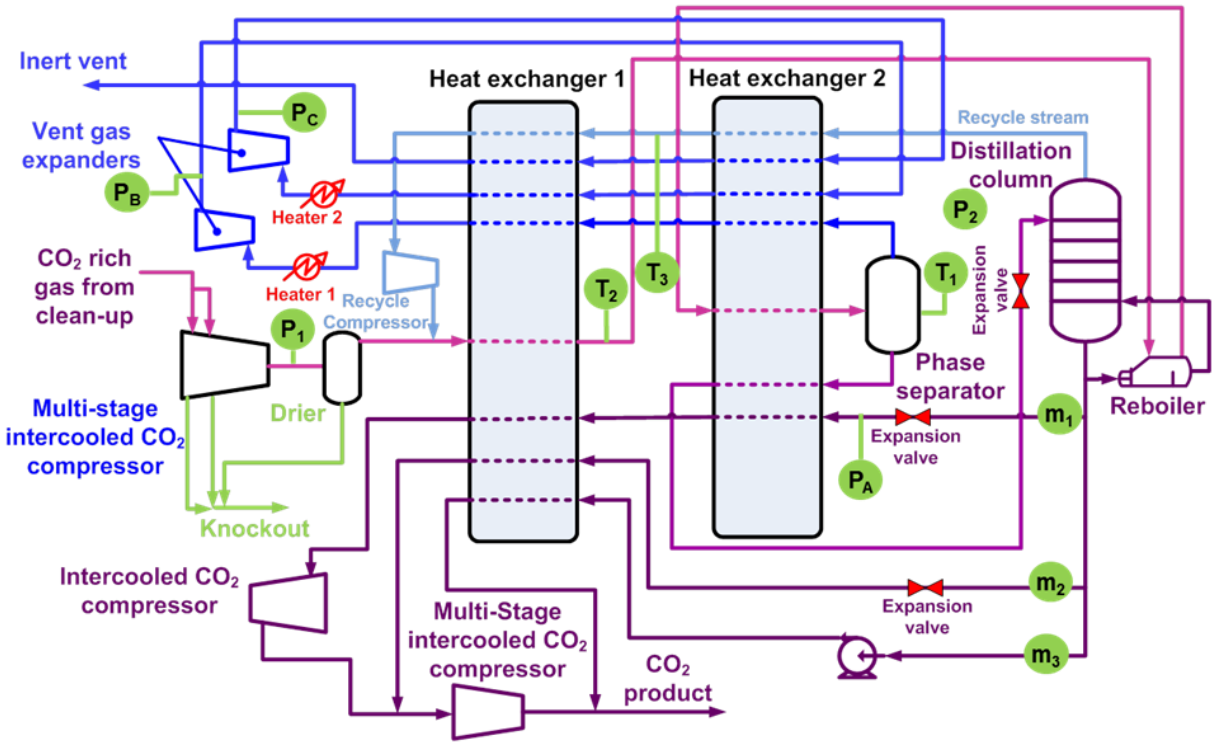

A surrogate black-box model was developed in IDAES using the Aspen Plus® (Aspen) model developed by NETL [5]. The inputs to the CPU surrogate model are the flue gas flow rate and composition (mole fractions of argon [Ar], CO_2, H_2O, N_2, and O_2). Exhibit 2-4 details the input variable bounds over which the surrogates were trained and can be expected to be accurate. The temperature and pressure of the flue gas to the CPU are assumed to be 37.8°C and 0.101 MPa, respectively. The case models include a flash unit operation prior to the CPU to ensure the proper inlet conditions. The CPU model then uses surrogate equations and mass balances to

compute the electric load and cooling duty of the CO_2 compressors and the states (flow, temperature, pressure, and composition) of the three outlet streams (pure CO_2, non-condensable vent gases, and H_2O knockout).

Exhibit 2-4. CPU surrogate input variables and bounds

Input Variable	Lower Bound	Upper Bound
Flue Gas Flowrate (mol/s)	350	1600
Flue Gas Ar Mole Fraction	0.0004	0.005
Flue Gas CO_2 Mole Fraction	0.8255	0.9211
Flue Gas H_2O Mole Fraction	0.0625	0.0675
Flue Gas N_2 Mole Fraction	0.014	0.016
Flue Gas O_2 Mole Fraction	0.00242	0.0856

2.1.4 Steam Cycle

The NGCC steam cycle uses the steam turbine model described by Liese [8] and a HRSG model based on the FEB [1]. The details of this model are provided in Section 3.

The SOFC-based flowsheets do not include a detailed steam cycle model as the steam cycle provides a relatively small proportion of the gross generation (around 10 percent versus 30 percent in the NGCC case). Instead, a nominal efficiency of 38.1 percent is assumed.

2.1.5 SOFC Model

The SOFC model represents the expected operating conditions and performance capabilities of current anode supported planar fuel cell technology operated at atmospheric pressure. The modeled cell performance provides 0.8 V at 400 mA/cm^2 operating at a temperature of 750 °C for a wet H_2 fuel (97 percent H_2, 3 percent H_2O) with 75 percent fuel utilization and 12.5 percent air utilization.

The SOFC performance is simulated using a surrogate model trained on data collected from the Pacific Northwest National Laboratory's SOFC-multi-physics (SOFC-MP) software. The underlying 1D channel cell model represents a 550 cm^2 active area anode-supported cell with metal interconnects in a counter-flow configuration. The development of the surrogate model is described in more detail in the NGFC Pathways study [5]. This work uses an updated surrogate model with a deep neural network (DNN) architecture. It is more accurate and contains fewer parameters than the Kriging interpolation used in the NGFC Pathways study. No changes were made to the underlying SOFC-MP simulation for this work.

The SOFC is represented as a combination of unit operations and the surrogate model that calculates the cell voltage and anode outlet temperature. Exhibit 2-5 shows the connectivity of the unit operations responsible for modeling mass and energy balances of the SOFC. On the cathode side, pure O_2 is separated from a stream of air, representing O_2 ions diffusing across the electrolyte. The pure O_2 is mixed with fuel entering the anode and supplied to a Gibbs reactor that calculates the composition of the anode outlet stream by minimizing its Gibbs free energy.

The outlet temperature of the Gibbs reactor is calculated by the surrogate model, imposing a negative heat duty (cooling duty) on the Gibbs reactor. The negative heat duty represents the power available for performing electric work and heating the cathode air stream. The electric power output is calculated by multiplying the current and the cell voltage. Electric current is directly proportional to the number of O_2 ions moving across the electrolyte and cell voltage is calculated by the surrogate model. The cathode heat duty must close the energy balance around the SOFC, determining the cathode outlet temperature.

Exhibit 2-5. SOFC model unit operations

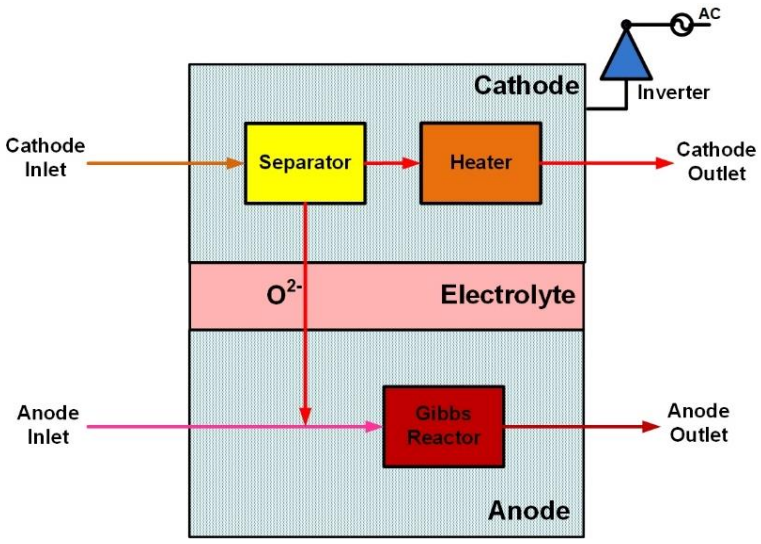

The surrogate model outputs also include the change in cell temperature and maximum cell temperature to serve as constraints preventing operation in regimes that would cause excess cell degradation. The change in cell temperature is constrained to be 100–750°C.

The performance of an SOFC is characterized by its operating current density and the states of its cathode and anode inlet streams. These are essentially the inputs to the SOFC surrogate model, but the stream states are represented through flowsheet-level variables such as recirculation fractions and overall fuel utilization. When the data for the surrogate model was being computed, these flowsheet level inputs were used to calculate the states of the SOFC inlet streams in the SOFC-MP simulation. Exhibit 2-6 depicts a block flow diagram of the SOFC power island and Exhibit 2-7 lists and describes the surrogate model input variables. The numbers on the block flow diagram correspond to the number in the table and show the streams where the input variables are calculated. Two occurrences of the same number indicate that information from two streams is needed to calculate that input variable.

Exhibit 2-6. SOFC power island block flow diagram

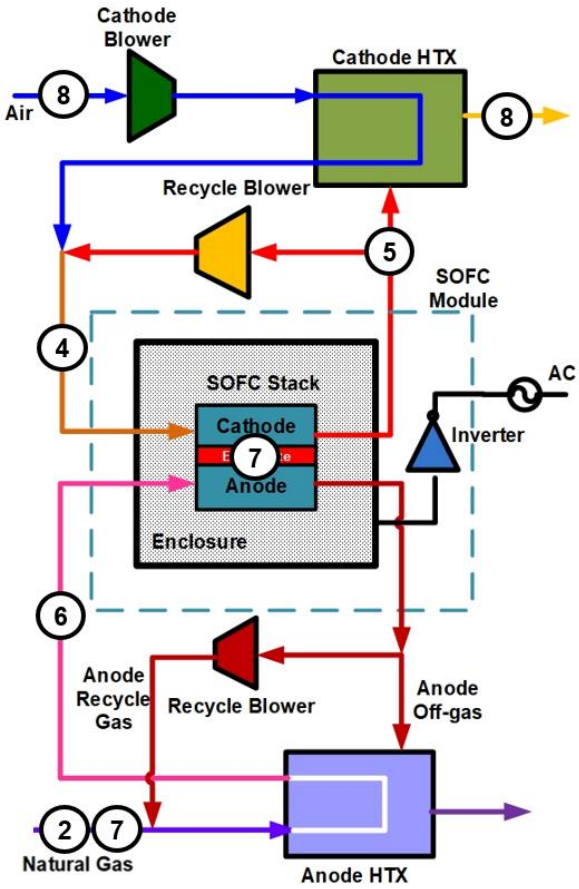

Exhibit 2-7. SOFC surrogate model input variables

No.	Input Variable	Lower Bound	Upper Bound	Description & Comments
1	Current Density	1500 A/m^2	6000 A/m^2	The current (O_2 ions) per unit area across the SOFC electrolyte In this study, current density is fixed to 4000 A/m^2 at full load; during partial load analysis it is decreased in proportion with the NG flowrate to maintain a constant SOFC area
2	Fuel Inlet Temperature	15 °C	600 °C	The temperature of the fuel entering the anode side of the SOFC power island determined by the NG temperature, which is fixed at 15 °C
3	Internal Reformation Percentage	0%	100%	The percentage of NG that is not externally reformed in an autothermal reformer. In this study, it is assumed that no external reforming is required, thus, the value is fixed to 100%
4	Air Inlet Temperature	550 °C	800 °C	Temperature of the air entering the cathode side of the SOFC stack
5	Air Recirculation	0%	80%	The percentage of the cathode exhaust recirculated to the cathode inlet

No.	Input Variable	Lower Bound	Upper Bound	Description & Comments
6	Oxygen to Carbon Ratio	1.5	3	The ratio of O_2 atoms to carbon atoms in the fuel entering the anode side of the SOFC stack. In this study, it is fixed to 2.1
7	Fuel Utilization	0.4	0.95	The ratio of the flowrate of O_2 across the electrolyte to the flowrate of O_2 needed to fully react the NG entering the SOFC power island. In this study, it is fixed to 0.85
8	Air Utilization	0.125	0.833	The ratio of O_2 in the air leaving the cathode side of the SOFC power island to O_2 in the air entering

2.1.6 SOEC Model

For the SOEC, a two-dimensional first-principles model of a planar rSOC is used. To avoid conflicting terminology between SOFC and SOEC modes, the electrodes are designated the "fuel electrode," where H_2 fuel is consumed or generated, and the "oxygen electrode," where O_2 is consumed or generated. See Exhibit 2-8 for a sketch of the SOFC structure, but note that the figure is not to scale, with several layers being only micrometers thick.

Exhibit 2-8. Structure of SOEC model

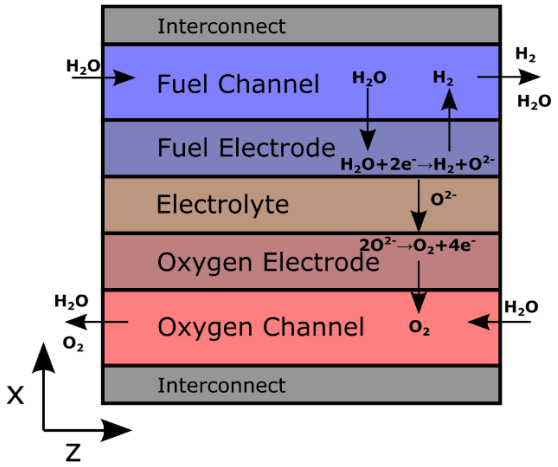

An electrolytic cell model's performance is characterized by its voltage-current (V-I) curve. The present SOEC model was calibrated using V-I curves[a] from a bench-scale planar fuel-electrode-supported short stack (two-cell deep) [9]. The fuel electrode is nickel (Ni)-yttria-stabilized zirconia (YSZ), the electrolyte is 8YSZ, and the O_2 electrode is lanthanum strontium cobalt ferrite.

In general, the SOEC potential is given by

[a] The V-I curves represent performance from a new stack. Stack degradation is over the life of the system is considered through an annual stack replacement cost.

$$E_{cell} = E_{Nernst} - (\eta_{Ohm} + \eta_{act,fuel} + \eta_{act,O_2})$$

where E_{cell} is the cell's potential, E_{Nernst} is the Nernst potential, η_{Ohm} is Ohmic polarization, and $\eta_{act,fuel}$ and η_{act,O_2} are activation polarization at the fuel and O_2 electrodes, respectively. Based on the electrolysis of H_2O represented by

$$H_2O \rightleftharpoons H_2 + \frac{1}{2}O$$

the Nernst potential is estimated as [10]:

$$E_{Nernst} = -\frac{\Delta G^0_{rxn}(T, P_{ref})}{2F} + \frac{RT}{2F}\ln\left(\frac{\left(\frac{P_{H_2}}{P_{ref}}\right)\left(\frac{P_{O_2}}{P_{ref}}\right)^{0.5}}{\frac{P_{H_2O}}{P_{ref}}}\right)$$

where ΔG^0_{rxn} is the standard Gibbs energy of reaction, F is the Faraday constant, R is the universal gas constant, T the electrode temperature, P_k the partial pressure of species k, and P_{ref} the reference pressure at which the standard Gibbs energy is computed.

Ohmic polarization is a function of the area-specific resistance of the different layers and the current density. For a planar cell with current paths generally along the normal to the cell layers,[b] the ohmic polarization can be calculated as

$$\eta_{Ohm} = \left(\rho_{int}\ell_{int} + \frac{\rho_{fuel}\ell_{fuel}}{1-\phi_{fuel}} + \rho_{el}\ell_{el} + \frac{\rho_{O_2}\ell_{O_2}}{1-\phi_{O_2}} + Я\right) i$$

where ρ_k and ℓ_k denote the resistivity and thickness of layer k, for the interconnect, fuel electrode, electrolyte, and O_2 electrode layers, ϕ_k is the void fraction of electrode k, $Я$ denotes the total contact resistance (cell to cell as well as current collectors to electrodes), and i denotes the current density.

Ohmic resistance from the metal interconnect was neglected because it is much more conductive than the electrodes and the electrolyte. The contact resistance $Я$ was also set to zero and all unaccounted Ohmic resistance was taken to come from the electrolyte. Neglecting the interconnect and contact resistance, the ohmic polarization can be calculated as

$$\eta_{Ohm} = \left(\frac{\rho_{fuel}\ell_{fuel}}{1-\phi_{fuel}} + \rho_{el}\ell_{el} + \frac{\rho_{O_2}\ell_{O_2}}{1-\phi_{O_2}}\right) i$$

Layer resistivity is strongly temperature dependent, often being modeled using the expression

$$\rho_k = \gamma_k \exp\left(\frac{C_k}{T}\right)$$

where the preexponential factor γ_k and the exponent C_k are both material specific.

Activation polarization at the electrodes is characterized by the Butler-Volmer equation [11]:

[b] The electrolyte usually offers a significantly high ohmic resistance relative to the cell electrodes, which tends to make the current density vectors line up along the cell (layer) planes.

$$i = i_{0,k}\left(\exp\left(\frac{\alpha_{1,k}F\eta_{act,k}}{RT}\right) - \exp\left(\frac{-\alpha_{2,k}F\eta_{act,k}}{RT}\right)\right)$$

where $\alpha_{1,k}$ and $\alpha_{2,k}$ are constants that depend on the charge transfer kinetics and $i_{0,k}$ is the exchange current density of electrode k. For the fuel electrode, the exchange current density is given by [10] [12]:

$$i_{0,fuel} = \kappa_{fuel} y_{H_2O}^{m} y_{H_2}^{n} \exp\left(-\frac{E_{act,fuel}}{RT}\right)$$

where y_j is the mole fraction of species j and the preexponential factor κ_{fuel}, the activation energy $E_{act,fuel}$, and the kinetic exponents m and n are all kinetic parameters. For the O_2 electrode, the exchange current density is given by [10] [12]:

$$i_{0,O_2} = \kappa_{O_2} y_{O_2}^{p} \exp\left(-\frac{E_{act.O_2}}{RT}\right)$$

where κ_{O_2}, E_{act,O_2}, and p are all also kinetic parameters.

Most of the parameters vary significantly with how the material and cell were prepared. Even the two cells in the short stack in Fang, Blum, and Menzler have noticeably different V-I curves [9]. As a result, most of these parameters were estimated using the values generally used in literature as shown in Exhibit 2-9.

Exhibit 2-9. SOEC parameters fixed at literature values

Parameter	Value	Source	Notes
ℓ_{fuel}	1000 µm	[9]	
γ_{fuel}	$2.5 \cdot 10^{-5}$ Ωm	[13]	material: Ni/YSZ, 35 vol% Ni, 1000°C
C_{fuel}	0 K		relatively insignificant
ϕ_{fuel}	0.326	[14]	
ℓ_{O_2}	40 µm	[9]	
γ_{O_2}	$7.8125 \cdot 10^{-5}$ Ωm	[15]	material LSM
C_{O_2}	0 K		relatively insignificant
ϕ_{O_2}	0.30717	[14]	
ℓ_{el}	10.5 µm	[9]	

Even with the reduced parameter space, there are 13 parameters to estimate (show in Exhibit 2-10). The experimental dataset was not rich enough to estimate all these parameters simultaneously, so constraints were added such that

$$\alpha_{1,k} + \alpha_{2,k} = 1$$

for both the fuel and O_2 electrode, which holds if the rate-limiting charge transfer reaction at the electrode is a one-step, single electron process [11]. The kinetic exponents m, n, and p were fixed at values in a ratio corresponding to the stoichiometric coefficients of their respective species. The final parameter estimation problem then had 8 remaining degrees of freedom.

Exhibit 2-10. SOEC parameters fitted from experimental V-I curves

Parameter	Value	Parameter	Value
γ_{el}	1.234e-4 Ωm	C_{el}	8988 K
κ_{fuel}	5.911e9 A/m^2	κ_{O_2}	1.187e11 A/m^2
$E_{act,fuel}$	110.8 kJ	E_{act,O_2}	112.1 kJ
$\alpha_{1,fuel}$	0.648	α_{1,O_2}	0.503
$\alpha_{2,fuel}$	0.352	α_{2,O_2}	0.497
m	0.5	p	0.25
n	0.5		

Data for both fuel-cell and electrolysis mode from Fang, Blum, and Menzler [9] was extracted using WebPlotDigitizer [16] and fitted using PARMEST [17]. Note that the SOEC model developed here is reversible and can model the fuel-cell mode, but only for pure H_2 fuel, i.e., not containing NG or carbon monoxide. In the experimental data, slightly different voltage values are reported for both individual cells in the stack at the same current density, so the average value was used for fitting. To consider the experimental stack thermal conditions, the temperature of the edge of the O_2 channel opposite the electrode was set to a uniform temperature; the temperature of the fuel channel opposite the fuel electrode was set equal to the temperature measured by the experimental thermocouple between both cells in the stack.

Both traditional sum-of-squares objectives and smooth L1 costs were posed, starting at a variety of initial conditions with different weighting of experimental data and deviation of parameters from their initial values. Plots were assessed visually to find which set of parameters fit the data best for relevant operating conditions. The final values are given in Exhibit 2-10, and compared to experimental data in Exhibit 2-11 and Exhibit 2-12.

Exhibit 2-11. Current-voltage characteristic curve for the modeled SOEC run in fuel-cell mode

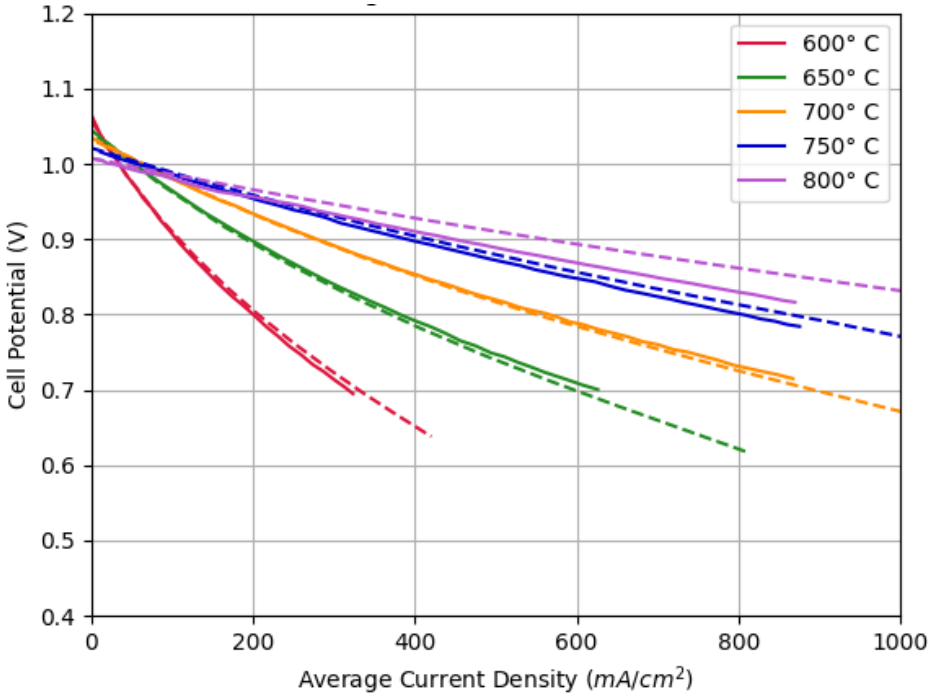

Note: Solid lines denote experimental data; dashed lines denote model predictions

Exhibit 2-12. Current-voltage characteristic curve for the modeled SOEC run in both fuel-cell and electrolysis

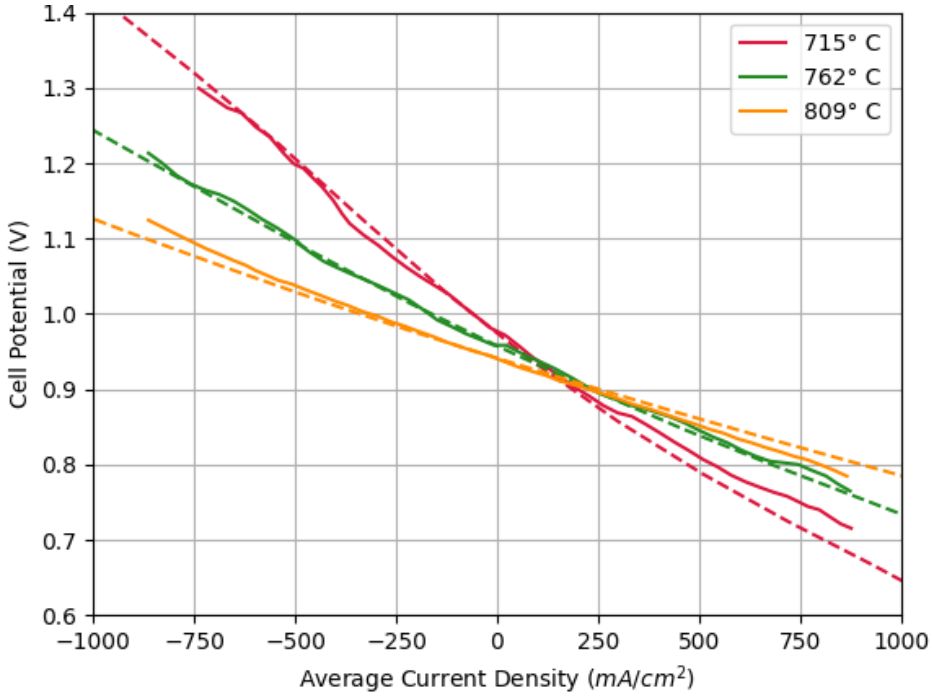

Note: Solid lines denote experimental data; dashed lines denote model predictions

2.1.7 Post-Combustion Capture

A post-combustion solvent-based CO_2 capture system is used for NGCC-based systems [1]. The capture system consists of an absorber where CO_2 is removed from the flue gas by contact with a solvent, and a stripper where CO_2 is removed from the solvent. The stripper requires heating, and this heat is provided to a reboiler by steam extracted from the intermediate pressure (IP)/low pressure (LP) crossover of the NGCC steam turbine. The reboiler steam requirement is most of the load imposed by CO_2 capture on the system.

The carbon capture system for the NGCC is not explicitly modeled, but the steam requirement is estimated based on specific reboiler duty (SRD), which is the steam energy required per mass of CO_2 captured. The SRD depends on the solvent, configuration of the capture system, and the capture fraction. Given a particular capture system and capture fraction, the SRD is nearly constant, and can be used to estimate the amount of steam that needs to be extracted from the NGCC. For 97 percent capture cases, the Piperazine Advanced Stripper (PZAS^{TM}) technology was used with an SRD of 2.4 MJ/kg CO_2 [18].

The power required to compress the CO_2 for post combustion capture is calculated from the FEB to be 0.2748 MJ/kg [1].

2.2 Overview of Costing Framework

This section describes the general methodology for estimating capital and fixed operating and maintenance (O&M) costs and scaling costs to different plant capacities. The variable O&M costs are dominated by fuel, electricity, and H_2O use. Variable costs are largely a result of the process model, so the details of these costs are provided in the sections describing each case.

2.2.1 Capital Costs

This study uses NETL's cost estimation methodology as the basis for determining capital costs [19]. NETL defines five levels of capital cost as follows:

1. Bare Erected Cost (BEC) comprises the cost of process equipment, on-site facilities, and infrastructure that support the plant, and the direct and indirect labor required for its construction and/or installation.
2. Engineering, Procurement, and Construction Cost (EPCC) comprise the BEC plus the cost of services provided by the engineering, procurement, and construction (EPC) contractor. The EPC services include detailed design, contractor permitting, and project/construction management costs.
3. Total Plant Cost (TPC) comprises the EPCC plus project and process contingencies.
4. Total Overnight Cost (TOC) comprises the TPC plus all other "overnight" costs, including inventory capital, financing costs, and other owner's costs.
5. Total As-Spent Cost (TASC) comprises the sum of all capital expenditures as they are incurred during the capital expenditure period for construction including their escalation. TASC also includes interest during construction, comprising interest on debt and a return on equity.

The primary source of capital cost estimates is the FEB [1]. It contains an itemized list of BECs based on vendor quotes for major systems and equipment found in a conventional NGCC plant (e.g., HRSG, cooling water system, cooling tower, and H_2O treatment system).

NETL developed a capital cost scaling methodology to account for differences in equipment sizes across studies in the Quality Guidelines for Energy System Studies (QGESS) report, "Cost Estimation Methodology for NETL Assessments of Power Plant Performance." [19] For each piece of equipment, the QGESS defines a process parameter for scaling the BEC via the following equation.

$$SC = RC\left(\frac{SP}{RP}\right)^{\alpha}$$

The variable names are defined as follows:

- RC is the reference BEC, taken from the FEB.
- RP is the reference process parameter defined in the QGESS. The actual value is taken from the FEB.
- α is the scaling exponent defined in the QGESS for each piece of equipment.
- SP is the scaled process parameter from the IDAES flowsheet.
- SC is the scaled BEC of the equipment in the IDAES flowsheet.

Equipment specific to the SOFC cases that is not included in the FEB was costed using correlations from the NGFC Pathways study [5]. The major systems costed with this method include the ASU, CPU, oxy-combustor, SOFC modules, and SOFC BOP components.

Wherever possible, correlations from the NGFC Pathways study were used to cost equipment in the SOEC flowsheets. For equipment where no correlations were available, the IDAES generic costing framework was used. The framework provides equipment cost estimates for common unit operations based on correlations from Process and Product Design Principles: Synthesis, Analysis, and Evaluation [20]. The installation labor cost was assumed to be 25 percent of the equipment cost, and the sum of the equipment and labor costs was taken to be the BEC.

The steps involved in converting BEC to TASC are summarized in Exhibit 2-13. TPC is equal to the BEC plus engineering fees and project and process contingencies, all of which are calculated as a percentage of the BEC. Each piece of equipment has its own set of percentages that can be found in the FEB report and the NGFC Pathways study. For equipment costed using the generic costing framework, the engineering fee is 20 percent, process contingency is 15 percent, and project contingency is 15 percent.

The TOC is equal to TPC plus owner's costs. In the FEB, the owner's cost calculation is complex with a large portion calculated as a percentage of the TPC and the remainder based on costs of consumables and fuel stockpiles. To simplify calculations in this report, owner's costs were assumed to be 21 percent of the TPC. This assumption has an insignificant effect on the overall conclusions of the report.

The TASC is obtained by multiplying the TOC by a TASC/TOC ratio of 1.093 to account for the impact of both escalation and cost of capital during construction. The ratio is valid for a plant with a three-year construction period and 30-year operating life. Other global economic and financial assumptions used in the calculation of the TASC/TOC ratio can be found in the QGESS [19].

The annualized cost is found by multiplying the TASC by a fixed charge rate (FCR) of 0.0707. It is based on the same assumptions as the TASC factor.

Exhibit 2-13. Capital cost structure

Capital Cost Level	Expression	Units
Total Plant Cost	$TPC = BEC + engineering\ fee + process\ contingency + project\ contingency$	$MM
Total Overnight Cost	$TOC = TPC + Owner's\ cost$	$MM
Total As Spent Cost	$TASC = TOC \times \frac{TASC}{TOC}$	$MM
Annualized Cost	$Annualized\ Cost = FCR \times TASC$	$MM/yr

2.2.2 NGCC

For the NGCC system, the configuration is the same as the FEB [1], aside from increasing the CO_2 capture from 90 to 97 percent. The capital and fixed O&M costs are taken directly from the report, and the capture system cost is adjusted to account for the additional capture and different capture process configuration.

Adjustments for the CO_2 capture system were derived from Du et al. [18], which presents capital costs for capture systems with capture rates of 90–99 percent. Percent increases in capital cost above 90 percent capture were calculated from the report (e.g., the capital cost increases by 7.8 percent from 90 percent capture to 95 capture). The percent increase for 97 percent capture was interpolated using a power law fit and applied to NETL's CO_2 capture system BEC.

Exhibit 2-14. CO_2 capture scaling

CO_2 Capture Percentage	EPRI Capital Cost, $MM	Capital Cost Increase Over 90% Capture	NETL CO_2 Capture Capital Cost with Increase Applied, $MM
90%	307	0%	373
95%	331	7.8%	402
97%	350 (interpolated)	13.9%	425
97.7%	358	16.6%	435

2.2.3 Fixed O&M Costs

Fixed O&M costs are calculated following the method in the FEB. A degradation rate of 0.2 percent/1,000 hr was assumed for both the SOFC and SOEC. The additional degradation rate of 0.2 percent/1,000 hr was also applied to the rSOC case excluding degradation due to mode switching. This assumption is consistent with one of the maturation goals of the rSOC technology, which is focused on minimizing effects of mode switching through research and development. The SOFC replacement cost, as $ per year per kW of SOFC alternating current (AC) power, is calculated based on the methodology presented in the NGFC Pathways report. SOFC replacement cost converted to a per cell basis was used for the SOECs. Exhibit 2-15 lists each component of fixed O&M costs and how it is calculated.

Exhibit 2-15. Fixed O&M costs

Fixed O&M Cost	Expression
Annual operating labor	$n_{operators} \times hourly\ rate \times 8760 \frac{hr}{yr} \times \left(1 + \frac{labor\ burden}{100}\right)$
Maintenance labor	$TPC \times 0.4 \times 0.019$
Maintenance material cost	$TPC \times 0.6 \times 0.019$
Admin & support labor	$0.25 \times (annual\ operating\ labor + maintenance\ labor)$
Property taxes and insurance	$TPC \times 0.02$
SOFC replacement cost	$\frac{\$25.14}{kW \times yr} \times P_{SOFC\_AC}$
SOEC replacement cost	$\frac{\$4.2765}{cell \times yr} \times n_{cells}$

The variables in Exhibit 2-15 are as follows:

- $n_{operators}$ is the number of plant operators. The NGCC, SOFC, and rSOC cases assume 6.3. The SOFC+SOEC case assumes 8.
- $hourly\ rate$ is the rate in $/hr paid to the operators. All cases assume $38.50/hr to be consistent with the FEB.
- $labor\ burden$ is the percentage of an operator's salary used to account for non-salary employee benefits such as healthcare. All cases assume 30 percent to be consistent with the FEB.
- P_{SOFC_AC} is the AC power output of the SOFC.
- n_{cells} is the total number of SOEC cells.

2.2.4 Fixed Cost Surrogates

The fixed cost surrogates presented in this report include the total fixed O&M cost and the annualized capital cost. Surrogate equations were generated by obtaining the fixed cost at

different plant sizes (maximum net power or maximum H_2 production) and fitting a power law in the form for the following.

$$FC = FC_{ref}\left(\frac{P_{\max}}{P_{\max\_ref}}\right)^{\alpha}$$

The variables are defined as follows:

- $P_{\max\_ref}$ is the maximum net power of the reference system. Power producing cases were sized for 650 $MW_{e,net}$ and H_2 producing cases were sized to 5 kg H_2/s.
- FC_{ref} is the fixed cost of the reference system.
- $P_{\max}$ is the maximum net power of the scaled system.
- α is the scaling exponent obtained via regression.

2.3 SURROGATE MODELS FOR PROCESS MARKET ANALYSIS

Detailed process models produced for this work can be time consuming to run and for large-scale problems such as market analysis, the models may present a tractability problem. Time and tractability issues can be addressed by generating surrogate models based on process model results. For profitability, the costs as a function of power and H_2 production are the only model results that are needed. Once a process design is fixed, fixed costs do not change, so only surrogate models for variable costs are needed.

Variable cost surrogates are written as a function of net power for systems that produce only power, as a function H_2 production for systems that only produce H_2, and net power and H_2 production for systems that produce both.

Since the price of electricity and fuel may vary, surrogates are also written with the fuel cost separated from other variable costs, so fuel cost can be adjusted. For systems that produce only H_2, electricity variable costs are also provided separately, so the electricity price can be adjusted.

With each set of variable cost surrogate models, bounds and/or inequality constraints are provided to define the feasible region for net power and H_2.

2.3.1 Data Generation

The detailed process models are run to generate sample points for the surrogate models. Process variables are optimized to produce the minimum operating cost. Costs are generated on a grid covering the entire feasible region.

2.3.2 Surrogate Modeling

In general, multivariate linear regression is used to fit surrogates for total, fuel, electricity, other variable costs as appropriate for each system. The model forms were determined by the Automatic Learning of Algebraic Models (ALAMO) surrogate modeling tool [21]. ALAMO determines the best combination of term to include in the models and selects the optimal

model size based on Bayesian information content. The IDAES/ALAMO surrogate modeling interface was used to generate the surrogate models. Settings used are provided in Exhibit 2-16.

Exhibit 2-16. ALAMO settings for variable cost surrogate fitting

Setting	Description	Value
linfcns	Include linear functions	True
constant	Include y-intercept	True
monomialpower	Monomial powers	[2, 3]
multi2power	Binomial powers	[1, 2, 3]
multi3power	Trinomial powers	[1, 2, 3]
ratiopower	Ratio powers	[1, 2]
maxterms	Maximum number of terms to include	8

Due to the large number of samples covering the entire feasible region coupled with the exclusion of extrapolation from the surrogates, over-fitting is not expected to be an issue. For each surrogate model, the R^2 value, a measure of the portion of the data variance explained by the mode, is reported. The large number of samples also allows for a good estimate of maximum and average surrogate model error, which is also reported.

2.4 Life Cycle Analysis of Greenhouse Gas Emissions

A life cycle analysis (LCA) is carried out to estimate the life cycle greenhouse gas (GHG) emissions for each technology. Cradle-to-gate life cycle GHG results were generated on a functional unit basis of 1 MWh net electricity produced for the power production technologies and 1 kg of H_2 produced for the H_2 production technologies. The life cycle impact assessment method used is from the International Panel of Climate Change Fifth Assessment Report (AR5) [22], which provides global warming potential (GWP) values for converting emissions of various GHG emissions into carbon dioxide equivalents (CO_2e) emissions. The computed results are generated using an assumption of a 100-year timeframe with atmospheric carbon feedback [4] using the values shown in Exhibit 2-17—GWP values for select GHG emissions.

Exhibit 2-17. GWP values for select GHG emissions

Greenhouse Gas	Chemical Formula	GWP Value
Carbon dioxide	CO_2	1
Methane	CH_4	36
Nitrous oxide	N_2O	298

The system boundaries considered for the cradle-to-gate LCA of the different technologies includes consumption of natural resources, utilities, and products. Exhibit 2-18 shows the system boundaries for the power production technologies, while Exhibit 2-19 shows the

boundaries for the H_2 production technologies. The parallelogram shapes represent upstream emissions data while the rectangle shapes represent outputs from the system.

Exhibit 2-18. Life cycle system boundaries for power production technologies

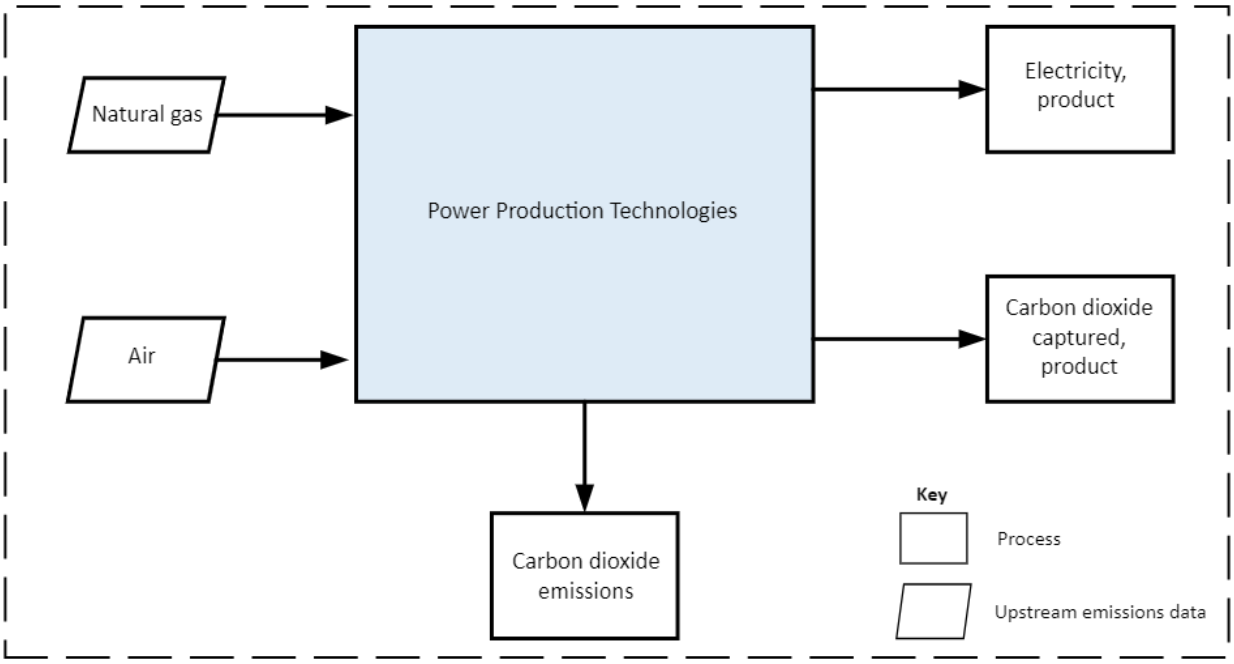

Exhibit 2-19. Life cycle system boundaries for H_2 production technologies

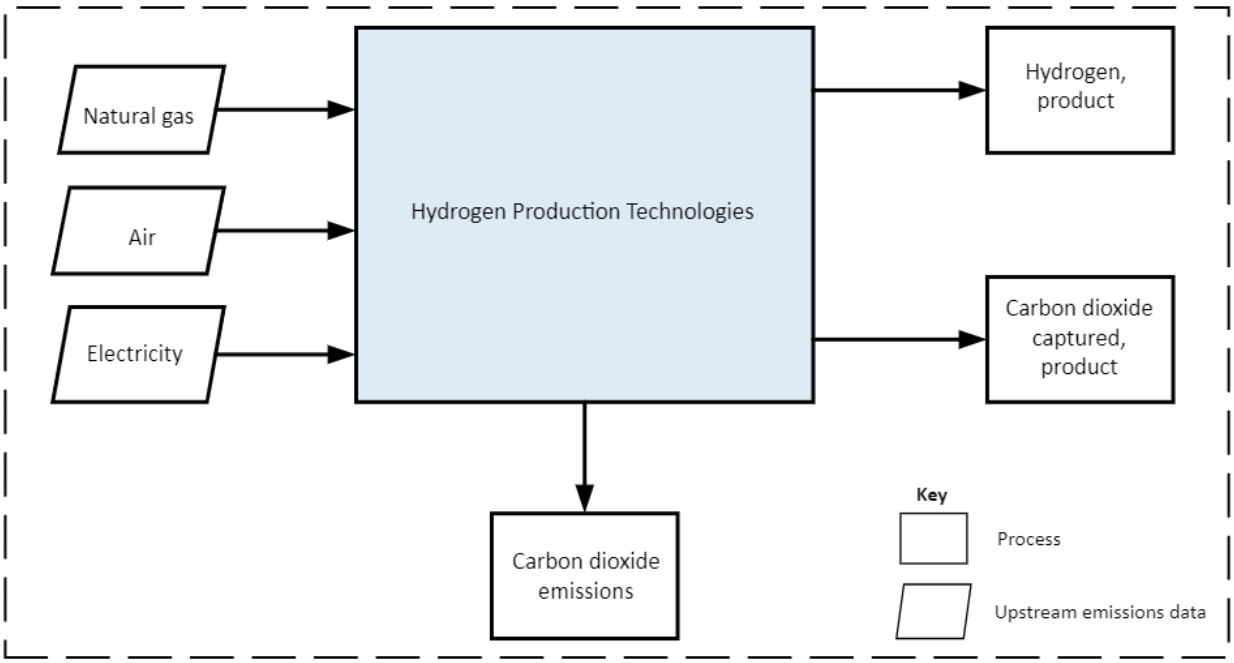

Data for the systems defined above were obtained from the technology simulations discussed in this report and literature sources. They include the following:

- Process emissions for the conventional and IES technologies discussed in this report were obtained from the simulation results.
- Process emissions for the steam methane reforming (SMR) technology with and without carbon capture were obtained from the NETL fossil-based H_2 production report [4]. Specifically, data from Case 1 of the report was used for the SMR without carbon capture case, while data from Case 2 was used for the SMR with carbon capture case.
- Process emissions for the NGCC without capture technology were obtained from case B31A of the FEB [1].
- Process emissions for the SOFC without capture technology were obtained from case ANGFC3B of the SOFC pathway studies report [2].
- U.S. average values for the life cycle GHG emissions of delivered NG were obtained from Rai et al. [23]. These values capture the emissions associated with extraction through the distribution of NG to the consumer.
- Life cycle cradle-to-gate GHG emissions of grid electricity from a U.S. average consumption mix were obtained from the U.S. Environmental Protection Agency (EPA) 2019 database [24]. The values obtained from the database are adjusted to account for losses during transmission and distribution to a user using values from the EPA eGRID2019 technical guide [25].

Life cycle cradle-to-gate GHG emissions of renewables electricity from solar photovoltaic (PV) cells are obtained from a National Renewable Energy Laboratory (NREL) report on life cycle GHG emissions from solar PVs [26]. These numbers are also adjusted to account for losses during transmission and distribution to a user [25]. The emissions values used include emissions associated with mining activities, production, and installation of the solar PV as well as power generation and decommissioning of the plant. The non-operational (power generation and plant maintenance) emissions contribute 74–79 percent of the overall life cycle emissions from the solar PV in comparison to less than 1 percent for traditional fossil technologies like coal [26].

3 NGCC

This section presents the IDAES process model used to estimate cost and performance of an NGCC plant with CCS[c]. The NGCC model is intended to represent current power generation technology providing a baseline for comparison of the different IES cases and their potential benefits over the current state-of-the-art. This model builds on case B31B of the FEB [1] and allows for off-design simulation and optimization. The model also provides a platform for integration of H_2 production systems, where the NGCC can provide heat, power, and steam.

3.1 System Description

The 90 percent carbon capture system in B31B that uses a conventional commercial solvent based CANSOLV (Shell) system was adjusted to provide 97 percent capture using PZAS™ [27]. The 97 percent capture case is used in this study, aside from verification of the model with the FEB.

The NGCC model can be divided into three major sections 1) gas turbine, 2) HRSG, and 3) steam cycle.

3.1.1 Gas Turbine

Exhibit 3-1 shows the gas turbine process flow diagram. This model is based on a dynamic NGCC model prepared by West Virginia University (WVU) [28, 29], corresponding to the FEB [1]. The WVU model provided performance curves for the turbine stages. The turndown performance of the turbine was verified against a similar turbine modeled in ThermoFlex [30]. Physical properties are modeled using the Peng-Robinson equation of state (EoS) and complete combustion of the NG is assumed.

The gas turbine flowsheet connects to the HRSG in three places: 1) turbine exhaust goes to the HRSG where heat is recovered to generate steam, 2) the NG preheater uses intermediate pressure hot H_2O from the HRSG, and 3) the NG preheater returns H_2O to the HRSG.

Pressure-driven flow is used to model the main flow through the gas turbine and flow of the blade cooling air. The turbine's performance is modeled with head and efficiency curves. A valve/compressor combination models the inlet air compressor that uses inlet guide vanes to control the flow. The compressor stage uses a fixed isentropic efficiency while the valve approximates adjustable inlet guide vanes. Increasing the valve pressure drop reduces the overall efficiency and pressure ratio of the compressor section. Lower compressor outlet pressure leads to lower flow through the turbine.

The exit pressure of the turbine is controlled by the pressure of exhaust gas leaving the HRSG, accounting for pressure drop through the HRSG. The turbine's exhaust temperature is controlled and assumed to be set based on limits of the HRSG. Setting the turbine power and exhaust temperature determines both the fuel and air flow rate. The valve used to control the fuel flow is not explicitly modeled.

[c] Found here: https://github.com/IDAES/publications/tree/main/netl_report_sofc_hydrogen_ies_2023/ngcc

Valves are used to simulate the flow of blade cooling air to the turbine stages. Since the blade cooling air requirements are not known and likely not significant, the valve openings were fixed at 85 percent and the valve flow coefficients were estimated based on the flow given in the FEB. In this configuration, blade cooling airflow is determined by pressure-driven flow, and the valve remains open at 85 percent.

Exhibit 3-1. NGCC gas turbine IDAES sub-flowsheet

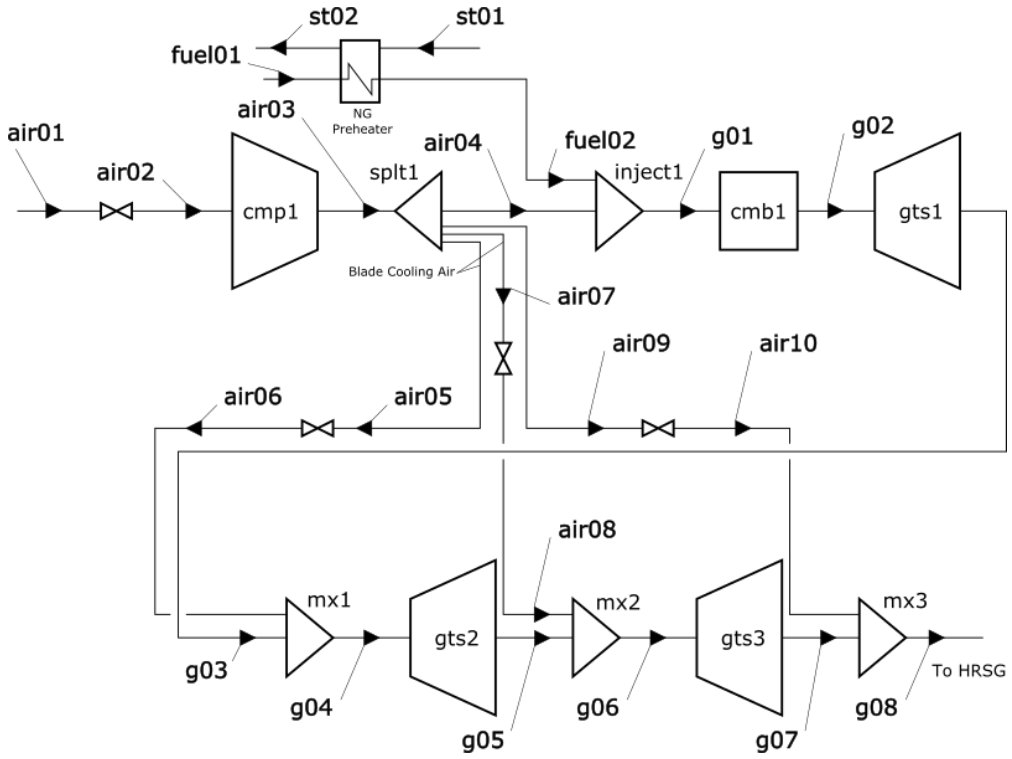

3.1.2 HRSG

Exhibit 3-2 shows the HRSG model process flow diagram. The HRSG uses heat from the NG turbine exhaust to provide high pressure (HP), IP, and LP steam to the steam cycle. The IP section includes a reheater for IP steam from the steam turbine.

Aside from the evaporators, the heat exchangers are modeled with detailed 0D models that include estimates for heat transfer coefficients and pressure drops on both the tube and shell side. The evaporator heat exchangers are modeled as simple 0D heat exchangers with fixed heat transfer coefficients. Since the exact dimensions and configuration of the HRSG are not known, a few correction factors were optimized to match key flows and temperatures reported in the FEB [1].

Control of the HRSG is based on the evaporators. Though level controllers and valves are not required in the steady state model, flow is regulated such that the H_2O fed to the IP and HP evaporators is vaporized and leaves as approximately 100 percent vapor saturated steam. These flow constraints set the main flow of feedwater to the HRSG and the split between IP and HP steam. A valve is included before the HP evaporator to include pressure drop induced by control valves and to ensure the steam in the HP evaporator is subcritical.

Exhibit 3-2. HRSG flowsheet

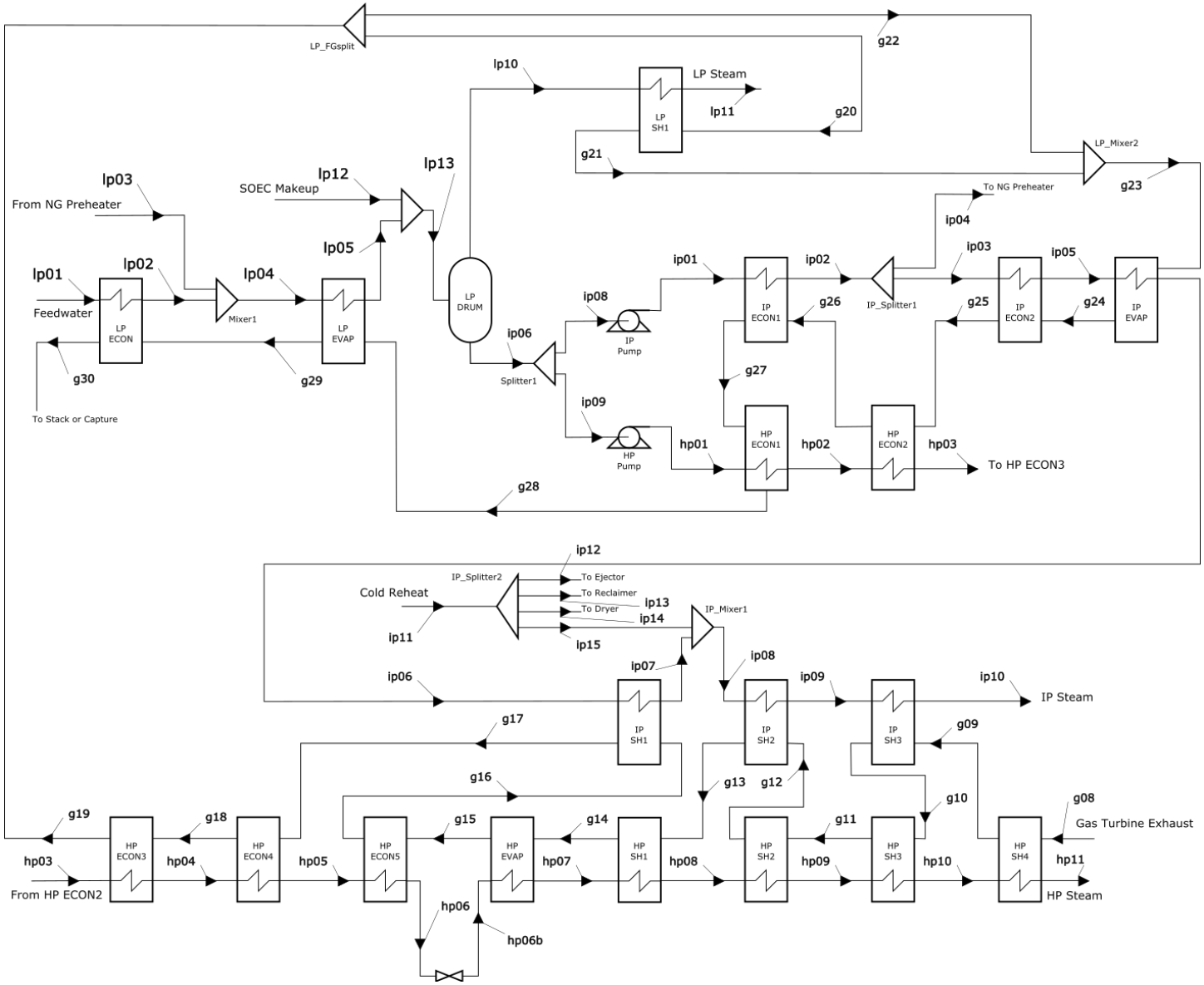

3.1.3 Steam Turbine

The steam turbine model is based on a model developed previously by Liese [8]. The flow coefficients and condenser size were estimated using the FEB conditions. Exhibit 3-3 shows the steam turbine process flow diagram.

Steam enters the turbine's throttle valve to the HP section from the HRSG. Steam from the HP turbine section is reheated and mixed with additional IP steam in the HRSG before being fed to the IP section. LP steam from the HRSG is added at the turbine IP/LP crossover. Steam for the carbon capture system is extracted from the IP/LP crossover, and an extraction point for the SOEC module is included for use in other cases. Turbine exhaust pressure is determined by the condenser. The carbon capture system is not explicitly modeled, but a heater block is used to determine the heat duty and steam conditions for the reboiler.

The main flow through the steam turbine is modeled as pressure driven flow. Constraints in the HRSG also determine the steam flow. Coupling the HRSG and steam turbine determines the turbine throttle valve position, or the HP steam pressure produced by the HRSG.

Exhibit 3-3. Steam cycle flowsheet

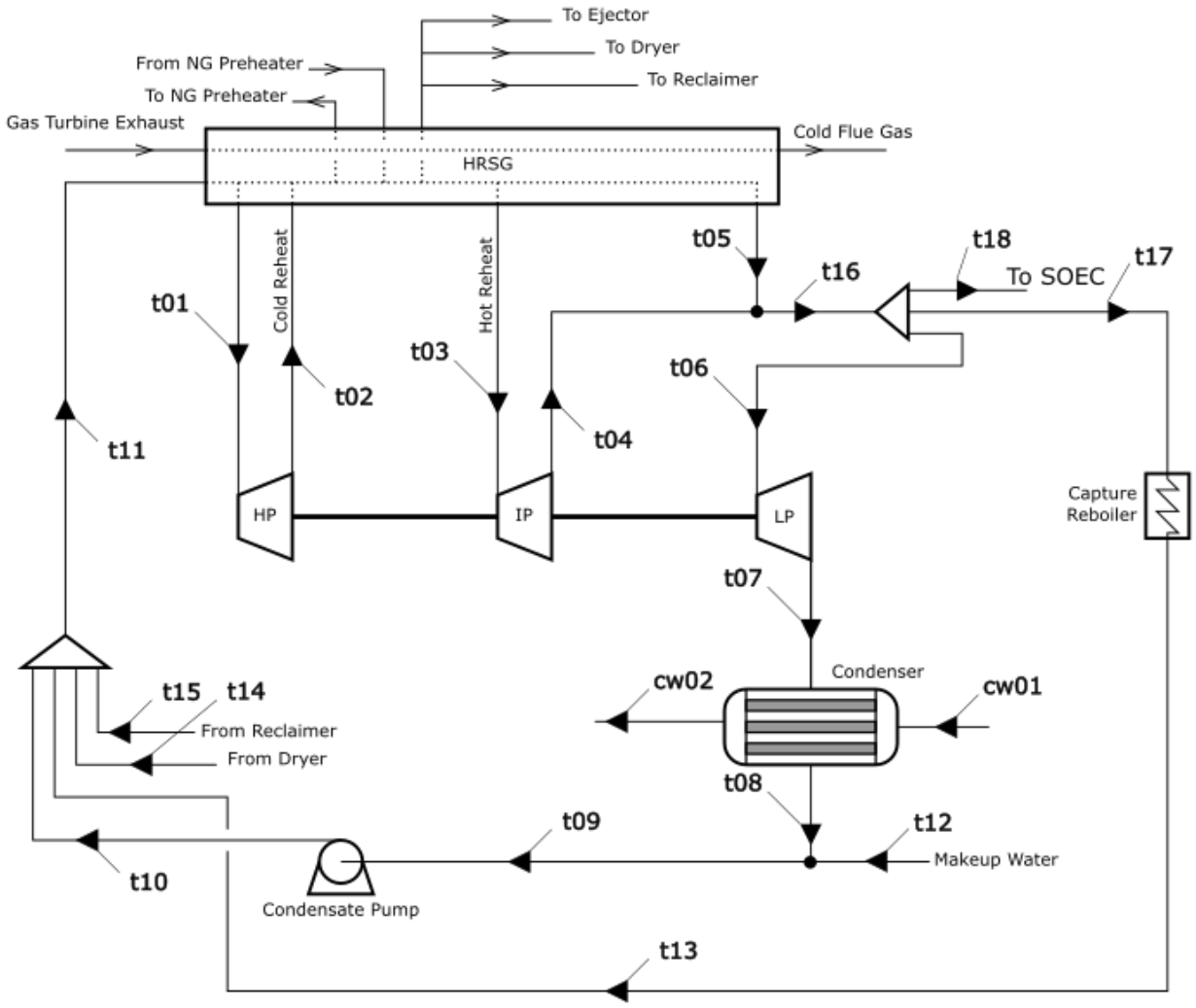

3.1.4 Carbon Capture

The carbon capture system is not explicitly modeled; however, capture fraction is an adjustable parameter and the specific reboiler duty and the compression power are estimated using surrogates described in Section 2.1.7 based on the amount of CO_2 captured and the capture fraction.

3.1.5 Full NGCC

Once all three sections of the NGCC are coupled, the model is configured so that the only significant adjustable parameter is net power. Some additional operating variables are described in the next section, but the system is configured to be very close to optimal operation.

The NGCC is modeled in detail and is capable of off-design simulation from 160 to 650 $MW_{e,net}$, so all major mass and energy flows can be obtained as well as temperatures, pressures, and enthalpies of all streams. The process efficiency and operating costs can be estimated from the model results across the load range.

3.2 Main Assumptions

Selected model parameters are provided in Exhibit 3-4. The specific reboiler duty and CO_2 compression power are obtained as described in Section 2.1.7.

Exhibit 3-4. Parameters used in the NGCC model

Parameter	Value
Specific Reboiler Duty at 90% Capture (MJ/kg) – CANSOLV	2.7
Specific Reboiler Duty at 97% Capture (MJ/kg) – PZAS	2.4
Specific CO_2 Compression Energy (MJ/kg)	0.2748
Gas Turbine Exhaust Temperature Limit (K)	898
Steam Turbine Flow Control	Throttle Valve

3.3 Performance and Cost Estimation

This section compares the IDAES model results to the FEB Case B31B [1].

3.3.1 System Performance

Exhibit 3-5 shows the comparison of the IDAES NGCC model predictions against the FEB. The results show good agreement between the reference and the IDAES flowsheet model. These results were obtained after tuning several parameters in the models (i.e., turbine efficiency, overall heat transfer coefficients, flue gas bypass in LP section, HRSG HP/IP ratio, HRSG heat transfer correction factors, and HRSG pressure drop correction factors). The costs are based on 2018 dollars.

Exhibit 3-5. Comparison of IDAES model results to FEB Case B31B

Item	FEB 90% Capture CANSOLV B31B	IDAES 90% Capture – CANSOLV	IDAES 97% Capture – PZAS
HHV Efficiency	47.7	47.7	47.6
Net Power (MW_e)	646	646	646
Gross Power (MW_e)	690	690	692
Gas Turbine Power (MW_e)	477	477	478
Steam Turbine Power (MW_e)	213	213	215
Fuel Cost ($/MWh)	31.65	31.68	31.71
Other Variable Costs ($/MWh)	5.63	5.64	5.64
TASC ($MM)	1,702	1,702	1,820

The model predictions under off-design conditions are shown in Exhibit 3-6 that shows the HHV efficiency as a function of net power.

Exhibit 3-6. Efficiency as a function of power output assuming 97% capture and a PZAS carbon capture system

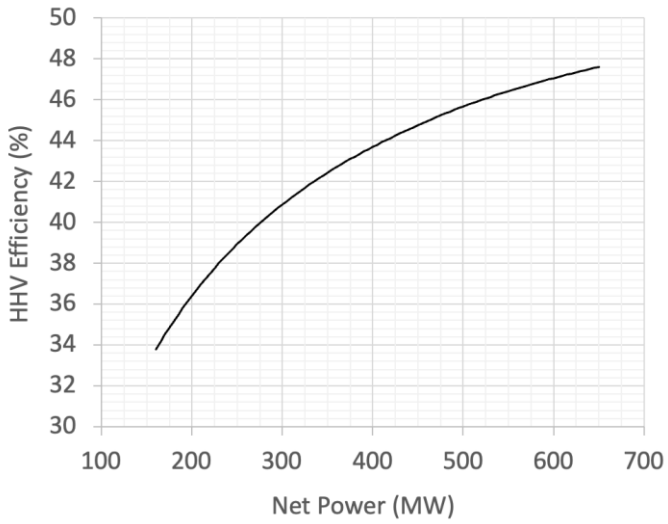

3.3.2 Fixed Costs

Fixed costs, taken from the FEB [1], are summarized in the 90 percent capture column of Exhibit 3-7. Costs for relevant subsystems were updated to 97 percent capture using the IDAES model and are summarized in the 97 percent capture column of Exhibit 3-7.

Exhibit 3-7. Fixed cost breakdown for the base case NGCC (2018 dollars)

Fixed Cost Breakdown	FEB 90% Capture – CANSOLV (B31B)	97% Capture – PZAS
TOC ($MM)	1,557.53	1,664.95
TPC ($MM)	1,281.32	1,369.78
Feedwater System	115.23	115.23
CO_2 Removal System	680.09	768.54
Combustion Turbine Generator	113.76	113.76
Heat Recovery Steam Generator	100.88	100.88
Steam Turbine Generator and Accessories	81.73	81.73
Cooling Water System	52.41	52.42
Generator Equipment and Accessories	66.68	66.68
Control System	23.46	23.46
Site Preparation, Improvement, and Facilities	28.76	28.76
Various Building Structures	18.31	18.31
Pre-Production Costs	39.83	42.58
Inventory Capital	8.34	8.91
Owner's, Financing, Other Costs	227.94	243.68
TASC (TOC x 1.093) ($MM)	1,701.83	1,819.79
Annualized Capital Cost ($MM/yr)	120.32	128.66
Fixed O&M ($MM/yr)	41.27	43.88
Total Fixed Cost ($MM/yr)	161.59	172.54

The following equation can be used to scale the total fixed cost to different maximum power outputs:

$$Fixed\ Cost\ \left[\frac{MM\$}{yr}\right] = 172.54\left(\frac{P_{max}}{650\ MW}\right)^{0.8}$$

3.3.3 Variable Costs

Turndown surrogate models for variable cost were developed for the NGCC with 97 percent capture by running the model from 650 down to 160 $MW_{e,net}$ in 5 MW_e increments.[d] The NGCC was operated at a fixed gas turbine exhaust temperature of 898 K using fixed pressure operation in the steam turbine.

[d] The model was not optimized, as it was previously determined that the degrees of freedom are limited and opportunity for improvement is not significant.

Exhibit 3-8 shows the variable costs as function of net power, where net power is in MW_e. Fuel costs make up the bulk of the variable costs. The remaining costs come from items like purchased H_2O, H_2O treatment, and chemicals. The surrogate model for total cost can be obtained for other fuel prices by adding the surrogate model for other costs to the fuel surrogate multiplied by ($x/MMBtu)/($4.42/MMBtu), where x is the fuel price based on HHV.

Exhibit 3-8. Variable cost surrogates

Variable Cost Component	Variable Cost Model ($/hr)	R^2

Total	`35.67538 * net_power`
	`- 0.7692752E-002 * net_power**2`
	`+ 0.5218480E-005 * net_power**3`
	`+ 2889.652`
		1.0000

Fuel	`30.28471 * net_power`
	`- 0.6530350E-002 * net_power**2`
	`+ 0.4429949E-005 * net_power**3`
	`+ 2453.015`
		1.0000

Other	`5.390678 * net_power`
	`- 0.1162402E-002 * net_power**2`
	`+ 0.7885309E-006 * net_power**3`
	`+ 436.6367`
		1.0000

Exhibit 3-9 shows percent error in the total variable cost surrogate model relative to the detailed process model.

Exhibit 3-9. Percent error in NGCC total variable cost surrogate model relative to the detailed process model

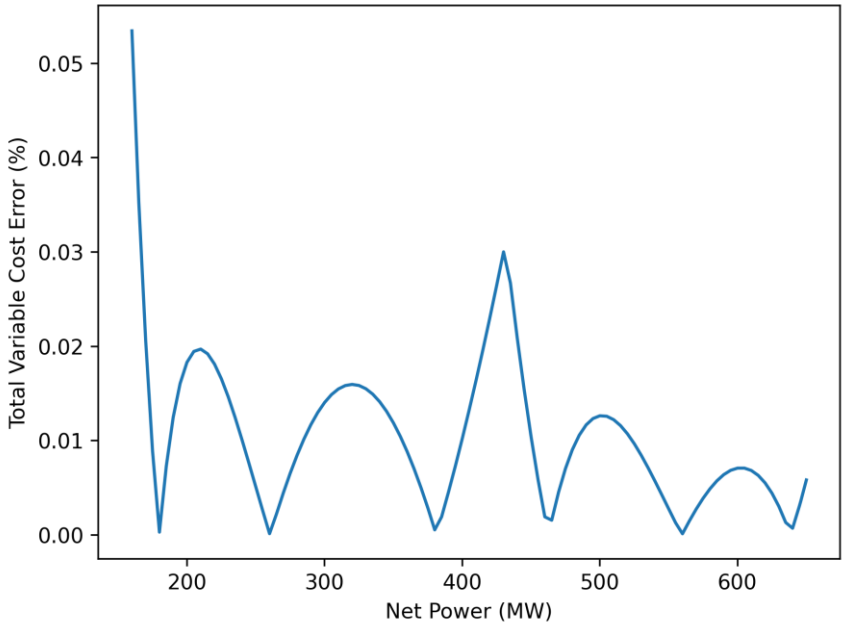

4 SOFC

This section describes the IDAES process model used to estimate cost and performance of a 650 $MW_{e,net}$ NG-fed SOFC plant with a steam turbine bottoming cycle and CPU (~98 percent CO_2 capture)[e]. The SOFC technology used in this case assumes that DOE's performance and cost goals for 2030 have been achieved. This model is based on Case ANGFC3B of the NGFC Pathways study [5] and is suitable for off-design simulation and optimization.

4.1 System Description

Exhibit 4-1 shows the block flow diagram of the SOFC plant and is largely based on Case ANGFC3B of the NGFC Pathways study [5]. The plant contains three major sections: 1) SOFC power island, 2) HRSG and steam cycle, and 3) CPU. De-sulfurized NG is supplied to the anode side of the SOFC power island. The incoming NG is pre-heated in the anode heat exchanger and sent to an adiabatic pre-reformer where higher hydrocarbons are reformed to prevent carbon deposition in the anode. Within the anode of the SOFC, methane is further reformed into H_2 and carbon monoxide on the Ni catalyst. A portion of the anode off-gas is recirculated at a rate that only provides the steam necessary for reformation of the incoming NG but also prevents any carbon deposition by maintaining an appropriate O_2 to carbon ratio. The cathode of the SOFC is supplied with air whose flow rate and temperature are modulated to maintain the stack within the desired temperature range. Driven by the electrochemical potential, O_2 ions diffuse across the electrolyte to react with the fuel on the anode side, generating an electrical current and power. Part of the cathode exhaust is recycled to minimize the size of the cathode heat exchanger. The unconsumed fuel in the anode off-gas is combusted in an oxy-combustor with O_2 supplied from a low-pressure ASU. The flue gas generates steam in a HRSG for use in a steam bottoming cycle. While drying of the flue gas will be sufficient to capture the CO_2, a CPU unit is required to purify the CO_2 to pipeline specifications (<10 ppm O_2). The process generally results in ~98 percent CO_2 capture.

[e] Found here: https://github.com/IDAES/publications/tree/main/netl_report_sofc_hydrogen_ies_2023/sofc

Exhibit 4-1. SOFC block flow diagram

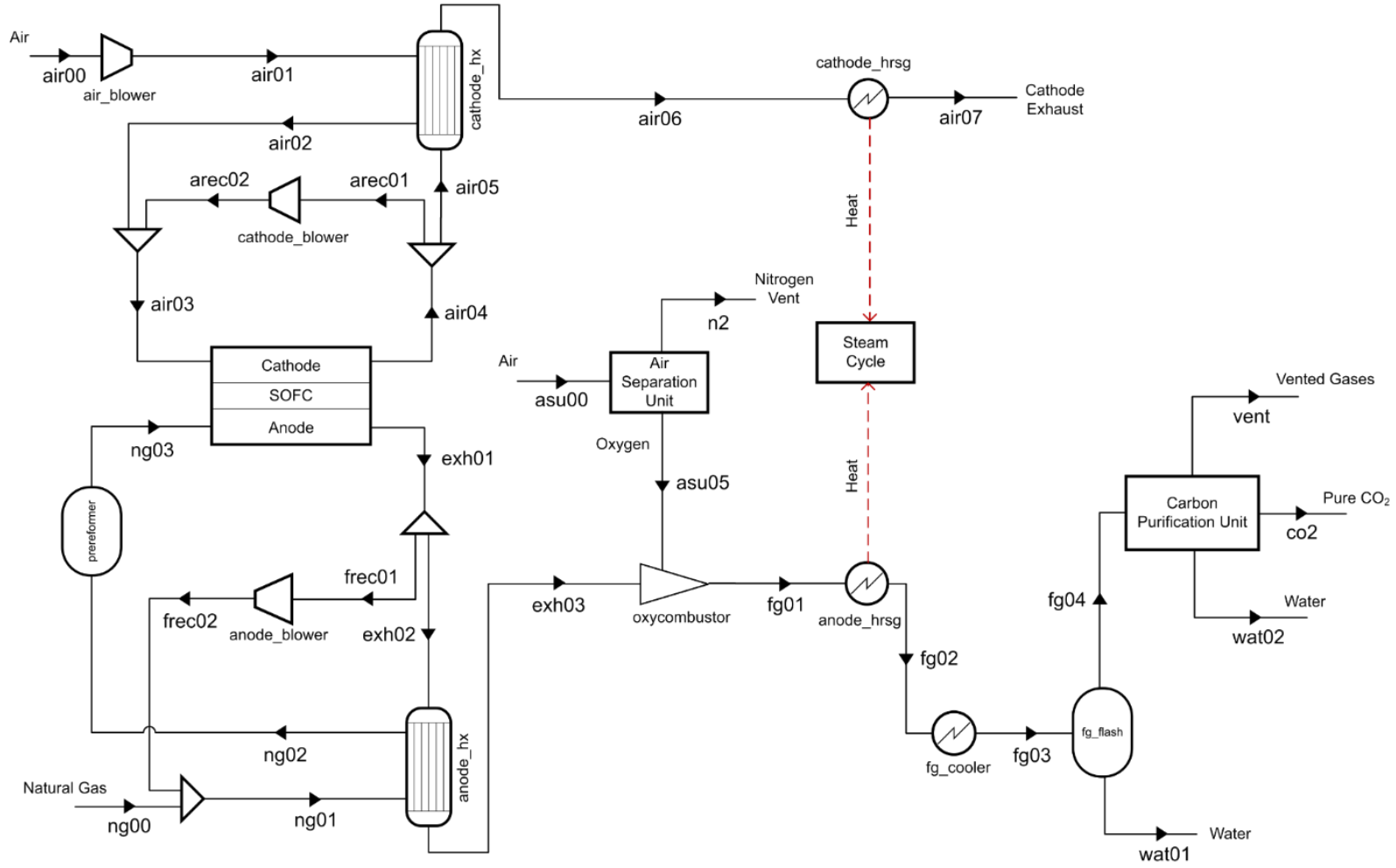

The desulfurization process is not explicitly modeled but is factored into the capital and operating costs. Blowers are modeled using the compressor model with fixed isentropic efficiency. The cathode and anode heat exchangers are modeled with 0D heat exchanger models. The pre-reformer is modeled as an adiabatic Gibbs reactor. The HRSG and steam cycle are not explicitly modeled, since it generates only a relatively small portion of the power (about 10 percent). The HRSG is represented as a heater that cools the flue gas to a fixed temperature. The steam cycle is assumed to have a 38.1 percent thermal efficiency. A surrogate model was developed based on a CPU process used (see Section 2.1.3). The surrogate CPU model provides the outlet stream conditions, compressor work, and cooling requirements based on an inlet composition.

The SOFC model involves four unit-operations (separator, heater, mixer, and Gibbs reactor) and the DNN reduced-order model (ROM) (described in Section 2.1.5). Based on the specified average current density at which the SOFC operates, O_2 is separated from the air entering the cathode and mixed with the fuel entering the anode (the current density along with the fuel utilization value determine the inlet NG flow). The outlet composition of the anode is determined by the Gibbs reactor with an outlet temperature calculated from the ROM. The ROM calculates the voltage of the SOFC, which is multiplied by the current to calculate the power. The heater sets the cathode outlet temperature to a value that closes the energy balance around the SOFC (anode duty = power + cathode duty).

4.2 Main Assumptions

Main assumptions of the SOFC model are listed in Exhibit 4-2.

Exhibit 4-2. Parameters used in the SOFC model

Parameter	Value
Blower Isentropic Efficiency, %	80
Current Density, mA/cm^2	400
Fuel Utilization, %	85
Internal Reformation, %	100
Oxygen to Carbon Ratio	2.1
Cathode Gas Recirculation Ratio	0.5
Steam Cycle Thermal Efficiency, %	38.1
Heat Exchanger Overall Heat Transfer Coefficient, W/m^2K	80
Cell Max Temperature (°C)	750
ΔT Across the Cell (°C)	100
HRSG Exit Temperature (°C)	132

4.3 Performance and Cost Estimation

The 650 $MW_{e,net}$ SOFC IDAES model is based on Case ANGFC3B from the NGFC Pathways study [3].

4.3.1 System Performance

A comparison of the gross and net power outputs and efficiencies between the IDAES model and Case ANGFC3B [5] can be found in Exhibit 4-3.

Exhibit 4-3. Comparison to Case ANGF3B

Variable	IDAES Model	Base Case – ANGFC3B
Gross Power, MW_e	693.8	694.4
Net Power, MW_e	650.0	650.0
HHV Efficiency, %	65.16	64.8

4.3.2 Fixed Costs

Capital, fixed O&M, and variable O&M costs for the SOFC plant were estimated using the costing methodology detailed in Section 2.2. The equation for fixed costs as a function of SOFC capacity is as follows:

$$Fixed\ Cost\ \left[\frac{MM\$}{yr}\right] = 69.88\left(\frac{P_{max}}{650\ MW}\right)^{0.77} + 49.13\left(\frac{P_{max}}{650\ MW}\right)^{0.779}$$

The first term represents the annualized capital cost and the second term the fixed O&M costs. The annualized capital cost contributes about 59 percent to the total fixed cost at 650 $MW_{e,net}$.

Exhibit 4-4. Fixed cost breakdown for the base case SOFC

Fixed Cost Breakdown	IDAES Model, 98% Capture
TPC ($MM)	**747.33**
SOFC Modules	216.35
SOFC BOP	22.17
Oxy-combustor	17.26
ASU	75.17
CPU	80.18
Feedwater & Miscellaneous BOP Systems	78.42
Heat Recovery Steam Generator	44.92
Steam Turbine Generator & Accessories	50.98
Cooling Water System	32.60
Generator Equipment and Accessories	67.16
Control System	20.49
Site Preparation, Improvement, and Facilities	28.84
Various Building Structures	12.81
TOC ($MM)	**904.27**

Fixed Cost Breakdown	IDAES Model, 98% Capture
Total As Spent Cost (TASC) ($MM)	**988.37**
Annualized Capital Cost ($MM/yr)	**69.88**
Fixed O&M ($MM/yr)	**49.13**
Annual Operating Labor ($MM/yr)	2.63
Maintenance Labor ($MM/yr)	5.68
Admin & Support Labor ($MM/yr)	2.08
Property Taxes & Insurance ($MM/yr)	14.95
Maintenance Material Cost ($MM/yr)	8.52
Stack Replacement Cost ($MM/yr)	15.27
Total Fixed Cost ($MM/yr)	**119.01**

4.3.3 Variable Costs

Surrogate models for the variable O&M costs were developed over an operating range of 190– to 650 $MW_{e,net}$. Contributions to the variable costs included NG, H_2O, H_2O treatment chemicals, sulfur adsorbent, and methanation catalyst costs. Plant design is fixed relative to the 650 $MW_{e,net}$ case. To reduce the net power of the IDAES model, the NG flowrate and stack current density were decreased by the same proportion. The equations for variable cost surrogates are given in Exhibit 4-5.

Exhibit 4-5. SOFC variable cost surrogate models

Variable Cost Component	Variable Cost ($/hr)	R^2

Total	`23.29340 * net_power`
	`+ 0.2875715E-003 * net_power**2`
	`+ 0.1155903E-005 * net_power**3`
	`+ 49.21504`
		1.0000

Fuel	`22.49809 * net_power`
	`+ 0.2714661E-003 * net_power**2`
	`+ 0.1073822E-005 * net_power**3`
	`+ 38.61723`
		1.0000

Other	`0.7953093 * net_power`
	`+ 0.1610535E-004 * net_power**2`
	`+ 0.8208137E-007 * net_power**3`
	`+ 10.59780`
		1.0000

Exhibit 4-6 shows the percent error in the total cost surrogate model relative to the detailed process model.

Exhibit 4-6. Percent error in the SOFC total variable cost surrogate model relative to the detail process model

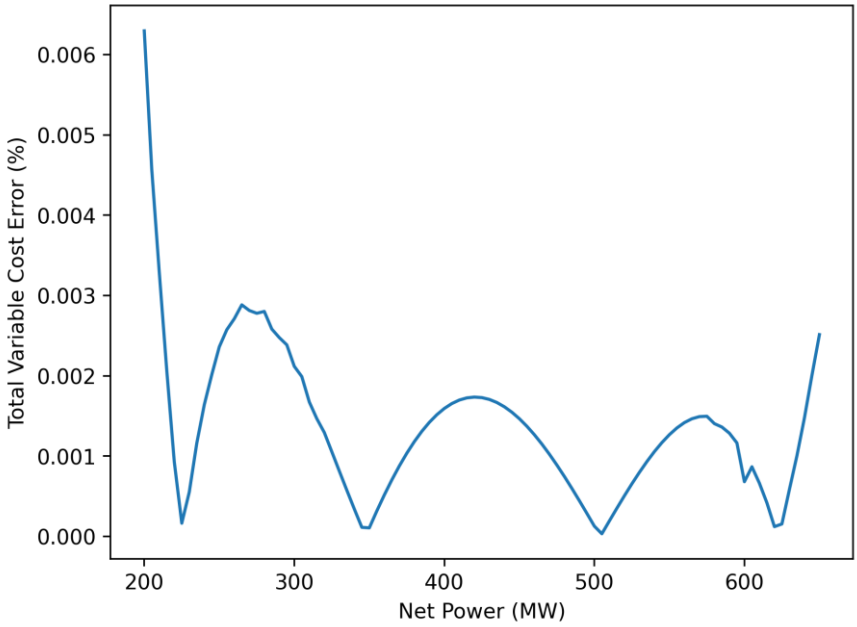

5 SOFC WITH CAES

This section presents a model for the 650 $MW_{e,net}$ NG-fed SOFC plant from Section 4 integrated with a 255 $MW_{e,net}$ CAES system[f]. The compressed air is stored in a sub-surface cavern at high pressure (4–7 MPa). Two different flowsheets are implemented to simulate the charge and discharge cycles of the integrated SOFC-CAES system. When discharging, the SOFC steam cycle (107 MW) is deactivated and the heat is used for the CAES system, so the maximum power output of the system is 798 MW. The storage capacity was sized to allow 10 hours of air storage. While charging, the compressor consumes 253 MW_e from the SOFC system (or potentially from the grid), this power allows the system to charge from minimum pressure to maximum in 10 hours.

5.1 SYSTEM DESCRIPTION

The CAES system consists of three components, 1) power conversion (compressors and turbines), 2) heat management, and 3) compressed air storage. The storage system can operate in three exclusive modes 1) charging, 2) discharging, and 3) idling. In charging mode, power from the SOFC is used to run the CAES compressors. In discharging mode, the steam cycle is turned off, and heat from the HRSG is used to heat stored compressed air, which is then sent to the CAES turbine to generate power. In idling mode, the SOFC can also operate as in Section 4, while not using the CAES system.

The primary unit operations in the CAES system are compressors, turbines, heat exchangers, and storage facility. The sub-surface storage cavern was assumed to be an adiabatic tank of fixed volume. A shell-and-tube type heat exchanger was used to model the air preheater. A heater was used to represent the air heating in the SOFC HRSG. Based on the temperatures involved, the heat that would be used by the steam cycle is available to heat the stored air. The Peng-Robinson EoS was used to model the thermodynamic properties of air (air composition is shown in the Exhibit 2-1).

While discharging, the SOFC and CAES systems were assumed to operate at full capacity to maximize the power output.

5.1.1 Charging Mode

Exhibit 5-1 shows the plant in charging mode. During periods with low electricity prices (or low power demand), a portion of the electricity produced from the SOFC module is used to drive the intercooled CAES compressor. After compression, the air is cooled to be stored in a sub-surface cavern. It was assumed that the usable heat recovered from the compressor intercoolers and aftercooler is not significant.

[f] Found here: https://github.com/IDAES/publications/tree/main/netl_report_sofc_hydrogen_ies_2023/caes

Exhibit 5-1. CAES integrated with the SOFC plant block flow diagram, charge mode

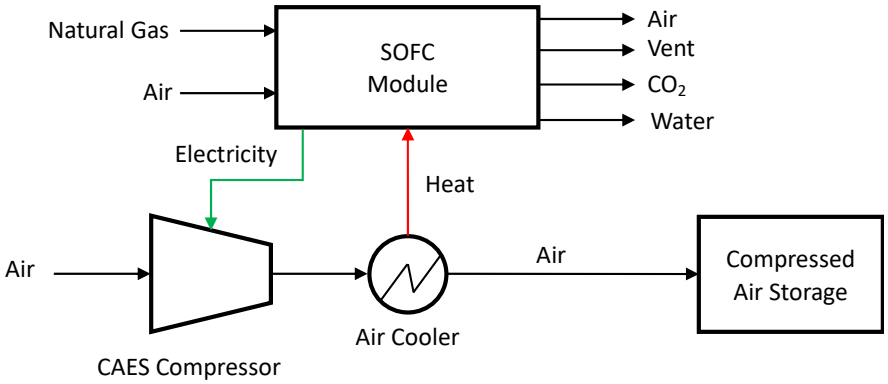

5.1.2 Discharging Mode

Exhibit 5-2 shows the integrated SOFC-CAES plant in discharging mode. During periods with high electricity prices (or high-power demand), compressed air from the storage is used to generate additional electricity. In this mode, the compressed air from storage is fed through a throttle valve to reduce the pressure to a specified CAES turbine inlet pressure. The air is preheated by the turbine exhaust and then heated to the turbine inlet temperature in the HRSG of the SOFC plant. The hot air is then sent to the CAES turbine to generate power.

Exhibit 5-2. CAES integrated with the SOFC plant block flow diagram, discharge mode

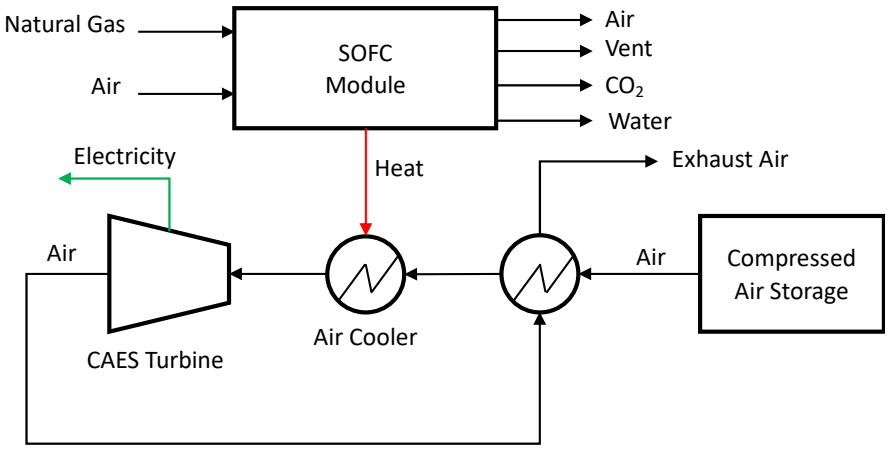

5.2 Main Assumptions

Key assumptions made in the CAES model are compiled in Exhibit 5-3.

Exhibit 5-3. Parameter used in the CAES model

Parameter	Value
Maximum allowable pressure for cavern (MPa)	7
Minimum allowable pressure for cavern (MPa)	4
Storage temperature (K)	323
Charging time from 4 to 7 MPa (hr)	10
Discharging time from 7 to 4 MPa (hr)	10
Discharging HRSG usable heat (MW_{th})	282.4
Turbine inlet pressure (MPa)	4
Turbine inlet temperature (K)	900
Turbine isentropic efficiency	0.9
Compressor isentropic efficiency	0.8
Number of compressor intercoolers	2
Compressor intercooler temperatures (K)	400

5.3 Performance and Cost Estimation

The base case scenario considers the same SOFC plant as described in Section **Error! Reference source not found.**with a 255 $MW_{e,net}$ CAES system. In discharge mode, the steam cycle is not active, so the additional power produced by the system overall increases by 148 MW, extending the overall plant's capacity to 798 $MW_{e,net}$. This section shows the system performance for both charging and discharging operations.

5.3.1 System Performance

The base case operation of the SOFC is presented in Section 4.3.1. This section provides key model results based on the CAES system specified in Exhibit 5-3. Key charging mode results are summarized in Exhibit 5-4 and key discharging results are summarized in Exhibit 5-5.

Exhibit 5-4. Charging mode results

Quantity	Result
Compressor power (MW)	253
Energy to fully charge from minimum pressure (MW_ehr)	1,481.67
Maximum stored air (kmol)	792,560
Minimum stored air (kmol)	451,680
Total usable stored air (kmol)	340,880

Exhibit 5-5. Discharging mode results

Quantity	Result
Cavern volume (m^3)	514,000
Electrical energy produced discharging from maximum pressure ($MW_e hr$)	1,496.99
Thermal energy input discharging from maximum pressure ($MW_{th} hr$)	1,654.68
Discharging power (MW)	255.48
Air flow (kmol/s)	16.16

The flow of air to the cavern in charging mode varies with cavern pressure. The model results were used to construct surrogate models for the air flowrate, the amount of air stored, and the charging time.

The following equation shows the air flowrate in charging mode as a function of pressure, where z is compressor power in MW, f is flowrate in kmol/s, and p is cavern pressure in kPa. The R^2 value is 0.9998.

$$\frac{f}{z} = 5.09587 \times 10^{-10} p^2 - 9.25337 \times 10^{-6} p + 0.0991564$$

The following equation shows the amount of air stored in the cavern as a function of the cavern pressure, where s is the amount of stored air in kmol and v is the cavern volume in m^3. The R^2 value is 1.0.

$$s = 3.7713 \times 10^{-4} pv$$

The following equation shows the time required to charge from one amount of stored air (s_1 in kmol) to another (s_2 in kmol), where t is the time to charge in seconds. Since the compressor power is constant (253 MW), the energy required to charge can be found by multiplying the compressor power by time:

$$t = \frac{-7.27796 \times 10^{-8}(s_2^3 - s_1^3)}{3(3.7713 \times 10^{-4} v)^2 z} + \frac{1.68254 \times 10^{-3}(s_2^2 - s_1^2)}{2(3.7713 \times 10^{-4} v) z} + \frac{8.6504163.5(s_2 - s_1)}{z}$$

In discharging mode, the turbine power is set by the amount of heat available from the SOFC, the CAES turbine inlet pressure, and the CAES turbine inlet temperature. The turbine inlet conditions are constant, so the flow and power are approximately constant, with minor variation due to temperature change in the adiabatic throttle valve, with cavern pressure. The constant turbine flow and power are given in Exhibit 5-5.

5.3.2 Fixed Costs

The overall costing methodology used in this study is detailed in Exhibit 2-13. The major equipment capital costs are estimated using a reference study [31]. The cavern cost was estimated to be \$3.66/kWh for a 960 $MWh_{e,net}$ cavern based on a literature survey average. The balance of plant and other miscellaneous costs (e. g. piping, instrumentation, controls, buildings, …) were estimated to be one third of the major equipment costs.

The fixed cost for the CAES system includes capital and fixed O&M (operating and maintenance) costs. Since the power generated by the CAES is determined by the heat available from the SOFC, the CAES power output cannot be scaled independent of the SOFC; however, the discharge time can be sized independently. For this study it is assumed that the charge and discharge time are equal going from full to empty or empty to full. The total annualized capital cost is given as the following:

$$Fixed\ Capital\ Cost\ \left[\frac{MM\$}{yr}\right] = \left(100.54 + 0.171 t_{discharge}^{0.8}\right)\left(\frac{P_{max}^{SOFC}}{650\ MW}\right)^{0.80}$$

Next, the total fixed O&M costs in MM$/y are given as the following:

$$Fixed\ O\&M\ Cost\ \left[\frac{MM\$}{yr}\right] = \left(77.23 + 0.099 t_{discharge}^{0.8}\right)\left(\frac{P_{max}^{SOFC}}{650\ MW}\right)^{0.80}$$

Exhibit 5-6. Cost breakdown for the base case simulation

Fixed Cost Breakdown	650 $MW_{e,net}$ SOFC, 10 hr charge and discharge	650 $MW_{e,net}$ SOFC, x hr charge and discharge
Total as Spent Cost (TASC) (MM$)	1,437.44	$1422.19 + 2.418x^{0.8}$
Total SOFC as Spent Cost (TASC) (MM$)	995.27	995.27
Total CASE as Spent Cost (TASC) (MM$)	442.17	$426.92 + 2.418x^{0.8}$
Total Plant Cost (MM$)	334.31	$322.77 + 1.8278x^{0.8}$
Bare Erected Cost (MM$)	222.87	$215.18 + 1.2185x^{0.8}$
Turbine (MM$)	71.89	71.89
Compressor (MM$)	42.54	42.54
Exhaust Heat Exchanger (MM$)	2.96	2.96
HRSG Heat Exchangers (MM$)	23.50	23.5
Cavern (MM$)	7.69	$1.2185x^{0.8}$
Misc. Balance of Plant (MM$)	74.29	74.29
Total Fixed Cost (MM$/yr)	179.78	$177.77 + 0.270x^{0.8}$
Annualized Capital Cost (MM$/yr)	101.63	$100.54 + 0.171x^{0.8}$
Fixed O&M Costs (MM$/yr)	78.15	$77.23 + 0.099x^{0.8}$
Annual Operating Labor (MM$/yr)	3.04	3.04
Maintenance Labor (MM$/yr)	11.15	$10.81 + 0.0184x^{0.8}$
Admin & Support Labor (MM$/yr)	3.55	$3.46 + 0.0046x^{0.8}$
Property Taxes & Insurance (MM$/yr)	28.75	$28.44 + 0.0484x^{0.8}$
Maintenance Material Cost (MM$/yr)	16.39	$16.21 + 0.0276x^{0.8}$
Stack Replacement Cost (MM$/yr)	15.27	15.27

5.3.3 Variable Costs

The variable costs can be calculated from the variable cost surrogate models for the SOFC given in Section 4.3.3, by adjusting the overall net power. This section describes how the surrogate models can be used in each mode.

When the CAES system is off, the SOFC surrogate models can be used directly.

When the CAES system is in charge mode, the SOFC must produce at least enough power to run the CAES compressor. The compressor power is assumed to be constant and is a design decision. The net power produced by the system in charge mode is the SOFC net power (which is the input to the surrogate model) minus the CAES compressor power.

When the CAES system is discharging, the power output should be maximized so that the SOFC and CAES will operate at full capacity. The input to the variable cost surrogates will be 650 MW_e and the system net power will be 798 MW_e.

6 NGCC+SOEC

In this case, an NGCC is coupled with an SOEC to produce H_2 and/or power[g]. The proposed design extracts steam from the steam turbine IP/LP crossover for use in the electrolyzer. The NGCC also provides electricity to the SOEC, and if the SOEC's electricity demand exceeds the NGCC's capacity, electricity can be purchased from the grid.

6.1 System Description

The block flow diagram of the NGCC+SOEC system is shown in Exhibit 6-1.

When electricity prices are low, the SOEC can produce H_2 by consuming power from the NGCC, allowing the NGCC to operate more frequently in the high-efficiency region near full capacity. Integration with the NGCC may be preferable to purchasing electricity from the grid depending on market conditions. Since the NGCC provides both electricity and steam to the SOEC, the integrated system is potentially more cost effective than using a standalone SOEC that would require an additional boiler and market-priced electricity.

The standalone NGCC capacity is 650 $MW_{e,net}$ with 97 percent carbon capture. The SOEC module is sized to produce a maximum of 5 kg/s of H_2. At maximum H_2 output, the steam extraction imposes a derate of 26 MW_e to the NGCC, requiring about 58 MW_e from the grid to supply the full SOEC load of 682 MW_e.

Exhibit 6-1. Block flow diagram for a NGCC integrated with SOEC

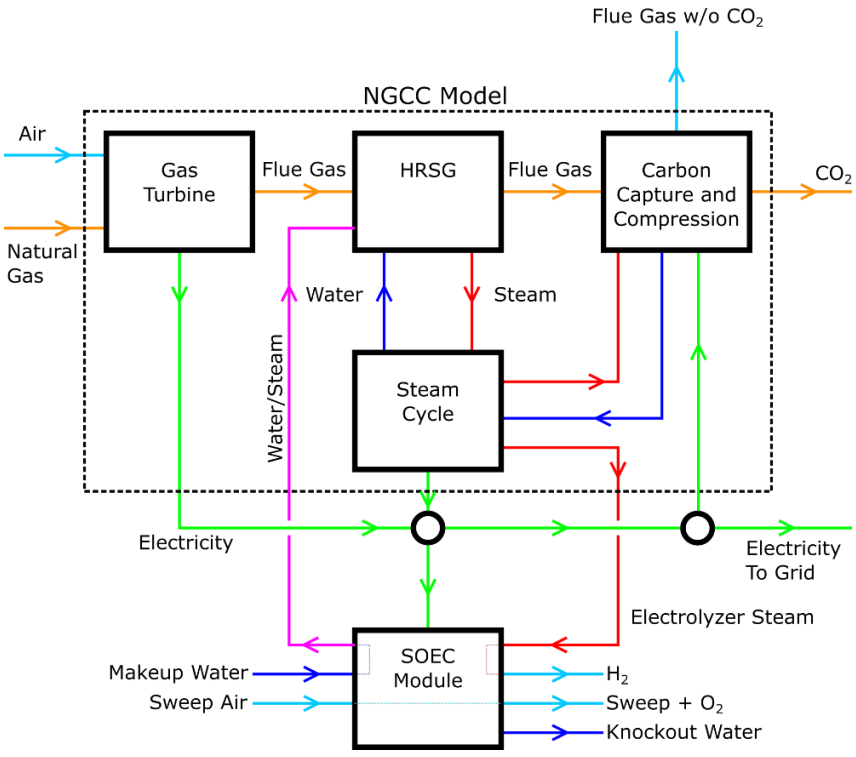

[g] Found here: https://github.com/IDAES/publications/tree/main/netl_report_sofc_hydrogen_ies_2023/ngcc

The SOEC module layout is shown in Exhibit 6-2. The steam supplied to the SOEC in stream "feed03" is extracted from the steam turbine IP/LP crossover. Makeup low-quality steam from streams "water04" and "water05" are fed to the LP drum in the HRSG. Steam extraction reduces the IP/LP crossover pressure, so a constraint of 2.9 bar minimum IP/LP crossover pressure is employed. This limits the amount of steam that can be extracted and the amount of turndown that can be achieved in the NGCC. This constraint ensures that the steam condensing temperature is high enough to operate the carbon capture system and that the steam extraction for the SOEC will not interfere with the steam turbine operation.

Exhibit 6-2. SOEC section

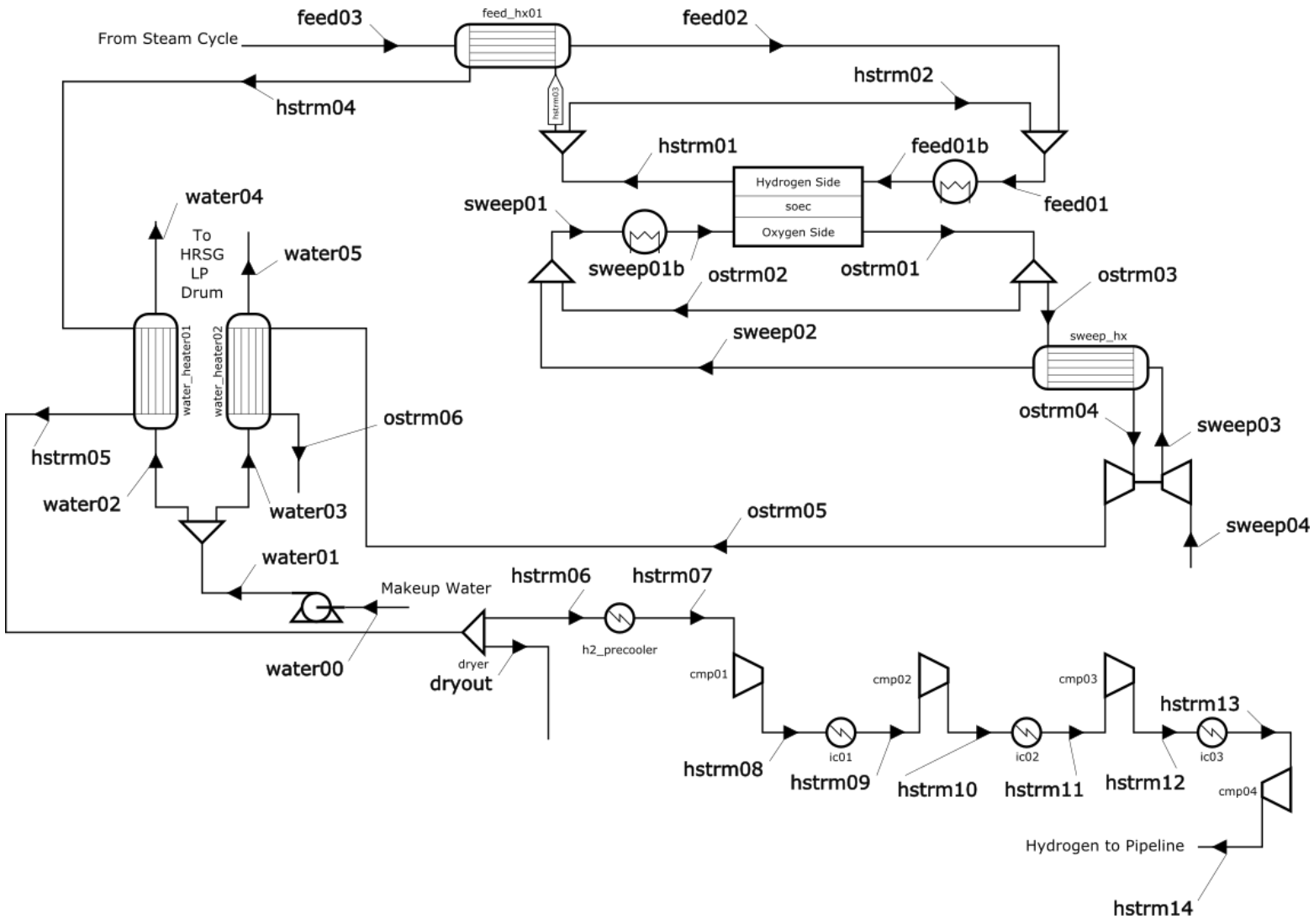

The H_2 compression section uses compression stages with fixed isentropic efficiency and intercoolers between stages. Currently, H_2 drying is not modeled. Zero-dimensional shell and tube heat exchangers with fixed heat transfer coefficients are used for the heat recovery. The two trim heaters for the SOEC feed and sweep are assumed to use resistance heating. Pressure drop is currently neglected.

The full NGCC model is described in Section 3. The operating conditions and some design parameters are optimized as will be described later in this section.

6.2 MAIN ASSUMPTIONS

The NGCC assumptions are described in Section 3. This section describes additional assumptions for the SOEC module.

The discretized SOEC model contains many design and model parameters. The SOEC is described in Section 2.1.6, and the model is available in the IDAES model repository. Compressors and expanders use a fixed isentropic efficiency and assume that the outlet pressure is set. Recovery heat exchangers use a fixed heat transfer coefficient and neglect pressure drop. The detailed SOEC model uses ideal gas properties. In the rest of the model, cubic EoS properties are used for multicomponent streams while the IAPWS-95 [32] proprieties are used for pure H_2O and steam.

6.3 PERFORMANCE AND COST ESTIMATION

The NGCC model from Case 0 is used to model the NGCC section. The NGCC includes 97 percent carbon capture and can produce 650 $MW_{e,net}$. The SOEC module can produce up to 5 kg/s of H_2 with LP steam extracted from the NGCC. When producing full H_2 output, about 58 MW_e must be purchased from the grid. While the SOEC can consume approximately 650 MW_e, the NGCC produces less due to steam extracted for the SOEC.

6.3.1 System Performance

Optimization was done in two steps. In the first step, design and operating parameters were optimized together at full load to determine optimal heat exchanger sizing and number of SOEC cells based on minimization of the fixed and variable costs. In the second step, design parameters were fixed, and operating parameters were optimized based on minimizing variable operating costs. The decision variables and constraints for optimization are shown in Exhibit 6-3, Exhibit 6-4, and Exhibit 6-5. Operating parameters can be optimized for off-design power and H_2 production, while design parameters cannot change.

Exhibit 6-3. Design decision variables

Variable	Lower	Upper	Optimal
Number of Cells	1,000,000	2,000,000	1,087,990
Sweep Recovery HX Area (m^2)	1,000	7,000	5,940
Feed Recovery HX Area (m^2)	1,000	7,000	6,990
Water Heater 1 Area (m^2)	1,000	7,000	5,700
Water Heater 2 Area (m^2)	1,000	7,000	7,000

Exhibit 6-4. Operating decision variables

Variable	Exhibit 6-2 Stream(s)/Unit	Lower	Upper	Full Capacity Optimal
Sweep Recycle Split Fraction	ostrm02, ostrm03	0.05	0.60	0.36
Steam Recycle Split Fraction	hstrm02, hstrm03	0.30	0.70	0.68
Makeup Water Heater Split Fraction	water02, water03	0.30	0.70	0.50
Sweep Inlet Flow (mol/s)	sweep04	100	8000	5653
SOEC Cell Potential (V)	soec unit	1.26	1.60	1.345
Sweep Trim Heater Temperature (K)	sweep01b	900	1020	933
Steam Trim Heater Temperature (K)	feed01b	900	1020	933
Sweep Trim Heater Duty (MW)	sweep_heater	0	8	0
Steam Trim Heater Duty (MW)	feed_heater	0	8	0

Exhibit 6-5. Constraints for optimization

Constraint
SOEC Makeup Water Flow = SOEC Extraction Steam Flow
Difference Between Any Two SOEC Cell Inlets/Outlets Temperatures ≤ 75 K
Local Temperature Gradient ≤ 750 K/m
Turbine Throttle Valve ΔP ≤ -0.5 Bar
SOEC Sweep/O_2 Outlet O_2 content ≤ 35%
SOEC Steam/H_2 outlet H_2O content ≥ 20%
SOEC Sweep/O_2 Outlet Temperature ≤ 1030 K
SOEC Steam/H_2 Outlet Temperature ≤ 1030 K
SOEC Sweep/O_2 Trim Heater Duty ≤ 8 MW
SOEC Steam/H_2 Trim Heater Duty ≤ 8 MW
Current Density ≤ 8000 A/m^2
IP/LP Crossover Pressure ≥ 2.9 Bar

The trim heaters were eliminated in the initial design optimization, but they are required for dynamic optimization, so the trim heater capacity was fixed to 8 MW. The components of the NGCC were only allowed to increase in capacity, so the NGCC can operate in standalone mode. For the off-design operation, constraints where add to prevent the system from exceeding design capacity.

6.3.2 Fixed Costs

The following equation can be used to scale the fixed cost to different maximum power outputs—in this case, maximum H_2 production cannot be scaled independently of power, so it is scaled by the same factor:

$$Fixed\ Cost\ \left[\frac{MM\$}{yr}\right] = 150.11\left(\frac{H_{2,max}}{5\ kg/s}\right)^{0.8} + 74.70\left(\frac{H_{2,max}}{5\ kg/s}\right)^{0.8}$$

Since steam is extracted from the NGCC steam turbine for the SOEC, the H_2 capacity cannot be independently resized. The following equation shows the relationship between power and H_2 capacity:

$$\frac{P_{max}}{H_{2,max}} = \frac{650\ MW}{5\ kg/s}$$

The fixed cost breakdown is given in Exhibit 6-6.

Exhibit 6-6. Fixed cost breakdown for the NGCC+SOEC

Fixed Cost Breakdown	97% Capture
TPC ($MM)	1,605.45
NGCC TPC ($MM)	1,437.79
Feedwater and Misc. BOP Systems	159.32
CO_2 Removal System	782.03
Combustion Turbine Generator	113.76
HRSG, Ductwork, and Stack	102.22
Steam Turbine Generator & Accessories	75.69
Cooling Water System	53.33
Accessory Electric Plant	80.41
Instrumentation and Control	24.83
Improvements to Site	28.38
Buildings and Structures	17.82
SOEC TPC ($MM)	167.68
SOEC Modules ($MM)	72.85
Trim Heaters ($MM)	25.18
H_2 compression ($MM)	21.10
Sweep Compressor/Turbine ($MM)	10.87
Heat Exchangers ($MM)	37.68
Total TASC ($MM)	**2,123.25**
Annualized Capital Cost ($MM/yr)	**150.11**
Fixed O&M Costs ($MM/yr)	**74.70**
Operating Labor ($MM/yr)	3.51
Maintenance Labor ($MM/yr)	12.20

Fixed Cost Breakdown	97% Capture
Admin & Support ($MM/yr)	3.93
Property Tax and Insurance ($MM/yr)	32.11
Maintenance Material ($MM/yr)	18.30
Stack Replacement ($MM/yr)	4.65
Total Annual Fixed Cost ($MM/yr)	**224.81**

6.3.3 Variable Costs

Optimization of the model is described in Section 6.3.1. To generate data points, the gas turbine power was varied from 480 MW_e to 305 MW_e in 5 MW_e increments, and H_2 was varied from 5 kg/s to 0.75 kg/s in 0.25 kg/s increments. This grid results in 528 data points. While gas turbine power can go lower, extending the range explored to lower net powers, the range explored was limited because 1) it was desired to operate in the relatively high efficiency range and 2) the NGCC at low output may reach a point where it produces insufficient steam for carbon capture and H_2 production.

Surrogate models for variable cost are provided as a function of net power in MW_e and H_2 production rate in kg/s. The net power includes the power used for the SOEC module, so it represents the power sold or purchased from the grid. Negative net power represents purchasing power. The fuel surrogate is also provided separately so the fuel price can be adjusted. The fuel cost used for the surrogate is $4.42/MMBtu. See Exhibit 6-7 for surrogates.

Exhibit 6-7. NGCC+SOEC variable cost surrogate models

Variable Cost Component	Variable Cost Model ($/hr)	R^2

Total	`27.34467 * net_power`
	`+ 3604.529 * h_prod`
	`+ 0.362858E-002 * net_power**2`
	`+ 202.2234 * h_prod**2`
	`- 18.72379 * h_prod**3`
	`+ 0.129705E-002 * (net_power*h_prod)**2`
	`+ 5125.909`
		0.9970

Fuel	`23.21237 * net_power`
	`+ 3027.882 * h_prod`
	`+ 0.308059E-002 * net_power**2`
	`+ 171.6582 * h_prod**2`
	`- 15.89132 * h_prod**3`
	`+ 0.1101224E-002 * (net_power*h_prod)**2`
	`+ 4351.539`
		0.9970

Other	`4.132305 * net_power`
	`+ 576.64691 * h_prod`
	`+ 0.5479886E-003 * net_power**2`
	`+ 30.565232 * h_prod**2`
	`- 2.8324722 * h_prod**3`
	`+ 0.1958348E-003 * (net_power*h_prod)**2`
	`+ 774.37067`
		0.9972

Constraints on the feasible range of operation are given in Exhibit 6-8, and plotted in Exhibit 6-9.

Exhibit 6-8. Net power and H_2 production feasible region constraints

Constraints
$P_{net} \geq 16.403 H_{prod} - 139.14$
$P_{net} \geq -146.02 H_{prod} + 475.62$
$P_{net} \leq -141.16 H_{prod} + 650.72$
$H_{prod} \geq 1.0$
$H_{prod} \leq 5.0$

Exhibit 6-9. Net power and H_2 production feasible region plot

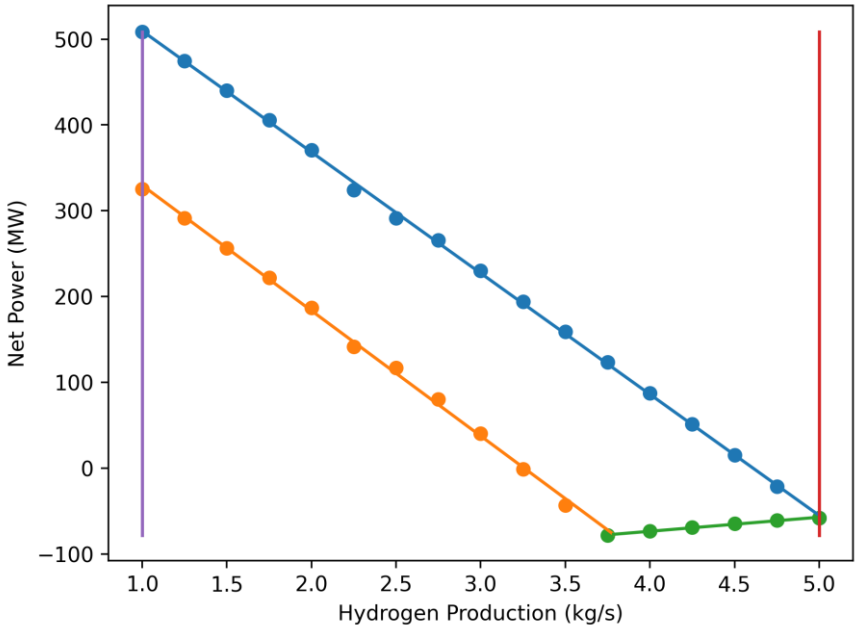

If there is no H_2 production, the NGCC surrogates for variable costs from Section 3.3.3 can be used along with the NGCC+SOEC fixed costs. There is some penalty for keeping the SOEC stack warm, but it is assumed to be negligible here.

Exhibit 6-10 shows the percent error in the total variable cost relative to the detailed process model for power and H_2 production.

Exhibit 6-10. Percent error in total variable cost surrogate model for NGCC+SOEC power and H_2 relative to the detailed process model

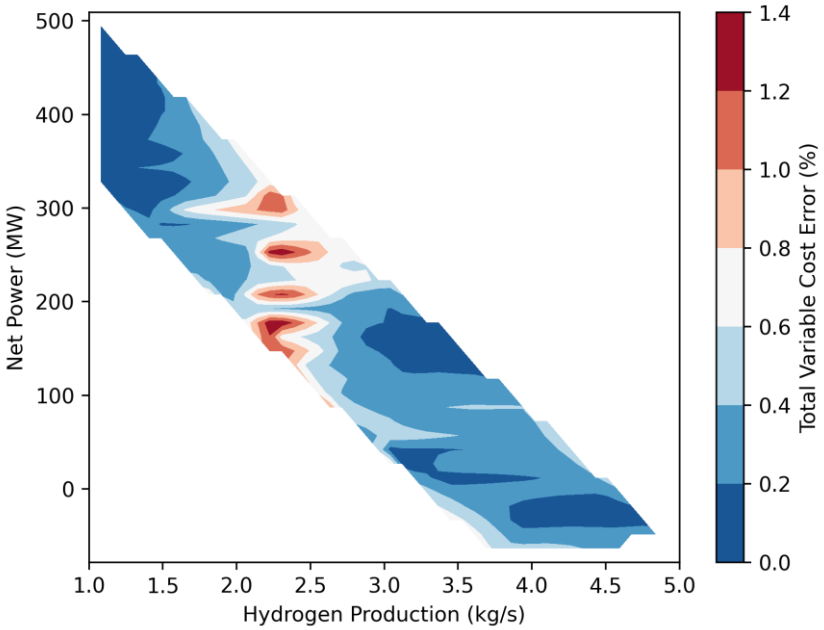

7 REVERSIBLE SOC

This section describes a NG-fed rSOC plant with a steam turbine bottoming cycle[h]. The rSOC plant operates in two distinct modes 1) SOFC mode in which power is produced by utilizing a NG feed and 2) SOEC mode in which H_2 is produced by utilizing electricity from the grid. The minimum carbon capture percentage in all operating modes is 98 percent.

7.1 SYSTEM DESCRIPTION

Exhibit 7-1 shows the process flow diagram of the rSOC plant in SOEC mode. The plant consists of five major sections: ASU, SOEC power island, CPU, HRSG, and steam cycle. Details and process description of the SOFC mode of the rSOC are provided in Section 4.1.

In the SOEC mode, the rSOC operates by using steam to produce H_2 on its fuel electrode side, while air is used as a sweep gas to remove O_2. To provide air to the air side of the rSOC, ambient air is compressed in a blower and preheated via two preheaters to reach the required temperature. The O_2-rich air stream that exits the air side of the rSOC is used to preheat the fresh air feed in the first air preheater; subsequently, it is used to both preheat the O_2 from the ASU in the O_2 preheater and the NG feed in the NG preheater. Finally, the O_2-rich air streams from both the O_2 and NG preheaters are sent to the HRSG where they are further cooled before release to the atmosphere.

To provide steam to the fuel side of the rSOC, H_2O at ambient conditions is pumped and heated to saturated conditions in a boiler feedwater heater. It then passes through the tube side (H_2O side) of an oxy-combustor boiler where it is superheated to the required temperature of the fuel side of the rSOC. In the rSOC, electricity from the grid is used to electrolyze the steam to produce H_2 and O_2. The O_2 diffuses across the electrolyte to the air side of the rSOC while the H_2/steam mixture exits from the fuel side. A part of the H_2/steam mixture is recycled through the fuel side to mitigate potential flow mal-distribution issues while the rest is used to heat H_2O in the boiler feedwater heater before being sent to the H_2 purification and compression unit where excess H_2O is removed and the H_2 is compressed to pipeline conditions.

To provide the required heat for the process, ambient air is compressed and sent to the ASU where a high-purity O_2 stream is produced. The O_2 stream is preheated and used to combust preheated NG in the fuel side of an oxy-combustor. The hot CO_2-rich flue gas from the oxy-combustor is used to preheat air (or sweep gas) to the required temperature for the air side of the SOEC in a second stage air preheater. The flue gas is then sent to the HRSG where it is further cooled to generate steam. Finally, H_2O is condensed and flashed out before the CO_2-rich gas is sent to the CPU where it is further dried, compressed, and purified to meet pipeline specifications.

[h] Found here: https://github.com/IDAES/publications/tree/main/netl_report_sofc_hydrogen_ies_2023/rsofc

Exhibit 7-1. SOEC process flow diagram

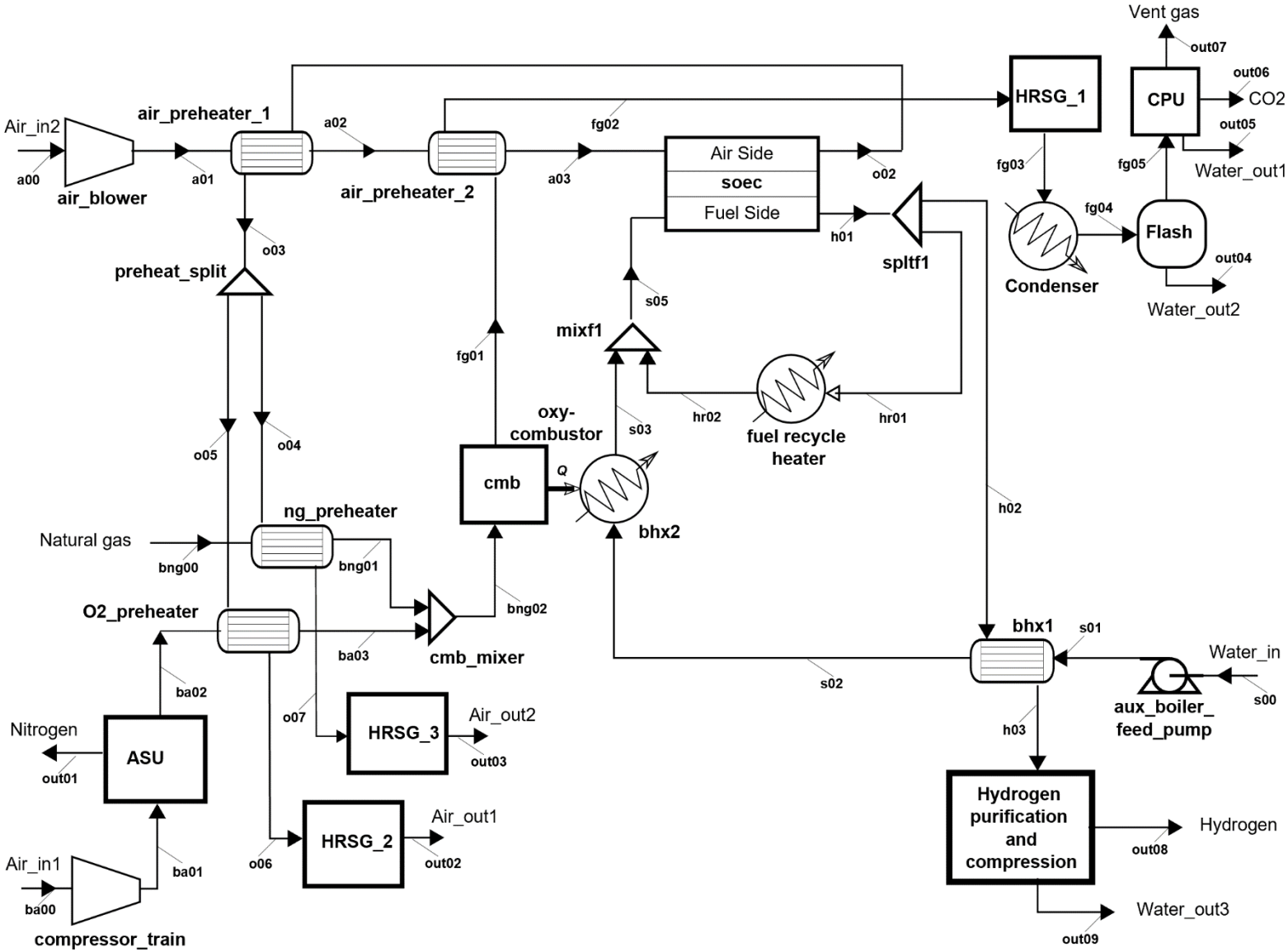

7.2 Main Assumptions

The assumptions for modeling the SOFC mode of the rSOC are the same as that of the SOFC case reported in Section 4.2. For the SOEC mode of the rSOC, the SOEC is modeled using the 2D SOEC cell model described in Section 2.1.6. Most of the flow sheet uses the generic IDAES cubic EoS property package, while the detailed SOEC model uses ideal gas properties. Exhibit 7-2 shows the main assumptions of the SOEC mode of the rSOC model.

Exhibit 7-2. Parameters used in the SOEC mode of the rSOC model

Parameter	Value
Blower isentropic efficiency, %	80
Air compressors isentropic efficiency, %	84
Intercooler outlet temperature, K	303.1
Number of cells of SOEC stack	3,222,000
Area per cell of SOEC stack, cm^2/cell	550
Steam cycle thermal efficiency, %	38.1
HRSG exit temperature, K	405

7.3 Performance and Cost Estimation

The rSOC plant is designed and costed with a maximum capacity of 650 $MW_{e,net}$ electricity output in the SOFC mode as basis. The SOFC mode flowsheet is based on Case ANGFC3B from the NGFC Pathways study [5] and is the same model reported for the SOFC in Section 4. Selecting this basis establishes the maximum electricity produced by the solid oxide cell (SOC) stack in the SOFC mode. Subsequently, this value is then used to calculate the number of cells the SOC stack has for a given area per cell. Since the SOC stack is used in both the SOFC and SOEC modes of the rSOC, the active cell area and the number of cells are the same in both modes. To be consistent with other cases, a maximum H_2 capacity of 5 kg/s was used. Since the current density in SOECs is generally higher than SOFCs, the stack is under-used in SOEC mode. Other SOEC mode equipment is sized for 5 kg/s H_2. There is some trade-off between electricity and H_2 price for varying H_2 capacity. Optimization of the H_2 capacity is a topic of potential further study and requires electricity and H_2 market forecasts.

The capital cost of the rSOC is a combination of equipment costs in both the SOFC and SOEC modes. Equipment that appears in both modes are costed at their maximum operational capacity between both modes. Fixed O&M costs are then calculated from the capital cost. The variable O&M cost is computed for the rSOC in both SOFC and SOEC modes. In the SOFC mode, the variable O&M cost is computed for variable electricity production, while in the SOEC mode it is computed for varying H_2 production.

7.3.1 System Performance

The operational performance of the rSOC in SOFC mode is reported in Case 1 for the SOFC (see Section 4.3.1). In the SOEC mode, the system performance for a given H_2 production capacity is

optimized to minimize the variable O&M costs. This is done by varying the recycle rate of H_2, sweep flow of air through the air side of the SOEC, the split ratio of hot air to the fuel and O_2 preheaters, the cell potential, the oxy-combustor outlet temperature, and the inlet temperatures into the SOEC subject to the flowsheet constraints (mass balance, momentum balance, energy balances etc.) of the flowsheet. A list of the operating decision variables for optimization is shown in Exhibit 7-3, while Exhibit 7-4 shows the optimization constraints. The base case operational performance of the system in SOEC mode is summarized in Exhibit 7-5.

Exhibit 7-3. Operating decision variables with optimal values for base case

Variable	Lower	Upper	Optimal
SOEC air inlet temperature (K)	273.15	1023.15	1023.15
SOEC fuel inlet temperature (K)	273.15	1023.15	1023.15
Oxy-combustor outlet temperature (K)	1100	2000	1264.70
Air sweep inlet flow (mol/s)	100	50000	5697.75
H_2O feed inlet flow (mol/s)	100	8000	3125.32
Steam recycle split fraction	0.02	0.50	0.481
Hot flue gas to O_2 preheater split fraction	0.30	0.99	0.528
SOEC cell potential (V)	1.03	1.40	1.251
Steam recycle heater temperature (K)	273.15	1023.15	1023.15

Exhibit 7-4. Constraints for optimization

Constraint
Difference Between Any Two SOEC Cell Inlets/Outlets Temperatures ≤ 40 K
SOEC Sweep/O_2 Outlet O_2 content ≤ 35%
SOEC Steam/H_2 outlet H_2O content ≥ 20%
SOEC Sweep/O_2 Outlet Temperature ≤ 1030 K
SOEC Steam/H_2 Outlet Temperature ≤ 1030 K
Current Density ≤ 8000 A/m^2
Single Pass H_2O Conversion ≥ 50 %

Exhibit 7-5. Base case operational performance summary of rSOC in SOEC mode

Variable	IDAES Model
SOEC power consumption (AC), MW_e	622.28
Net power process consumption, MW_e	660.31
H_2 production, kg/s	5
CO_2 captured, kg/s	10.271
NG feed, kg/s	3.94
H_2O utilization, %	80

7.3.2 Fixed Costs

Capital, fixed O&M, and variable O&M costs for the rSOC plant were estimated using the costing methodology detailed in Section 2.2. The equation for fixed costs as a function of the rSOC capacity is as follows:

$$Fixed\ Cost\ \left[\frac{MM\$}{yr}\right] = 73.65\left(\frac{P_{max}}{650\ MW}\right)^{0.77} + 51.69\left(\frac{P_{max}}{650\ MW}\right)^{0.779}$$

The first term represents the annualized capital cost and the second term the fixed O&M costs. The annualized capital cost contributes about 59.33 percent to the total fixed cost at 650 $MW_{e,net}$.

Since equipment is shared between the SOFC model and SOEC, the capacities cannot be resized independently. The equation below gives the relationship between the power and H_2 mode capacities:

$$\frac{P_{max}}{H_{2,max}} = \frac{650\ MW}{5\ kg/s}$$

The cost breakdown for total fixed cost is shown in Exhibit 7-6.

Exhibit 7-6. Cost breakdown for the rSOC base case simulation

Fixed Cost Breakdown	Model/Case
TPC ($MM)	**787.73**
Existing SOFC Equipment (Section 4.3.2)	**752.55**
SOEC Mode Equipment	**35.18**
H_2O/Steam Side Heat Exchangers	10.40
Steam Side Resistive Heater	1.20
Air Side Heat Exchangers	1.76
NG and O_2 Preheaters	0.60
H_2 Compressor	21.22
Owner's cost	165.42
TOC ($MM)	953.15
TASC ($MM)	**1041.79**
Annualized Capital Cost ($MM/yr)	**73.65**
Fixed O&M Costs ($MM/yr)	**51.69**
Annual Operating Labor	3.04
Maintenance Labor	5.99
Admin & Support Labor	2.26
Property Taxes & Insurance	15.75
Maintenance Material Cost	8.98
Stack Replacement Cost	15.68
Total Fixed Cost ($MM/yr)	**125.35**

7.3.3 Variable Costs

Variable costs for the operation of the rSOC system include costs of NG, H_2O, H_2O treatment chemicals, sulfur adsorbent, and electricity costs (during SOEC mode). Data for developing the surrogate models of the variable costs is generated by minimizing the total variable costs at each operating point. Details about the surrogate model development procedure and results in the SOFC mode are provided in Section 4.3.3. The rSOC mode models are provided here. The base case cost of electricity and NG used in generating the surrogate models in the SOEC mode are $30/MWh and $4.42/MMBtu, respectively. To develop the surrogates, the optimization was carried out over a range of H_2 production from 1.25 kg/s to 5.0 kg/s in step sizes of 0.25 kg/s for the rSOC in SOEC mode. The resulting variable cost surrogates are given in Exhibit 7-7. To adjust the electricity cost surrogate to a new electricity price, multiply the surrogate by x/($30/MWh), where x is the electricity price in $/MWh. To adjust the NG price for the gas surrogate, multiply the surrogate by y/($4.42/MMBtu), where y is the natural gas price in $/MMBtu based on HHV.

Exhibit 7-7. Variable cost surrogates

Variable Cost Component	Variable Cost Model ($/hr)	R^2
Total	`4594.055 * h_prod` `+ 3.341725 * h_prod**2`	0.9996
Electricity	`3957.829 * h_prod`	1.0000

Fuel	`506.8802 * h_prod`
	`+ 41.73345 * h_prod**2`
	`- 4.208053 * h_prod**3`
	`+ 86.31713`
		0.9783

Other	`23.36639 * h_prod`
	`- 0.1954561E-008 * h_prod**2`
	`+ 0.2203011E-009 * h_prod**3`
	`- 0.49380473E-008`
		1.0000

Exhibit 7-8 shows the percent error in the surrogate model for total variable cost for H_2 production relative to the detailed process model.

Exhibit 7-8. Percent error in total variable cost surrogate model for rSOC in H_2 mode relative to the detailed process model

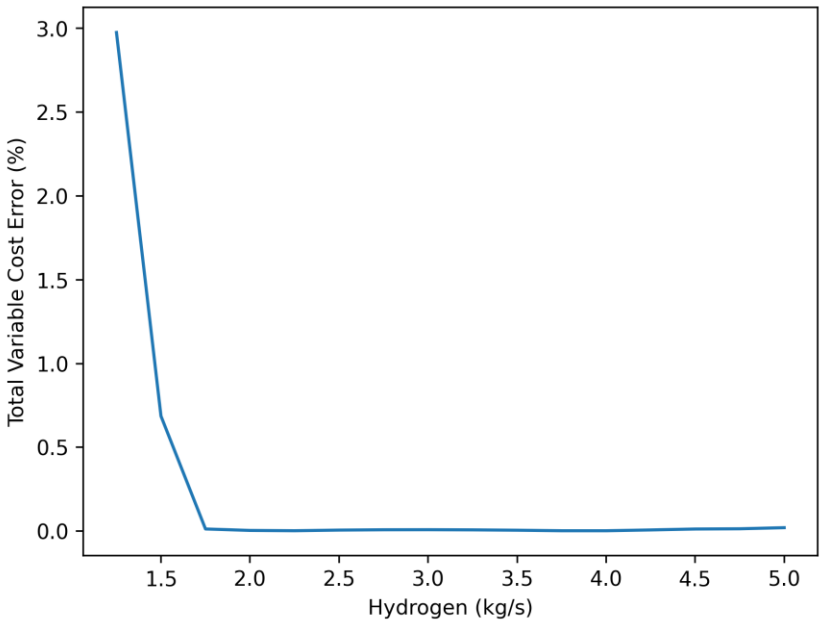

8 SOFC+SOEC

This section describes an electricity and H_2 co-generation plant containing SOFC and SOEC modules[i]. The modules can be operated independently allowing the plant to produce either electricity, H_2, or a combination of both. Waste heat from the SOFC module can be used to generate steam for the SOEC. The minimum carbon capture fraction in all models is 98 percent.

8.1 SYSTEM DESCRIPTION

Exhibit 8-1 shows the block flow diagram for the SOFC+SOEC plant illustrating the major mass and energy flows between sections of the plant. Air and NG are supplied to the SOFC to produce electricity. Unconsumed fuel in the anode exhaust is combusted in the oxy-combustor with O_2 supplied from an ASU. The maximum power generation capacity of the entire system is 712 $MW_{e,net}$ with the SOEC turned off.

If the SOEC heat duty requirement is larger than the SOFC anode exhaust can provide, additional NG and O_2 is supplied to the oxy-combustor to satisfy the steam demand. There are two options for the flue gas leaving the oxy-combustor. First, it can be used in the HRSG to power a steam cycle, or it can be used to generate steam for electrolysis. In either case, flue gas is sent to the CPU for carbon capture.

When both the SOFC and SOEC modules are operating, electricity from the SOFC and steam cycle can be used to power the SOEC. The system has been designed such that the SOFC can fully power the SOEC when both are operating at full capacity. If the SOECs are not operating, the power is supplied to the grid. The system also has the flexibility to supply excess power to the grid if electricity generated by the SOFC and steam cycle exceeds the SOEC demand.

[i] Found here: https://github.com/IDAES/publications/tree/main/netl_report_sofc_hydrogen_ies_2023/sofc_soec

Exhibit 8-1. Block flow diagram of the SOFC+SOEC IES

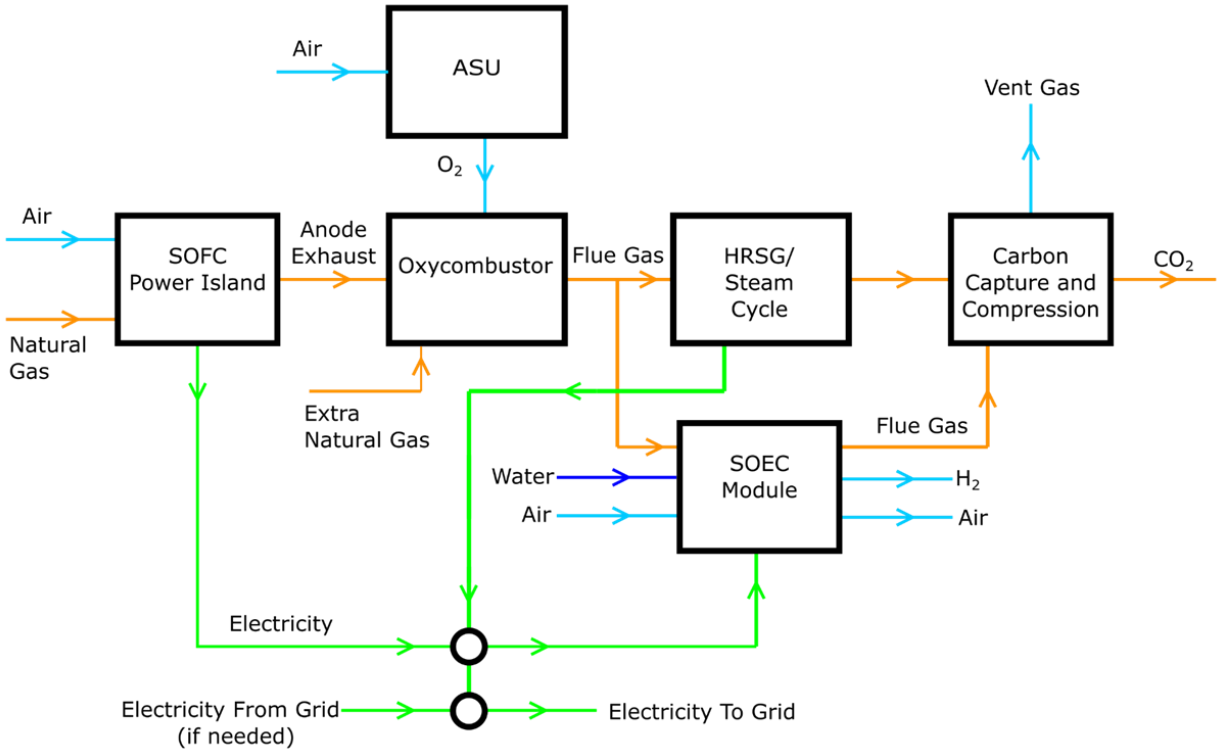

The SOFC power island, ASU, HRSG, and CPU are the same as in the SOFC case (Section 4) and will not be described again in this section. Exhibit 8-2 shows the process flow diagram for the SOEC section of the plant. The SOEC operates as described in previous cases, but the heat integration is different. Steam is generated with heat from the oxy-combustor, which is fueled by NG and/or SOFC anode exhaust. The fuel gas from the oxy-combustor can be used to generate steam for the SOEC or diverted to the HRSG to run a steam cycle. The flue gas passes through a steam superheater, a high-temperature air sweep heater, and a steam boiler before being sent to the CPU for capture and storage. Heat from the anode and cathode streams is also recuperated to heat the incoming streams.

Exhibit 8-2. SOEC process flow diagram

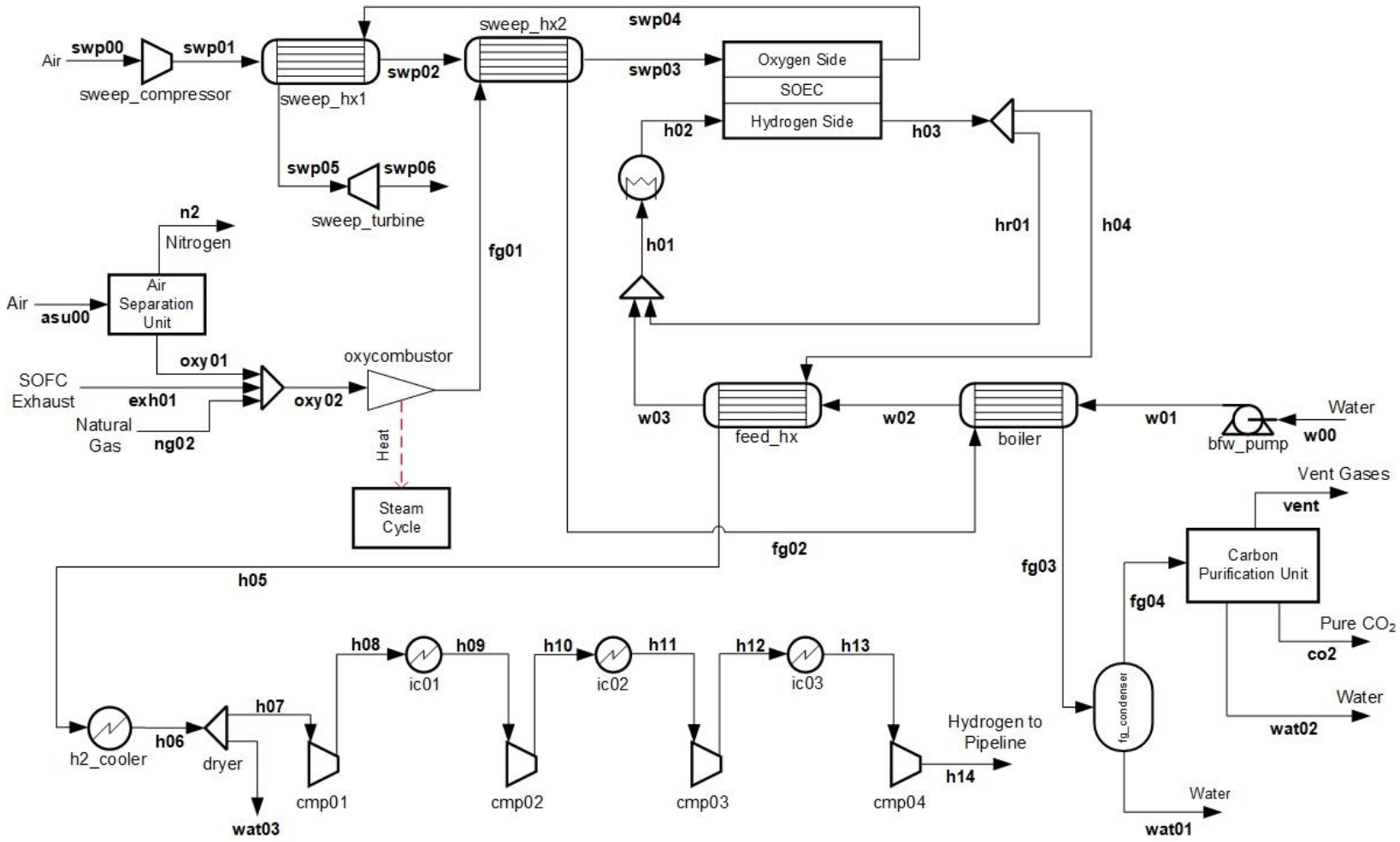

8.2 Main Assumptions

The assumptions for modeling the SOFC section of the SOFC+SOEC plant are identical to Case 1 and are reported in Section 4.2. The SOEC is modeled using the SOEC model described in Section 2.1.6. Exhibit 8-3 shows the main assumptions of the SOEC mode of the SOFC+SOEC plant.

Exhibit 8-3. Parameters used in the SOEC mode of the SOFC+SOEC model

Parameter	Value
Pump Isentropic Efficiency, %	85
Air Compressor Isentropic Efficiency, %	90
Air Expander Isentropic Efficiency, %	90
Heat Exchanger Overall Heat Transfer Coefficient, $W/m^2/K$	100
Area per SOEC Cell, cm^2	550

8.3 Performance and Cost Estimation

The SOFC+SOEC plant is sized to produce 5 kg/s of H_2 with 712 MW_e. The SOFC is large enough to cover the entire electricity demand of the SOEC. The SOFC section of the flowsheet is based on Case ANGFC3B from the NGFC Pathways study and is the same model reported in sections 4 and 7. Unlike the rSOC case, the SOFC and SOEC cells can be different sizes in this case.

The capital cost of the SOFC+SOEC plant is a combination of equipment costs from the SOFC and SOEC sections. Equipment that appears in both modes is costed at its maximum operational capacity. Fixed O&M costs are then calculated from the capital cost. The variable O&M cost is computed for the SOFC+SOEC system in both SOFC and SOEC modes. In the SOFC mode the variable O&M cost is computed for variable electricity production, while in the SOEC mode it is computed for varying H_2 production.

8.3.1 System Performance

An optimization of the design and operation of the SOFC+SOEC system was performed at maximum power and H_2 production by minimizing the sum of fixed and variable costs. The decision variables and constraints use in the optimization are shown in Exhibit 8-4 and Exhibit 8-5.

Exhibit 8-4. Design and operating decision variables

Variable	Lower	Upper	Optimal
Number of SOEC cells	1,000,000	2,000,000	1,101,995
Sweep HX 1 Area (m^2)	100	10,000	100
Sweep HX 2 Area (m^2)	100	10,000	1,137
Boiler Area (m^2)	100	10,000	4,865
Feed Recovery HX Area (m^2)	100	10,000	10,000
Steam Recycle Split Fraction	0.25	0.95	0.83
Air Sweep Flowrate (mol/s)	100	8,000	5,636
Oxy-combustor NG Flowrate (mol/s)	0	50,000	0
Steam Trim Heater Temperature (K)	900	1,020	990
SOEC Cell Potential (V)	1.26	1.38	1.303

Exhibit 8-5. Constraints for optimization

Constraint
Difference Between Any Two SOEC Cell Inlets/Outlets Temperatures ≤ 75 K
SOEC Sweep/O_2 Outlet O_2 Content ≤ 35%
SOEC Steam/H_2 Outlet H_2O content ≥ 20%
SOEC Sweep/O_2 Outlet Temperature ≤ 1030 K
SOEC Steam/H_2 Outlet Temperature ≤ 1030 K
Current Density ≤ 8000 A/m^2
H_2 Cooler Outlet Temperature ≥ 350 K
Flue Gas Cooler Outlet Temperature ≥ 350 K

8.3.2 Fixed Costs

Capital, fixed O&M, and variable O&M costs for the SOFC+SOEC plant were estimated using the costing methodology detailed in Section 2.2. The equation for fixed costs as a function of H_2 production is as follows:

$$Fixed\ Cost\ \left[\frac{MM\$}{yr}\right] = 119.45\left(\frac{H_{2,max}}{5\frac{kg}{s}}\right)^{0.8} + 77.92\left(\frac{H_{2,max}}{5\frac{kg}{s}}\right)^{0.8}$$

The first term represents the annualized capital cost and the second term the fixed O&M costs. The SOFC and SOEC sections must be scaled together to maintain the validity of the net power bounds given in the next section.

Since some equipment is shared between the SOFC and SOFC plants, the two sections cannot be independently sized. Only H_2 capacity is used to scale the fixed costs. The equation below relates the power capacity with H_2 production off to H_2 capacity:

$$\frac{P_{max}}{H_{2,max}} = \frac{712\ MW}{5\ kg/s}$$

The cost breakdown for total fixed cost is shown in Exhibit 8-6.

Exhibit 8-6. Cost breakdown for the SOFC+SOEC base case simulation

Fixed Cost Breakdown	IDAES Model, 98% Capture
TPC ($MM)	**864.94**
SOFC Modules	233.58
SOFC BOP	31.55
SOEC Modules	73.79
SOEC BOP	34.49
H_2 Compressor	21.10
Oxy-combustor	52.66
ASU	240.46
CPU	97.68
Feedwater & Miscellaneous BOP Systems	98.44
Heat Recovery Steam Generator	71.36
Steam Turbine Generator & Accessories	77.70
Cooling Water System	43.50
Generator Equip. and Access.	129.34
Control System	25.09
Site Preparation, Improvement, and Facilities	31.09
Various Building Structures	15.62
TOC ($MM)	**1,545.73**
TASC ($MM)	**1,689.48**
Annualized Capital Cost ($MM/yr)	**119.45**
Fixed O&M ($MM/yr)	**77.92**
Annual Operating Labor ($MM/yr)	3.51
Maintenance Labor ($MM/yr)	9.71
Admin & Support Labor ($MM/yr)	3.30
Property Taxes & Insurance ($MM/yr)	25.55
Maintenance Material Cost ($MM/yr)	14.56
SOFC Replacement Cost ($MM/yr)	16.58
SOEC Replacement Cost ($MM/yr)	4.71
Total Fixed Cost ($MM/yr)	**197.37**

8.3.3 Variable Costs

Contributions to the variable costs included NG, H_2O, H_2O treatment chemicals, sulfur adsorbent, and pre-reformer catalyst costs. Electricity costs are not included in the surrogates. If the amount of electricity required exceeds what is produced, the net power will be negative, and an appropriate cost can be assigned. The surrogates are written as a function of net power and H_2 production in Exhibit 8-7. Since net power was not directly manipulated to generate the surrogate models, the bounds on net power are given in Exhibit 8-8 and plotted in Exhibit 8-9.

Exhibit 8-7. Variable surrogates

Variable Cost Component	Variable Cost Model ($/hr)	R^2
Total, Hydrogen + Power Mode	3.501711 * net_power + 2771.341 * h_prod + 0.582662E-001 * net_power**2 - 0.571072E-004 * net_power**3 + 13.85955 * h_prod**3 + 4.485434 * net_power*h_prod - 0.197652E-002 * (net_power*h_prod)**2 + 1775.732	0.9972
Fuel, Hydrogen + Power Mode	4.578016 * net_power + 2685.456 * h_prod + 0.526439E-001 * net_power**2 - 0.515940E-004 * net_power**3 + 12.73327 * h_prod**3 + 4.057687 * net_power*h_prod - 0.178612E-002 * (net_power*h_prod)**2 + 1570.231	0.9975
Other, Hydrogen + Power Mode	-1.076292 * net_power + 85.88541 * h_prod + 0.562227E-002 * net_power**2 - 0.551328E-005 * net_power**3 + 1.126261 * h_prod**3 + 0.427743 * net_power*h_prod - 0.190403E-003 * (net_power*h_prod)**2 + 205.4984	0.9882
Total, Power Mode	23.29340 * net_power + 0.2625301E-003 * net_power**2 + 0.9633594E-006 * net_power**3 + 53.909399	1.0000
Fuel, Power Mode	22.49809 * net_power + 0.2478272E-003 * net_power**2 + 0.8949507E-006 * net_power**3 + 42.30072	1.0000
Other, Power Mode	0.7953093 * net_power + 0.1470292E-004 * net_power**2 + 0.6840869E-007 * net_power**3 + 11.60867	1.0000

Exhibit 8-8. Net power bounds

Model
$P_{net} \leq -142.06h_{prod} + 711.8$
$P_{net} \geq -120.46h_{prod} + 220.31$
$h_{prod} \leq 5.0$
$h_{prod} \geq 1.0$

Exhibit 8-9. Net power bounds plot

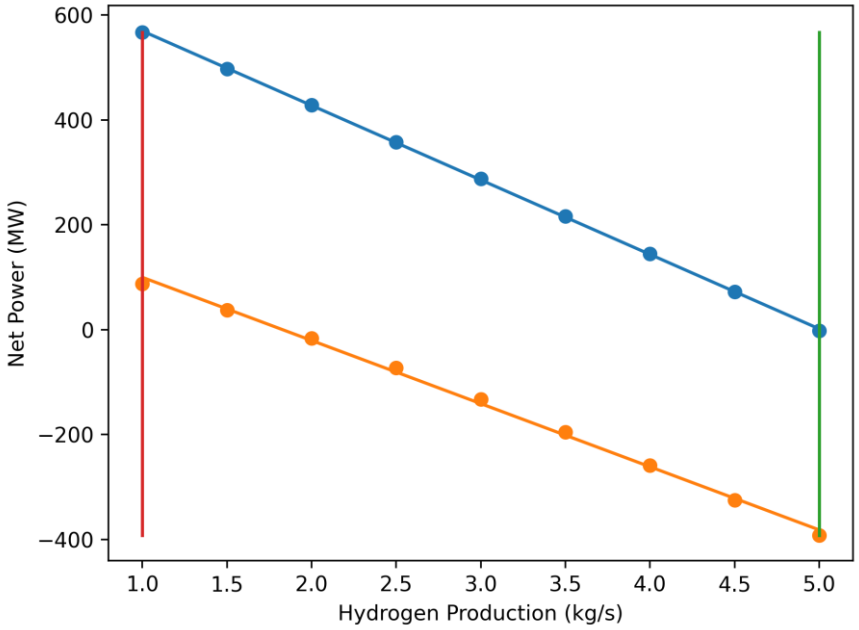

Exhibit 8-10 shows the percent error in the total cost surrogate model for power and H_2 production relative to the detailed process model.

Exhibit 8-10. Percent error in total variable cost surrogate model for SOFC+SOEC producing H_2 and power relative to the detailed process model

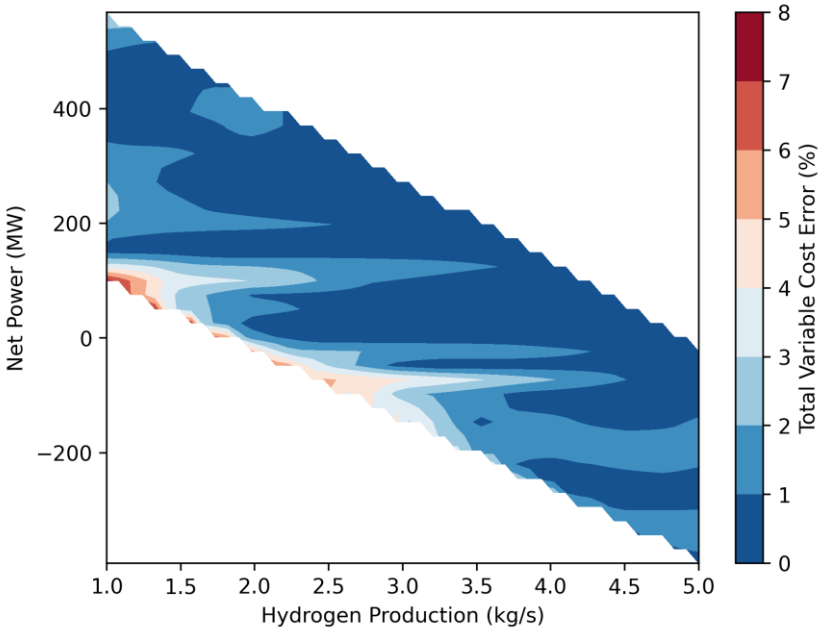

9 STANDALONE SOEC

This section describes a plant designed to produce 5 kg/s of H_2 gas by H_2O electrolysis in an SOEC[j]. The main feature distinguishing this plant from the rSOC plant in Section 7 is that it uses electrical heating instead of NG, eliminating the need for carbon capture equipment (i.e., the ASU and CPU). The SOEC is also designed specifically for electrolysis allowing a higher current density and smaller SOEC stack than the rSOC. Furthermore, there is no steam bottoming cycle, all electricity is imported from the grid. The electrolysis process described here requires only air, H_2O, and electricity as inputs.

9.1 SYSTEM DESCRIPTION

Conceptually, the plant can be divided into three main parts, 1) SOEC and associated auxiliary equipment, 2) H_2O evaporation system that provides steam, and 3) H_2 compression and drying. H_2 is compressed to a pressure of 64.8 bar. A heat pump is used to upgrade low-temperature heat from the drying and compression process to heat that can be used to evaporate H_2O. Exhibit 9-1 is a block flow diagram of the plant.

Exhibit 9-1. Block flow diagram of standalone SOEC plant

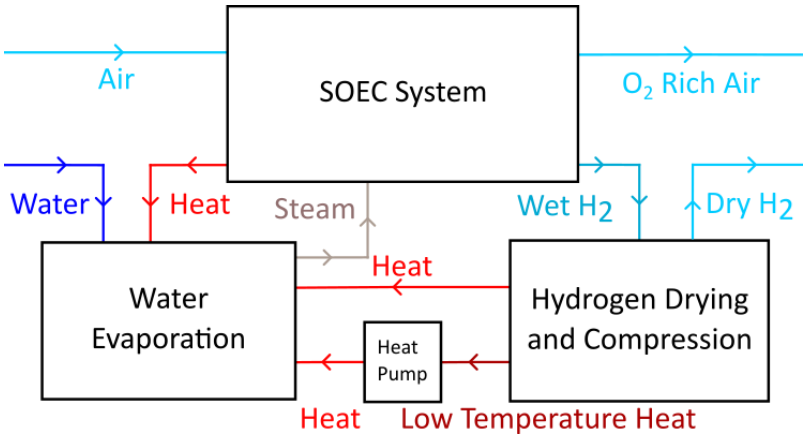

While these components can be separated conceptually, the actual process flow diagram cannot be separated easily. Exhibit 9-2 shows the full SOEC process. The H_2 drying and compression block is tightly linked with the H_2O evaporation block. This tight heat integration is primarily driven by a desire to avoid evaporation using resistive heating, which is expensive. Instead, heat from H_2 compression and the latent heat of H_2O in the H_2 stream is used to evaporate feedwater. The H_2 stream is repeatedly compressed, cooled in the H_2O evaporators, and run through a flash vessel to eliminate any condensate before being compressed again. Before the first compressor, the H_2 stream is diverted to preheat the H_2O feed to the evaporators, allowing more H_2O to be removed before the compression process begins.

[i] https://github.com/IDAES/publications/tree/main/netl_report_sofc_hydrogen_ies_2023/soec

Exhibit 9-2. SOEC flow diagram

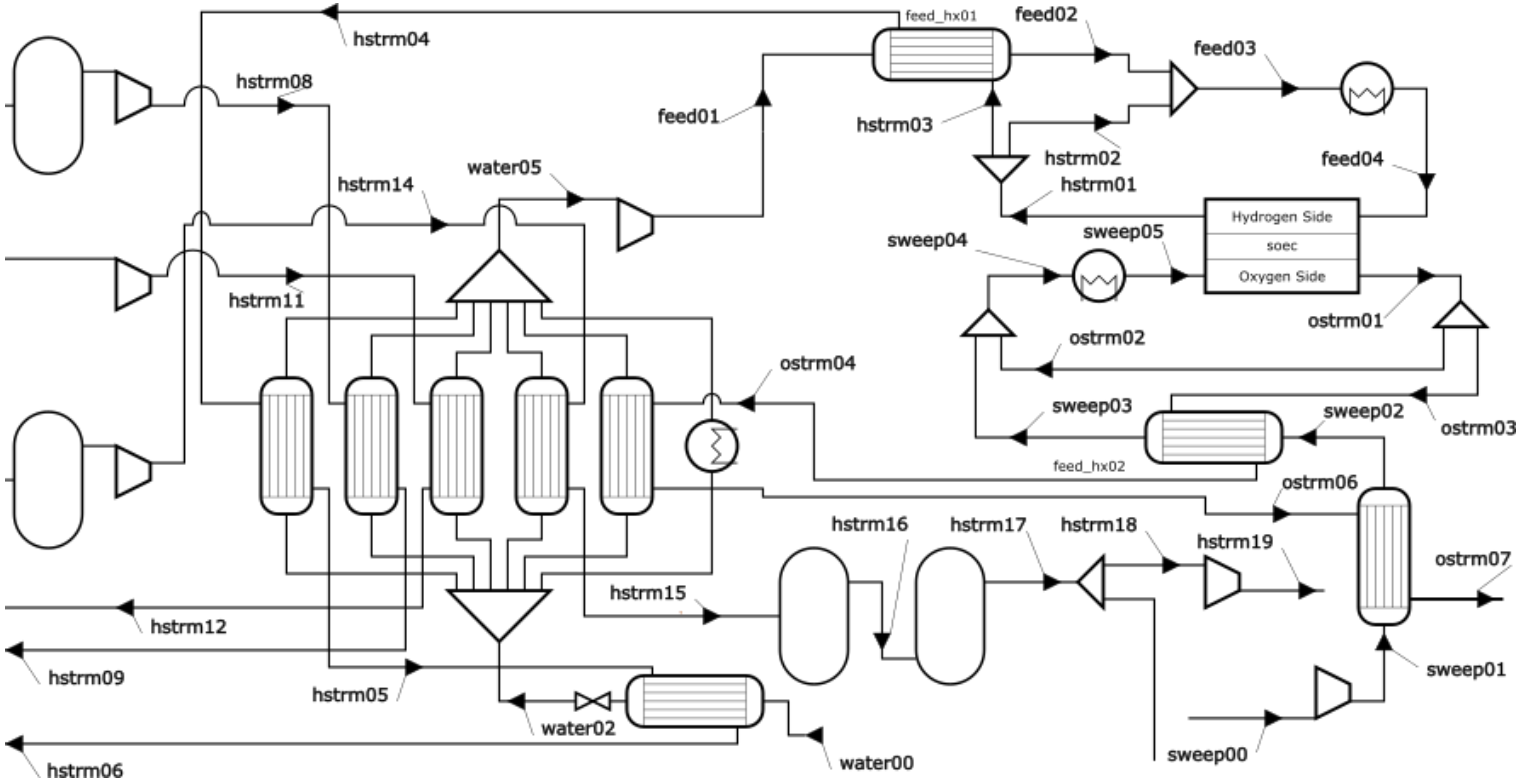

H_2O evaporation takes place at 0.4 bar to reduce the boiling point of H_2O to 76°C. This allows more H_2O to be condensed in the H_2 stream, and as a result, more of the latent heat can be utilized. However, even with this reduced evaporation temperature, after four passes through the evaporator, there are diminishing returns in H_2O removal from the H_2 stream. Chilled H_2O is then used to condense almost all H_2O remaining in the H_2 stream. The resulting stream has only 0.06 percent (mole basis) H_2O remaining in it, but H_2 pipeline specifications require it to have even less moisture. Industrially, either temperature-swing adsorption or a zero-loss adsorption dryer are used to reduce the H_2O content to below 1 ppm (mole basis) [33]. This final stage is not modeled, but the use of chilled H_2O in the prior condenser results in a relatively small drying burden.

In addition to using heat from the H_2 compression process, heat from the O_2-rich air from the SOEC is used to evaporate a portion of the feedwater. The remainder of the feedwater is evaporated using heat from the heat pump, which adsorbs heat from spent chilled H_2O, regenerating it in the process, and rejects heat to the final evaporator. Initially the idea of using a local body of H_2O as an additional source of heat for the heat pump was explored, but numerical optimization resulted in that heat source being eliminated in the steady state flowsheet. Nevertheless, some external source of heat may be necessary for plant startup and shutdown.

After evaporation, the H_2O vapor is compressed to 1.2 bar before being sent to the SOEC system. The steam is heated by the hot H_2 effluent from the SOEC. Air for use as sweep gas is pressurized to 1.2 bar by a blower before being preheated by the O_2-rich air stream. Because O_2 gas is generated in the SOEC, the returning stream has more heat available than the incoming air stream can use. As a result, the air stream is heated by the O_2-rich stream in two segments, with the O_2-rich stream being diverted to a H_2O evaporator between segments.

Some of the H_2 product stream is recycled and mixed with the steam feed, both to prevent degradation in the SOEC that may occur if no H_2 is present and to allow for a greater overall conversion while limiting the single-pass conversion to avoid risking steam starvation from gas maldistribution. The O_2-rich sweep is also partially recycled and mixed with incoming sweep gas to reduce the thermal gradient across the SOEC. Two trim heaters then bring the SOEC feeds to the SOEC inlet temperature.

9.2 MAIN ASSUMPTIONS

The main assumptions of the SOEC flowsheet model are listed in Exhibit 9-3.

Exhibit 9-3. SOEC flowsheet parameters

Parameter	Value
Blower Isentropic Efficiency (%)	80
Max Average Current Density (mA/cm$^{2)}$	800
Max Overall H_2O Conversion (%)	80
Max Fuel/Sweep Recycle Ratio	1.0
Max Sweep O_2 Content (%)	35
Min SOEC feed H_2 Content (%)	5
Condenser Overall Heat Transfer Coefficient (W/m^2/K)	200
Other Heat Exchanger Overall Heat Transfer Coefficient (W/m^2/K)	100
Cell Max Temperature (°C)	750
ΔT Across the Cell (°C)	75
Reciprocating Piston Compressor Efficiency (%)	85
Centrifugal Compressor Efficiency (%)	80
Heat Pump Coefficient of Performance	3.5

One tacit assumption is that the reciprocating piston compressors used for H_2 compression can handle the high outlet temperatures that are present in the flowsheet—some reach as high as 250°C. Because high temperatures are typically avoided in compression for process performance reasons, it is difficult to find information about technical limitations of the equipment. In this process, large pressure ratios are used across the reciprocating piston exchangers to ensure the partial pressure of H_2O in the H_2 product stream is large enough to condense at the temperature that the feed H_2O is being evaporated. The compression train could be reconfigured to have smaller pressure ratios across the individual compressors at the cost of additional heat exchangers to reject heat to the feedwater stream.

9.3 Performance and Cost Estimation

9.3.1 System Performance

Several unit models that are not present in the other cases require some explanation. The heat pump is modeled via a fixed coefficient of performance taken from a vendor brochure [34] for performance conditions close to those present in this flowsheet. Heat exchangers involving the heat pump are not modeled explicitly.

To determine the number of cells in the SOEC and heat exchanger sizing, optimization of the design and operating conditions at full H_2 capacity were optimized to minimize fixed and variable costs. Once the design is optimized at full capacity, the design variables are fixed. At H_2 capacities under 5 kg/s, only operating variables are optimized, and the objective includes only variable costs, since the fixed costs are constant.

Exhibit 9-4. Design decision variables

Variable	Lower	Upper	Optimal
Number of Cells	None	None	1,087,915
Water Evaporator 1 Area (m^2)	400	None	2018
Water Evaporator 2 Area (m^2)	400	None	1632
Water Evaporator 3 Area (m^2)	400	None	1513
Water Evaporator 4 Area (m^2)	400	None	5245
Water Evaporator 5 Area (m^2)	400	None	5267
Water Preheater Area (m^2)	400	None	1746
Feed Hot Exchanger Area (m^2)	400	None	4640
Sweep Hot Exchanger Area (m^2)	400	None	5522
Sweep Medium Exchanger Area (m^2)	400	None	8511

Exhibit 9-5. Operating decision variables

Variable	Exhibit 9-2 Stream(s)	Lower	Upper	Full Capacity Optimal
Sweep Recycle Split Fraction	ostrm02	0.03	0.50	0.5
Steam Recycle Split Fraction	hstrm02	0.02	0.50	0.5
Sweep Inlet Flow (mol/s)	sweep00	1,000	None	5,653
SOEC Cell Potential (V)	SOEC Stack	1.1	1.6	1.334
Sweep Trim Heater Outlet Temp. (K)	sweep05	873	1023	945
Steam Trim Heater Outlet Temp. (K)	feed04	873	1023	929

Exhibit 9-6. Constraints for optimization

Constraint
Difference Between Any Two SOEC Cell Inlets/Outlets Temperatures ≤ 75 K
Local Temperature Gradient ≤ 750 K/m
SOEC Sweep/O_2 Outlet O_2 Content ≤ 35%
SOEC Steam/H_2 Outlet H_2O Content ≥ 20%
SOEC Sweep/O_2 Outlet Temperature ≤ 1030 K
SOEC Steam/H_2 Outlet Temperature ≤ 1030 K
Average Current Density ≤ 8000 A/m^2
Maximum Current Density ≤ 10400 A/m^2

9.3.2 Fixed Costs

Capital, fixed O&M, and variable O&M costs for the standalone SOEC plant were estimated using the costing methodology detailed in Section 2.2. The heat pump was costed based on

costs from a vendor white paper [35] containing costs of a variety of installed systems. The cost from the largest installed system was multiplied by a factor of 2 to account for the fact that the systems contained in that white paper interfaced with an existing refrigeration system while this heat pump must be standalone and adjusted for process and project contingencies. A scaling exponent of 1 was used when scaling the cost by heat duty to generate a conservative estimate of costs.

$$Heat\ Pump\ Fixed\ Cost\ [MM\$] = 3.446\left(\frac{Q_{out}}{10.275\frac{MMBTU}{hr}}\right)$$

The centrifugal compressor had a detailed cost estimate in the original technical report [36]. This price was adjusted upward slightly to add a final cooler and adjust for inflation. A larger issue, however, is that the original design is constrained by material limitations, so it cannot be scaled larger. Therefore, for this process, two compressors in parallel are used with a cost exponent typical for centrifugal compressors:

$$Centrifugal\ Compressor\ Fixed\ Cost\ [MM\$] = 2 \times 4.241\left(\frac{F_{H_2}}{2 \times 240000\frac{kg}{day}}\right)$$

The overall fixed costs can be scaled for different H_2 capacities with the equation below:

$$Fixed\ Cost\ \left[\frac{MM\$}{yr}\right] = 41.08\left(\frac{H_{2,max}}{5\frac{kg}{s}}\right)^{0.8} + 26.08\left(\frac{H_{2,max}}{5\frac{kg}{s}}\right)^{0.8}$$

Exhibit 9-7 gives a detailed breakdown of the fixed costs for a 5 kg/s H_2 plant.

Exhibit 9-7. Fixed cost breakdown for the SOEC

Fixed Cost Breakdown	Cost
TPC ($MM)	**439.37**
SOEC Stack ($MM)	72.84
Trim Heaters ($MM)	25.18
Heat Pump ($MM)	34.77
H_2 Compression ($MM)	25.80
Water Compression ($MM)	45.96
Sweep Blower ($MM)	2.88
Heat Exchangers ($MM)	49.34
Flash Vessels ($MM)	0.45
Feedwater and Treatment Systems ($MM)	31.12
Accessory Electric Plant ($MM)	93.02
Instrumentation and Controls ($MM)	23.19

Fixed Cost Breakdown	Cost
Improvements to Site ($MM)	27.19
Buildings and Structures ($MM)	7.34
Total TASC ($MM)	**581.09**
Annualized Capital Cost ($MM/yr)	**41.08**
Fixed O&M Costs (MM/yr)	**26.08**
Operating Labor ($MM/yr)	2.76
Maintenance Labor ($MM/yr)	3.34
Admin & Support ($MM/yr)	1.53
Property Tax and Insurance ($MM/yr)	8.77
Maintenance Material ($MM/yr)	5.01
Stack Replacement ($MM/yr)	4.65
Total Annual Fixed Cost ($MM/yr)	**67.16**

9.3.3 Variable Costs

The SOEC variable costs consist primarily of electricity and H_2O. Although the H_2O cost is calculated, relative to the fixed costs, the H_2O cost is not significant. The price of electricity is assumed to be $30/MWh for the variable cost surrogates, so to adjust the electricity price, multiply the electricity price surrogate by ($x/MWh)/($30/MWh). To get the total adjusted variable cost, add other costs to the adjusted electricity cost. The other costs for this case consist entirely of H_2O.

Exhibit 9-8. Variable cost surrogates

Variable Cost Component	Variable Cost Model ($/hr)	R^2

Total	`4616.003 * h_prod`
	`- 59.29895 * h_prod**2`
	`+ 1.091159 * h_prod**3`
		1.0000

Electricity	`4128.190 * h_prod`
	`+ 37.92668 * h_prod**2`
	`+ 8.676711`
		1.0000

Other	`469.8077 * h_prod` `- 88.73857 * h_prod**2`	0.9946

Exhibit 9-9 shows percent error in the total variable cost surrogate model relative to the detailed process model.

Exhibit 9-9. Variable cost surrogates fit metrics

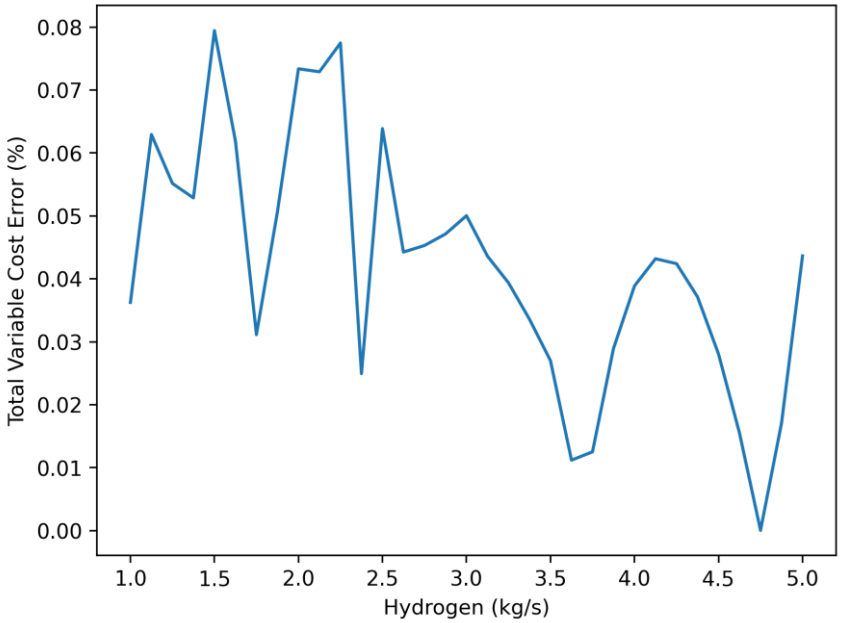

10 DISCUSSION OF RESULTS

This work provides steady state process and cost models for several types of SOFC/SOEC-based IES.

10.1 POWER GENERATION RESULTS

This section examines all cases capable of producing electricity in power only mode. The SOFC-based systems show significantly higher efficiency than NGCC-based systems and do not suffer from a loss of efficiency at part load. Exhibit 10-1 shows the estimated HHV efficiency over the load range for the 650 $MW_{e,net}$ capacity for NGCC and SOFC power plants.

Exhibit 10-1. NGCC and SOFC efficiency across load range

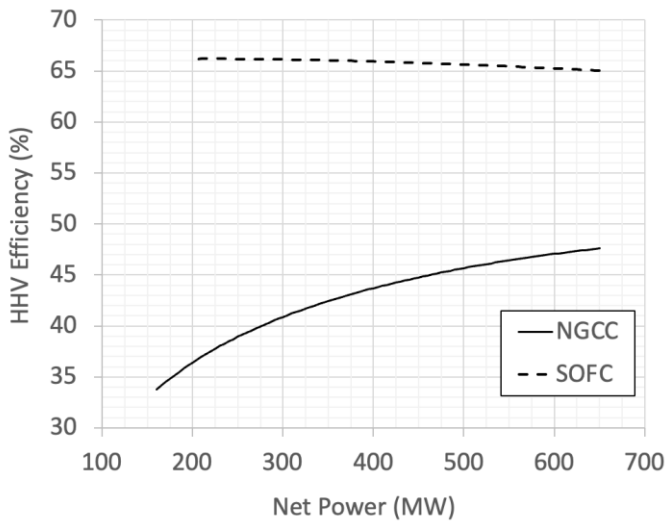

Exhibit 10-2 shows the cost breakdowns of systems producing 650 $MW_{e,net}$ (100 percent capacity) with two NG prices ($4.42 and $8.0/MMBtu) and no H_2 production. Key observations include the following:

- SOFC-based systems are lower cost than NGCC-based systems due to their higher efficiencies as well as lower capital and fixed O&M.
- Ranking the systems from lowest to highest cost of electricity gives 1) SOFC, 2) rSOC, 3) SOFC+SOEC, 4) NGCC, and 5) NGCC+SOEC.
- Electricity costs from the SOFC, rSOC, and SOFC+SOEC systems are similar.

Exhibit 10-2. Power production cost breakdown (2018 dollars)

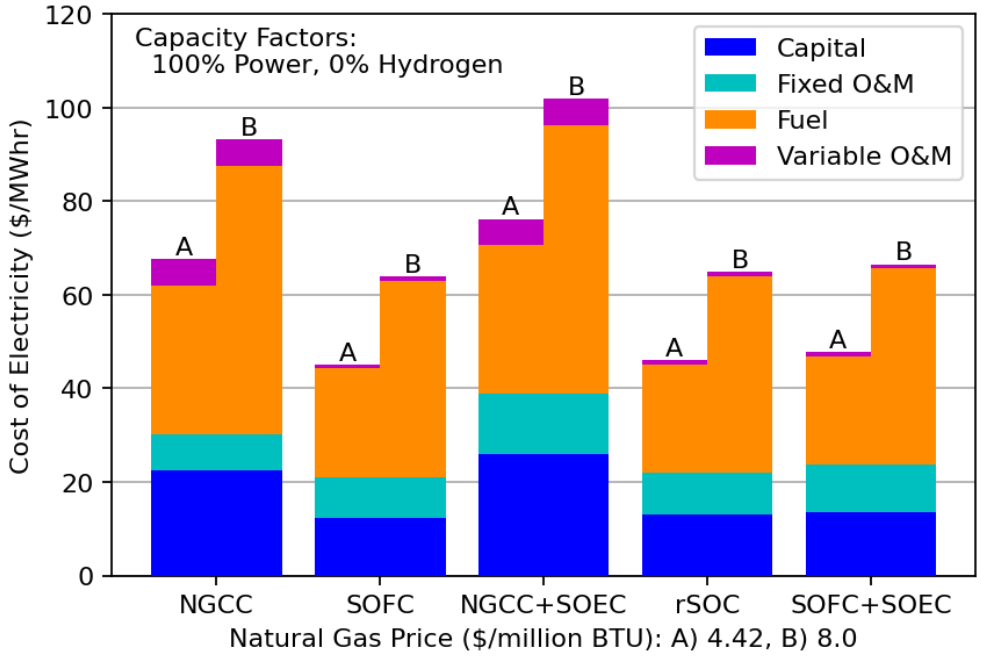

The break-even electricity prices are shown in Exhibit 10-3 as a function of NG prices. As expected, the SOFC-based cases can achieve a profit at much lower NG and electricity prices than the NGCC-based processes due to their higher efficiencies.

Exhibit 10-3. Break-even NG prices (2018 dollars)

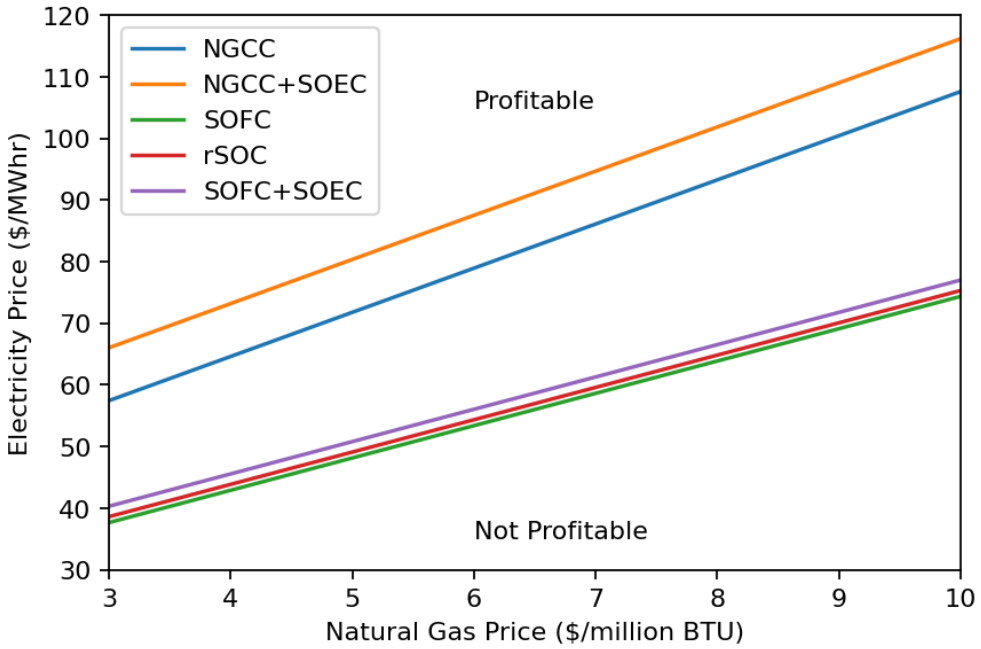

10.2 HYDROGEN GENERATION RESULTS

The cost breakdown for systems producing 5 kg/s of H_2 (100 percent capacity) is shown in Exhibit 10-4 at different NG and electricity prices. Key observations include the following:

- The system capable of producing H_2 at the lowest cost depends on the assumed prices of electricity and NG.
- The cost of H_2 produced from the NGCC+SOEC system is more dependent on NG price than the SOFC+SOEC system due to the lower efficiency of NGCC compared to SOFC-based power generation.
- At the lowest electricity price ($30/MWh), the SOEC enables lowest cost H_2 production followed closely by the SOFC+SOEC and rSOC systems.
- At the highest electricity price ($100/MWh), the systems with the flexibility to produce their own electricity, the SOFC+SOEC and NGCC+SOEC, can provide H_2 at the lowest cost.

It should be noted, however, that at electricity prices of $71.7/MWh and $100/MWh, the rSOC system has the flexibility to operate in electricity generation mode at a profit rather than produce H_2 at such a high cost. The SOEC system does not have this flexibility.

Exhibit 10-4. Cost breakdown for H_2 production (2018 dollars)

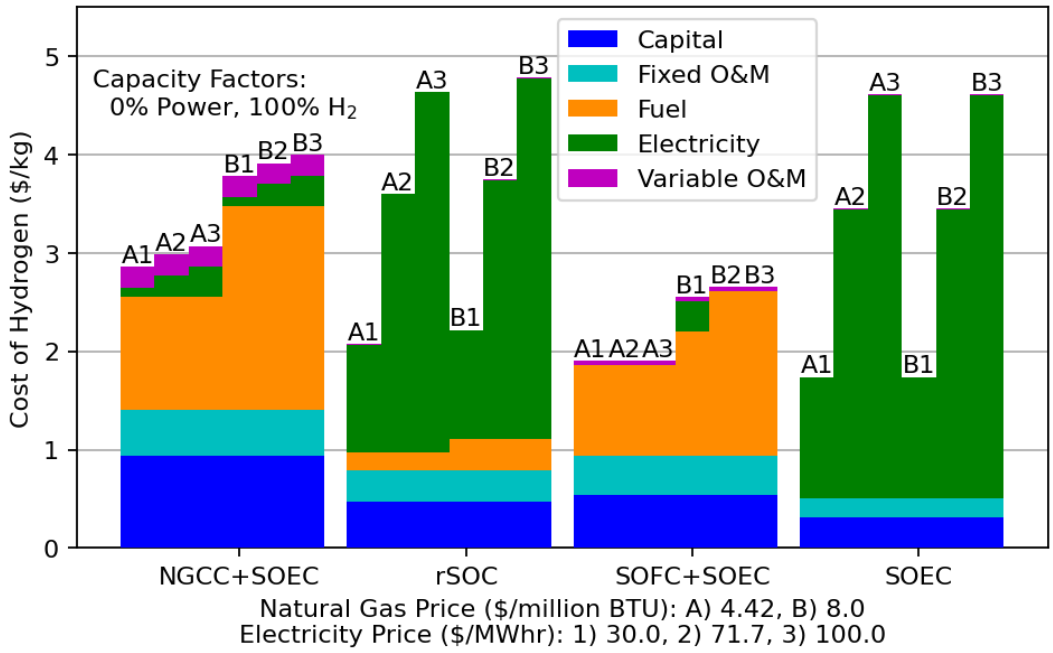

Exhibit 10-5 shows the comparison of performance indicators between all H_2 generating systems. These indicators were calculated over the full system including power generation where applicable. The rSOC and SOEC do not generate power while producing H_2, so their efficiencies are higher since they do not include power generation efficiency. The SOFC+SOEC has a significantly higher overall efficiency than the NGCC+SOEC due to the significantly higher efficiency of the SOFC relative to the NGCC. The rSOC is less efficient than the SOEC since it

burns some NG and requires carbon capture. The efficiency is calculated as the H_2 HHV with units of kWh/kgH_2 divided by the sum of the thermal input and the electricity input with units of kWh/kgH_2.

Exhibit 10-5. Key performance indicators for H_2 generating systems

Performance Indicator	Case 3 NGCC+SOEC	Case 4 rSOC	Case 5 SOFC+SOEC	Case 6 SOEC
H_2 production (kg/s)	5.0	5.0	5.0	5.0
H_2O flow to SOEC (kg/s)	55.9	56.3	55.9	55.9
Single pass stack conversion (%)	56.4	66.7	71.1	66.7
Overall conversion (%)	80.0	80.0	80.0	80.0
Number of cells (MM cells)	1.088	3.220	1.107	1.088
Cell voltage (V)	1.35	1.25	1.30	1.33
Current density (A/m^2)	8,000	2,725	8,000	8,000
SOEC AC load (MW_e)	663.6	622.2	638.2	638.5
Balance of plant load (MW_e)	18.3	45.2	98.1	81.3
Gross power generated (MW_e)	623.9	0.0	734.7	0.0
Total load (MW_e)	681.9	667.5	736.3	719.8
NG flow (kg/s)	26.0	3.9	21.0	0.0
Electrical input ($kWhr/kgH_2$)	37.9	36.8	0.1	40.0
Thermal input ($kWhr/kgH_2$)	81.6	11.4	61.1	0.0
H_2 efficiency (%)	-	81.7	-	83.3
Power/H_2 efficiency (%)	46.4	-	64.4	-

Exhibit 10-6 and Exhibit 10-7 show the break-even costs for the H_2 producing systems at NG prices of $4.42/MMBtu, and $8.0/MMBtu. The curves represent zero-profit for each system. Areas under the curves toward lower electricity and H_2 prices are not profitable, while areas above the curves toward higher H_2 and electricity prices are profitable. To simplify this analysis, it was assumed that the sale and purchase price of electricity are the identical. Key observations include the following:

- At low electricity prices, the standalone SOEC is the lowest cost system for H_2 production, followed by the rSOC, SOFC+SOEC, and NGCC+SOEC, respectively.
- At electricity prices higher than $38/MWh (for $4.42/MMBtu NG) and $52/MWh (for $8.0/MMBtu NG), the SOFC+SOEC system becomes more favorable than the standalone SOEC due to its ability to generate its own electricity for H_2 production.
- At electricity prices higher than $60/MWh (for $4.42/MMBtu NG) and $82/MWh (for $8.0/MMBtu NG), the NGCC+SOEC system becomes more advantageous than the standalone SOEC.

Regarding the integrated systems, there are different price points where the rSOC or SOFC+SOEC are the most favorable, due to the rSOC using mostly purchased electricity from the grid and the SOFC+SOEC mostly generating its own electricity. For example, the rSOC system is preferred over the SOFC+SOEC system below $25/MWh and above $45/MWh (for $4.42/MMBtu NG) and below $41/MWh and above $62/MWh (for $8.0/MMBtu NG). Between those ranges, the SOFC+SOEC process is the preferred system due to its ability to generate its own electricity for H_2 production. The NGCC+SOEC is the least favorable among the IES processes.

This analysis suggests that the value proposition for the SOFC/SOEC IES concepts centers on future electricity prices being bimodal (e.g., distinct periods of low and high electricity prices)—a reasonable possibility in future high variable renewable energy grids. If electricity prices are anticipated to be consistently low, the standalone SOEC process (or even reforming-based processes) will outperform the integrated systems. If electricity prices are anticipated to be very high, the standalone SOFC process will outperform the integrated systems as it is the least-cost means to generate electricity. However, if electricity prices are expected to fluctuate frequently between low and high values, then the rSOC process may confer a distinct advantage over the standalone systems by enabling a higher overall capacity factor. Furthermore, although the SOFC+SOEC process is higher cost than the rSOC process under most electricity-H_2 price pairings, it has a major advantage over the rSOC in that it can insulate itself from high electricity prices by producing its own electricity. This can be quite useful if minimum H_2 demands are placed on the system and turning down at high electricity prices is not possible.

Exhibit 10-6. Break-even prices for $4.42/MMBtu gas (2018 dollars)

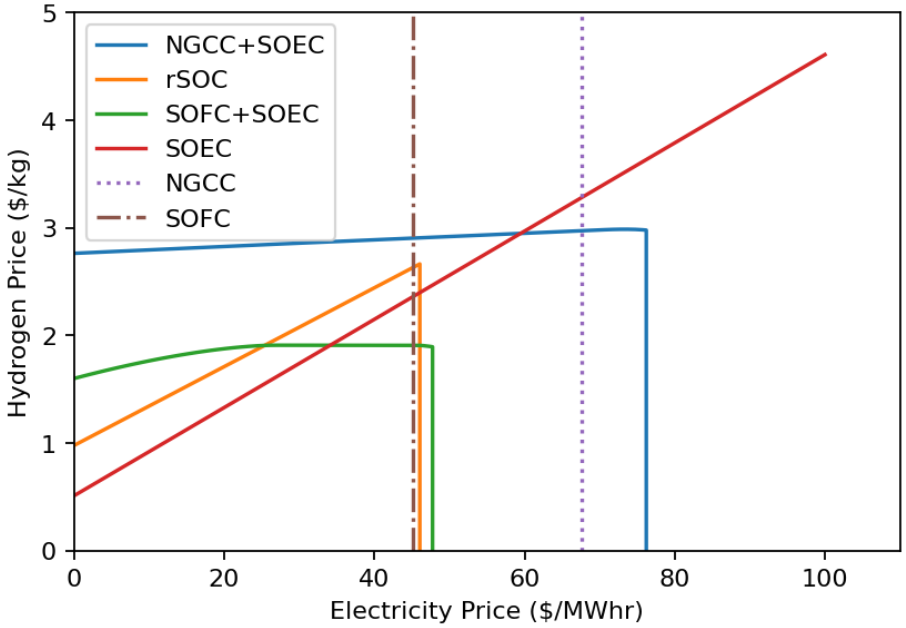

Exhibit 10-7. Break-even prices for $8/MMBtu gas (2018 dollars)

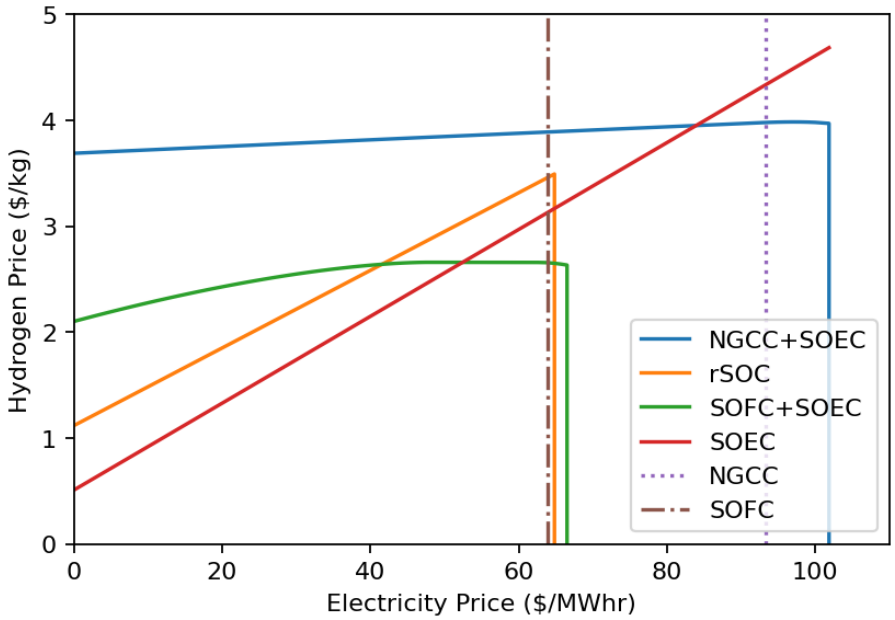

10.3 Greenhouse Gas Emission Results

A cradle-to-gate LCA was carried out to quantify the CO_2 equivalent emissions and determine the GWP for each of the technologies studied. The LCA was carried out for the technology operations in both power generation and H_2 generation modes. Emissions considered across all modes include emissions associated with the import of NG and electricity, and the direct emissions from the plant. In the case of the power production technologies, the emissions of each technology are evaluated at the base case net power production, while for the H_2 production technologies, the emissions are evaluated at the base case H_2 production. Two scenarios are evaluated for the H_2 production technologies. In the first scenario, electricity import is assumed to have emissions equivalent to a grid with a U.S. average consumption mix, while for the second scenario electricity import is assumed to have emissions equivalent to a solar PV-based grid. These scenarios allow the impact of different electricity grids on the GWP of each technology to be evaluated.

For the H_2 production technologies, two cases are evaluated for the SOFC+SOEC technology. In the first case, the SOFC is run at minimum load and the maximum amount of electricity possible is imported to run the SOEC and produce the base case amount of H_2 (5 kg/s), while in the second case there is no net electricity import nor export and the SOFC is run to provide only the electricity needed to run the SOEC and BOP equipment to produce the base case amount of H_2.

Exhibit 10-8 and Exhibit 10-9 summarize the breakdown of the calculations for GHG emissions for the power production and H_2 production technologies, respectively. Total GHG emissions associated with NG import to the plants are calculated from the cradle-to-gate emissions intensity of the NG import (14.1 $kgCO_2e/GJ$) [23], the HHV of NG (52.295 MJ/kg), and the flowrate of NG (kg/hr) into the plant for each technology. Total GHG emissions associated with electricity import to the plants are computed as cradle-to-gate emissions intensity of the

electricity import (403.345 $kgCO_2e/MWh$ for a U.S. average consumption mix [24], and 46 $kgCO_2e/MWh$ for solar PVs) [26], and the electricity consumption (MW_e) of each technology. The cradle-to-gate emissions values are adjusted by a factor of 5.1 percent [25] to account for transmission and distribution losses. Finally, direct plant emissions are obtained from the simulation results for each technology and include CO_2 emissions from combustion of natural gas and air used in the processes.

Exhibit 10-8. Breakdown of GHG emissions for power production technologies

Parameter	NGCC w/o capture	SOFC w/o capture	NGCC w capture	SOFC w capture	SOFC+SOEC
Natural gas input, kg/hr	93,272	65,408	93,409	67,973	77,196
Net power produced, $MW_{e,net}$	727	650.125	646	647.1	654
% CO_2 capture at plant	0	0	97	98	98
Plant emissions, $kgCO_2e/hr$	248,466	172,099	7,508	5,676	6,713
NG emissions, $kgCO_2e/hr$	68,775	48,229	68,876	50,120	56,921
CO_2 emissions ($kgCO_2e/MWh$-net)	**317,241**	**220,328**	**76,384**	**55,796**	**63,635**

Exhibit 10-9. Breakdown of GHG emissions for H_2 production technologies

Parameter	SMR w/o capture	SMR w capture	NGCC+ SOEC	rSOC, SOEC mode	SOFC + SOEC, max. power import	SOFC + SOEC, zero power import	SOEC
Natural gas input, kg/hr	70,979	75,472	93,424	14,186	50,510	77,196	0
Electricity input, MW_e	13	41	49	641.6	505.8	0	719.3
H_2 production rate, kg/hr	20,125	20,125	18000	18000	18000	18000	18000
% CO_2 capture at plant	0	96.2	97	98	98	98	0
Plant emissions, $kgCO_2e/hr$	188,070	7,661	7,778	7,807	7,274	6,955	269
NG emissions, $kgCO_2e/hr$	52,337	55,650	68,887	10,460	37,244	56,921	0
Electricity emissions, $kgCO_2e/hr$							
U.S. average consumer mix	5,525	17,426	20,826	272,711	214,988	-	305,715
Solar PV	630	1,987	2,375	31,102	24,519	-	34,866
Total CO_2 emissions, $kgCO_2e/kgH_2$							
U.S. average consumer mix	**12.22**	**4.01**	**5.42**	**16.17**	**14.42**	**3.55**	**17.00**
Solar PV	**11.98**	**3.24**	**4.39**	**2.74**	**3.84**	**3.55**	**1.95**

Exhibit 10-10 and Exhibit 10-11 show the life cycle emissions for the power production and H_2 production technologies, respectively.

The following observations can be made for the power production technology results shown in Exhibit 10-10:

- The technology with the highest GWP is the NGCC without capture, which has emissions of 436.37 $kgCO_2e$/MWh-net. The biggest contributor to its emissions is the direct emissions from the plant, which account for 78 percent.
- The technology with the lowest GWP is the SOFC with capture, which has emissions of 86.23 $kgCO_2e$/MWh-net with NG emissions contributing 90 percent to the total emissions. Note that the SOFC with capture model is also the same model for the rSOC operating in SOFC mode so the emission results are the same.
- The SOFC without capture technology has lower emissions than the NGCC without capture technology. This is primarily due to the lower amount of natural gas per MWh-net required by the SOFC without capture technology. The same analogy applies to the comparison between the SOFC with capture technology and the NGCC with capture technology.
- Finally, the SOFC+SOEC technology has the second lowest emissions ($kgCO_2e$/MWh-net) after the SOFC with capture. This is because though the SOFC+SOEC produces the maximum net amount of power possible, the SOEC is not totally shutdown, and a minimum amount of H_2 (0.5 kg/s) is still produced meaning that extra power and, thus, extra natural gas (and its associated emissions) in comparison to the SOFC with capture technology is needed.

For the H_2 production technology results shown in Exhibit 10-11, the following observations can be made:

- The type of grid greatly impacts which technology has the highest and lowest emissions. For example, when a U.S. average grid is considered, the standalone SOEC has the highest emissions of ~17 $kgCO_2e/kgH_2$ while the solar PV grid it has the lowest emissions of ~2 $kgCO_2e/kgH_2$.
- The rSOC has a similar emissions profile to the standalone SOEC but with slightly fewer extremes. When the U.S. average grid is considered, the rSOC has the second highest emissions of ~16.2 $kgCO_2e/kgH_2$ while for the solar PV grid, it has the second lowest emissions of ~2.7 $kgCO_2e/kgH_2$. For the U.S. average grid scenario, the grid electricity emissions constitute 94 percent of the rSOC emissions, while it accounts for 64 percent of the emissions of the corresponding case for the solar PV scenario albeit at a significantly lower value.
- The SOFC+SOEC with zero power import has the third lowest emission profile among the technologies considered for both the U.S. average grid and the solar PV grid (both have emissions of ~3.6 $kgCO_2e/H_2$), as no electricity import emissions are associated with it. However, the SOFC+SOEC with maximum electricity import has the second highest emissions (~14.4 $kgCO_2e/kgH_2$) for the U.S. average grid scenario because of the large amount of electricity import (~506 MW_e) needed.
- When the current U.S. average grid is considered, the SMR w/o capture technology has lower emissions than several of the assessed technologies such as the standalone SOEC, the rSOC and the SOFC+SOEC with maximum electricity import, which all consume a large

amount of electricity for H_2O electrolysis. This highlights the need for these technologies to use carbon-free electricity to play an attractive role in decarbonization.

- The SMR with capture technology has lower emissions across both grid scenarios than the NGCC+SOEC technology mainly because of the higher amount of NG per unit of H_2 product that is needed by the NGCC+SOEC (5.19 kg/kgH_2) in comparison to the SMR with capture (3.75 kg/kgH_2).

When considering IES technology options and looking at the CO_2 emissions results from both the power production and H_2 production modes, it can be observed that the rSOC technology is promising across both modes only when electricity imports from a renewable-based grid such as a solar PV grid is an option. However, the SOFC+SOEC technology is promising across both power and H_2 production modes when H_2 production is carried out without electricity import from the grid (SOFC+SOEC zero power import case).

Exhibit 10-10. CO_2e life cycle emissions for technologies in power production mode

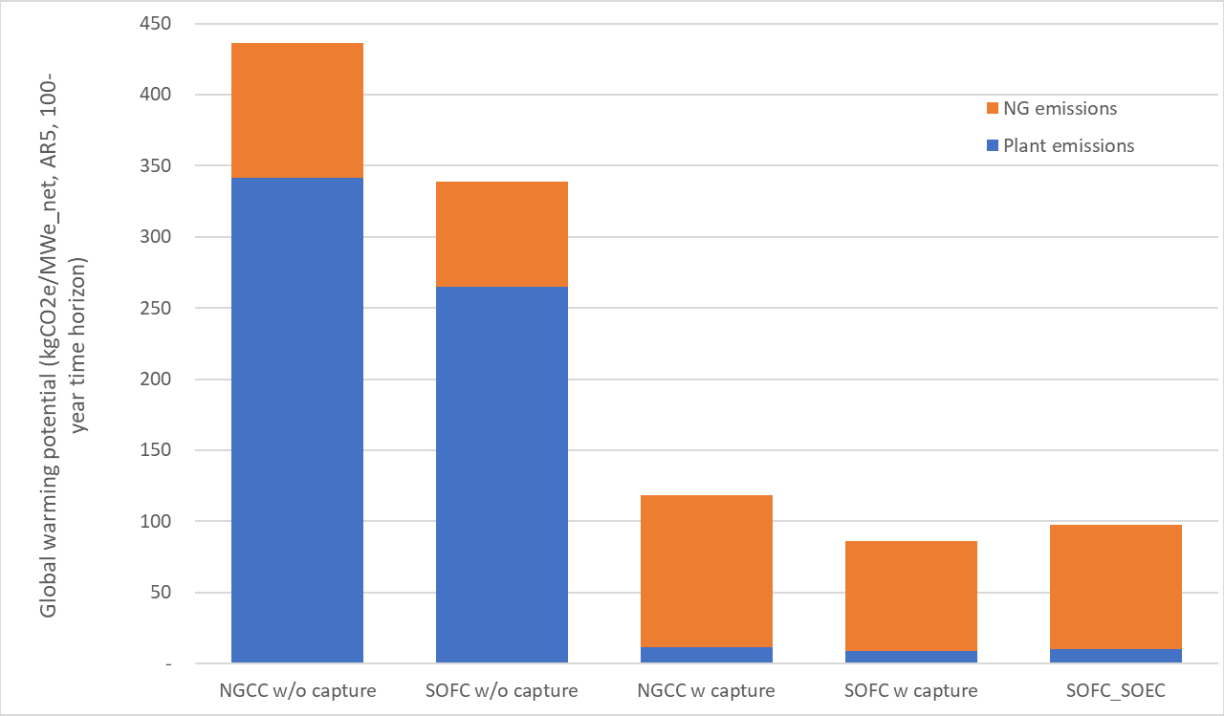

Exhibit 10-11. CO_2e life cycle emissions for technologies in H_2 production mode

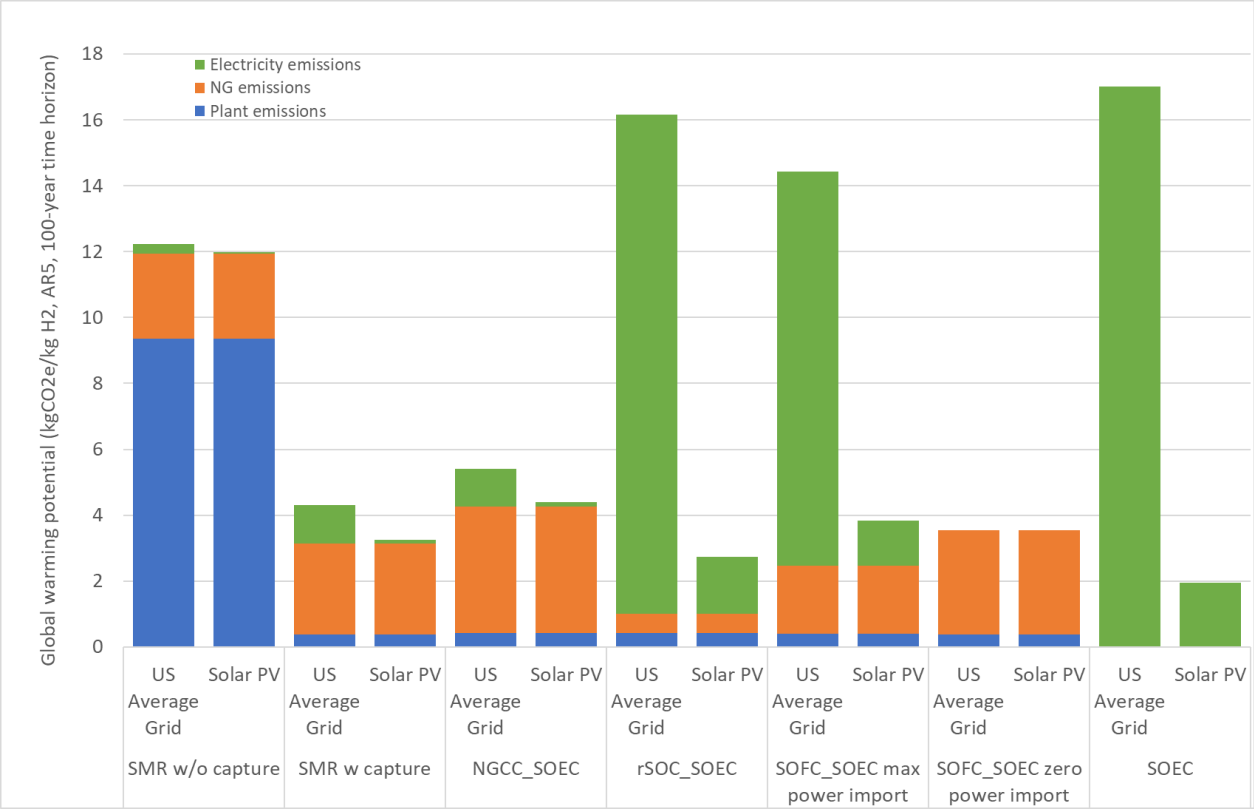

11 CONCLUSIONS

Models and cost surrogates for six different integrated energy systems were developed and presented in this report. A preliminary sensitivity analysis is also presented to understand the relative performance and costs of these IES. However, a detailed market analysis is needed to derive more insight into which system will be more profitable given different market forecasts. Nevertheless, the results from the sensitivity analysis included in this report provide useful information to inform the detailed market analysis.

11.1 MODEL CONCLUSIONS

Relative to the SOFC-based systems, NGCC systems are not competitive. SOFC systems are almost always preferred if SOFC development goals assumed in this report are met. The SOFC/SOEC technology is not currently commercially available and is at an approximate TRL of 6.

The analysis described herein reveals that the best overall system is highly dependent on the assumed prices and demands of electricity and H_2. The SOFC+SOEC configuration appears to be the best choice when the market is expected to have a reasonably stable midrange electricity price. The rSOC seems to be most beneficial when the electricity price shows a bimodal distribution with prices being low roughly the same amount of time as they are high. Bimodal distributions may be expected in high renewable energy markets. When wind and solar output are high electricity may be cheap, but at peak demand or when wind and solar are not producing sufficient power, electricity may be expensive. Where there is a significant amount of cheap electricity, the SOEC option may be best. The SOEC running only on electricity does not need power generating or carbon capture equipment. This makes fixed costs relatively low among the systems studied. As the electricity costs approach zero the SOEC can produce the cheapest H_2 relative to other options.

Depending on the level of deployment of renewable energy and carbon capture in a particular market, SOFC-IES systems have the potential to produce fewer greenhouse gas emissions than SMR with capture and depending on natural gas and electricity prices may produce less costly H_2 than SMR.

11.2 FOLLOW-UP WORK

The market analysis work considering varying prices of natural gas, power, and H_2 over time will follow this report and will be submitted to a peer-reviewed journal.

11.3 POTENTIAL FURTHER WORK

This section provides suggestions for additional work based on the conclusions of this work.

- Design optimization was done at maximum capacity for this work. Additional work could use the expected market conditions to develop a set of scenarios assigned different probabilities to get a better estimate of actual plant operation over time. This can be

used in a design-under-uncertainty-like problem to find a design that performs better under the actual expected operating conditions.

- This work focused on paired power and H_2 capacities, such that the power generation was roughly matched to the electrical capacity. Further work can examine smaller H_2 generation capacity. This would allow for continuous co-generation and allow the power and H_2 capacities to be independently scaled in the market optimization problem. Smaller H_2 capacities may also improve integration opportunities, since the extraction of steam or heat from the power system will have less impact.
- A smaller rSOC system that generates more H_2 relative to the power production could be modeled to more fully use the SOC stack in SOEC mode. Market analysis could then look at the trade-off in power to H_2 ratio. Increasing the H_2 production capacity relative to electric power capacity decreases the cost of H_2 but increases the cost of electricity generated.
- A modular rSOC system could be considered where some portion of rSOC modules can generate power while other modules generate H_2. This option potentially combines benefits of rSOC and SOFC+SOEC cases and greatly increases flexibility.
- The SOEC system makes sense in a market with a high portion of renewables where low electricity prices can be expected much of time. At peak demand, electricity prices may be high in such a market when renewables cannot meet demand. Peak demand can be met by fossil energy systems such as NGCCs or SOFC, but also through energy storage. The SOEC could operate as an SOFC at peak power prices potentially serving as an energy storage solution in addition to generating H_2.
- Systems including compressed air storage, whether the SOFC+CAES system presented here or other configuration, could potentially take advantage of the increased CO_2 partial pressure in the compressed air to enhance direct air capture. There is potential to leverage the models developed in this work to develop novel synergistic systems that integrate CAES, H_2 generation and storage, and direct air capture.

12 REFERENCES

[1] R. James, A. Zoelle, D. Keairns, M. Turner, M. Woods and N. Keuhn, "Cost and Performance Baseline for Fossil Energy Plants Volume 1: Bituminous Coal and Natural Gas to Electricity," DOE/NETL, Morgantown, 2019.

[2] R. Newby and D. Keairns, "Analysis of Natural Gas Fuel Cell Plant Configurations - Revision 1," DOE/NETL, Pittsburgh, 2013.

[3] A. Lee, J. H. Ghouse, J. C. Eslick, C. D. Laird, J. D. Siirola, M. A. Zamarripa, D. Gunter, J. H. Shinn, A. W. Dowling, D. Bhattacharyya, L. T. Biegler, A. P. Burgard and D. C. Miller, "The IDAES process modeling framework and model library—Flexibility for process simulation and optimization," *Journal of Advanced Manufacturing and Processing,* vol. 3, no. 3, 2020.

[4] E. Lewis, S. McNaul, M. Jamieson, M. S. Henriksen, S. H. Matthews, J. White, L. Walsh, J. Grove, T. Shultz, T. J. Skone and R. Stevens, "Comparison of commercial, state-of-the-art, fossil-based hydrogen production technologies, DOE/NETL-2022/3241," NETL, 2022.

[5] A. Iyengar, A. Noring, J. K. Mackay and D. Keairns, "Techno-economic Analysis of Natural Gas Fuel Cell Plant Configurations," DOE/NETL, Pittsburgh, 2020.

[6] NETL, "Quality Guidelines for Energy System Studies: CO2 Impurity Design Parameter," DOE/NETL, March 2012.

[7] NETL, "Advanced Oxy-combustion Technology for Pulverized Bituminous Coal Power Plants," DOE/NETL, April 20, 2015.

[8] E. Liese, "Modeling of a Steam Turbine Including Partial Arc Admission for Use in a Process Simulation Software Environment," *Journal of Engineering for Gas Turbines and Power,* vol. 136, no. 11, 2014.

[9] Q. Fang, L. Blum and N. H. Menzler, "Performance and Degradation of Solid Oxide Electrolysis Cells in Stack," *Journal of The Electrochemical Society,* vol. 162, no. 8, pp. F907-F912, 2015.

[10] D. Bhattacharyya, R. Rengaswamy and C. Finnerty, "Dynamic modeling and validation studies of a tubular solid oxide fuel cell," *Chemical Engineering Science,* vol. 64, no. 9, pp. 2158-2172, 2009.

[11] D. A. Noren and M. A. Hoffman, "Clarifying the Butler-Volmer equation and related approximations for calculating activation losses in solid oxide fuel cell models," *Journal of Power Sources,* vol. 152, no. 1-2, pp. 175-181, 2005.

[12] P. Kazempoor and R. J. Braun, "Model validation and performance analysis of regenerative solid oxide cells: Electrolytic operation," *International Journal of Hydrogen Energy,* vol. 39, no. 6, pp. 2669-2684, 2014.

[13] B. Shri Prakash, S. Senthil Kumar and S. T. Aruna, "Properties and development of Ni/YSZ as an anode material in solid oxide fuel cell: A review," *Renewable and Sustainable Energy Reviews,* vol. 36, pp. 149-179, 2014.

[14] F. R. Bianchi, R. Spotorno, P. Piccardo and B. Bosio, "Solid Oxide Fuel Cell Performance Analysis through Local Modelling," *Catalysts,* vol. 10, no. 5, p. 2020.

[15] P. Pianko-Oprych, T. Zinko and Z. Jaworski, "Computational Fluid Dynamics calculation of a planar solid oxide fuel cell design running on syngas," *Chemical and Process Engineering,* vol. 38, no. 4, pp. 513-521, 2017.

[16] A. Rohatgi, "WebPlotDigitizer," August 2021. [Online]. Available: https://automeris.io/WebPlotDigitizer.

[17] K. A. Klise, B. L. Nicholson, A. Staid and D. L. Woodruff., "Parmest: Parameter Estimation Via Pyomo," *Computer Aided Chemical Engineering,* vol. 47, pp. 41-46, 2019.

[18] Y. Du, T. Gao, G. T. Rochelle and A. S. Bhown, "Zero and negative-emissions fossil-fired power plants using CO2 capture by conventional aqueous amines," *International Journal of Greenhouse Gas Control,* vol. 11, p. 1034732, 2021.

[19] NETL, "Quality Guidelines for Energy System Studies: Cost Estimation Methodology for NETL Assessments of Power Plant Performance," DOE/NETL, Feb 2021.

[20] W. D. Seifer, J. D. Seader, D. R. Lewin and S. Windagdo, Process and Product Design principles: Synthesis, Analysis, and Evaluation, John Wiley and Sons, 2009.

[21] A. Cozad, N. V. Sahinidis and D. C. Miller, "Learning surrogate models for simulation-based optimization," *AIChE Journal,* vol. 60, no. 6, pp. 2211-2227, 2014.

[22] IPCC, "Climate Change 2014: Synthesis Report. Contribution of Working Groups," IPCC, Geneva, 2014.

[23] S. Rai, J. Littlefield, S. Roman-White, G. G. Zaimes, G. Cooney and T. J. Skone, "Industry partnerships and their role in reducing natural gas supply chain GHG emissions - phase 2," DOE/NETL, 2021.

[24] EPA, "eGRID Download Data," 2019. [Online]. Available: https://www.epa.gov/egrid/download-data. [Accessed 7 June 2022].

[25] EPA, "eGRID2019 Technical Guide," 2019. [Online]. Available: https://www.epa.gov/sites/default/files/2021-02/documents/egrid2019_technical_guide.pdf.

[26] NREL, "Life Cycle Greenhouse Gas Emissions from Solar Photovoltaics (Fact Sheet)," DOE/NREL, Golden, 2012.

[27] G. T. Rochelle, "Piperazine Advanced Stripper (PZASTM) Front End Engineering Design (FEED) Study on NGCC," DE-FE0031844, August 17, 2020.

[28] Y. Wang, D. Bhattacharyya and R. Turton, "Multiobjective Dynamic Optimization for Optimal Load-Following of Natural Gas Combined Cycle Power Plants under

Stress Constraints," *Industrial & Engineering Chemistry Research,* vol. 60, pp. 14251-14270, 2021.

[29] Y. Wang, D. Bhattacharyya and R. Turton, "Evaluation of Novel Configurations of Natural Gas Combined Cycle (NGCC) Power Plants for Load-Following Operation using Dynamic Modeling and Optimization," *Energy & Fuels,* vol. 34, pp. 1053-1070, 2020.

[30] Thermoflow Inc., "Thermoflow," 2022. [Online]. Available: https://www.thermoflow.com/index.html.

[31] K. Mongird, V. Viswanathan, J. Alam, C. Vartanian, V. Sprenkle and R. Baxter, "2020 Grid Energy Storage Technology Cost and Performance Assessment," PNNL, 2020.

[32] W. Wagener and A. Pruß, "The IAPWS Formulation 1995 for the Thermodynamic Properties of Ordinary Water Substance for General and Scientific Use," *Journal of Physical and Chemical Reference Data,* vol. 31, no. 387, 2002.

[33] A. Peschel, "Industrial perspective on hydrogen purification, compression, storage, and distribution," *Fuel Cells,* vol. 20, no. 4, pp. 385-393, 2020.

[34] Emerson Climate Technologies, Inc, "Emerson.com," 2018. [Online]. Available: https://climate.emerson.com/documents/vilter-heat-pump-brochure-en-us-5411192.pdf. [Accessed 23 June 2022].

[35] Emerson Climate Technologies, Inc, "Industrial heat pumps," 2011. [Online]. Available: https://climate.emerson.com/documents/vilter-heat-pump-white-paper-en-us-5411194.pdf. [Accessed 23 June 2022].

[36] F. A. Di Bella, "Development of a centrifugal hydrogen pipeline compressor," Concepts ETI, Inc. dba Concepts NREC, 2015.

www.netl.doe.gov

Albany, OR • Anchorage, AK • Morgantown, WV • Pittsburgh, PA • Sugar Land, TX

(800) 553-7681